Activated Carbons from Bituminous Coals by Reaction with H_3PO_4 : Influence of Coal Cleaning

Marit Jagtoyen, Brian McEnaney, John Stencel, Michael Thwaites and Frank Derbyshire

University of Kentucky Center for Applied Energy Research
3572 Iron Works Pike, Lexington, KY 40511-8433

Keywords: Activated Carbon, Phosphoric acid, Coal cleaning

Introduction

Previous publications have described the results of research in this laboratory to investigate the conversion of coals to activated carbons through reaction with phosphoric acid (1-5). These studies have examined the compositional, morphological, and porosity changes in subbituminous and bituminous coals, resulting from reaction with H_3PO_4 at temperatures up to 650°C.

Most of the present studies has been concerned with the use of Illinois bituminous coals as activated carbon precursors. These coals have high sulfur and high mineral matter contents. Phosphoric acid reacts with both of these components, promoting the substantial removal of organic and inorganic sulfur as H_2S (5), and combining with mineral matter constituents, thereby increasing the ash content of the carbon.

The second of these effects is particularly undesirable from the standpoint of producing a quality adsorbent carbon. A possible solution is to lower the coal mineral matter content, by some physical separation process, prior to carbon synthesis. This paper describes the effects of coal cleaning by pentane agglomeration, for three bituminous coals with ash contents between about 8 to almost 40%, on the synthesis and properties of activated carbons.

Experimental

Three bituminous coals, IBC 101, IBC 104 and IBC 106, were studied as precursors. The coals were obtained from the Illinois Basin Coal Sample Program and were of high volatile C rank, as determined by vitrinite reflectance measurement. Properties of the coals are summarized in Table 1. The coals were selected to show significant differences in ash content and organic and inorganic sulfur: IBC 104 is a high ash content coal (39.3%) in which about two-thirds of the sulfur is in the pyritic form; IBC 101 and 106 both have lower ash contents (10.5 and 8.9%, respectively) but the first coal has a high proportion of organic sulfur and the second has an organic/pyritic sulfur ratio of about one.

The parent coals were ground to -20 mesh before reaction with phosphoric acid. Finer grinding (-200 mesh) was required for coal cleaning. Physically cleaned coal samples were produced using a laboratory scale flotation unit. Fuel oil or pentane was vigorously mixed with a coal/water slurry to render the coal particles hydrophobic and to selectively agglomerate them. The agglomerated slurry was then screened; the free ash particles flowed through the screen and the agglomerated coal was retained.

The procedure for preparing chemically activated carbons from both parent and cleaned coals has

been described in detail elsewhere (5). Briefly, a 20 g sample of coal was thoroughly mixed with 30 cm^3 of 50% strength phosphoric acid solution. The mixture was then heated to 170°C and held at this temperature for 30 minutes in flowing nitrogen(80 $ml.min^{-1}$). Each sample was then heated to the higher heat treatment temperature of 550°C for 60 minutes in the same inert atmosphere. The solid products were leached with distilled water to pH=6 and vacuum dried at 110°C before further analysis.

Results and Discussion

The compositions of the cleaned coals are shown in Table 1. The reduction in ash content ranges from around 60%, for IBC 101 and IBC 106, to 90% for the high ash coal IBC 104. With all three coals, cleaning produces a significant rejection of pyritic sulfur. There is effectively no change in organic sulfur. For IBC 106, Si is also removed, and for IBC 104, there is substantial removal of both Si and Al.

The compositions of carbons produced from parent and cleaned coals by acid treatment, are shown in Table 2. In all cases, the carbons have much higher ash contents, by a factor of about two, than the corresponding precursor. Some increase is to be expected due to the loss of material to volatile products. However, the ash contents of the chemically-activated carbons are much higher than expected from devolatalization, and the trend is paralleled by increases in phosphorus content, as observed previously (5,6). Iron, silicon and aluminum can all form insoluble phosphates when reacted with phosphoric acid, and X ray diffraction data have shown that P is present as $FePO_4$, $Si_2P_2O_7$, $Al(PO_3)_3$ in carbons produced from both parent and clean coals. The formation of such species can account for the increased ash content and high phosphorus content of the synthesized carbons, even after extensive leaching.

The carbon phosphorus content is found to correlate almost linearly with both the total ash content of the parent coal and that of the carbon product, Figure 1, although the slopes of the curves differ. A high ash content is detrimental to the mechanical strength of the carbon product and its specific adsorptive capacity, and to the effective use of phosphoric acid: its consumption through these reactions means that less acid is available to promote the synthesis process, and less will be recoverable for recycle in an industrial process. The significant reductions in mineral matter, that are effected by coal cleaning, certainly help to minimize phosphorus retention and produce adsorbent carbons with much lower ash contents.

The data in Table 2 show that acid treatment causes extensive removal of sulfur: the concentrations of pyritic and organic sulfur are lowered by as much as 100% and 88%, respectively. The pyritic sulfur content is reduced to lower levels in the carbons from the parent coals and is almost completely eliminated in the carbons from the cleaned coals. More organic sulfur is also removed from the cleaned coals. The greater extent of S removal from the cleaned coals may relate to their smaller particle size and lower mineral matter content, both of which could facilitate access of the acid to the interior of the particles. The data for the parent high ash coal, IBC 104, provide evidence that the consumption of acid, by reaction with mineral matter, limits the extent of its reaction with the organic matrix, shown here by the extent of sulfur removal. After cleaning, the reduced mineral matter content allows more acid to be available for the removal of organic and pyritic sulfur, and other reactions involved in carbon synthesis.

The greater part of the coal sulfur is released in the form of H_2S, Figure 2. Approximately 60% of the sulfur in the starting coal is converted to H_2S for IBC 101, 47% for IBC 104, and 40% for IBC 106. This is considerably higher than can be attained by thermal treatment, as shown by other published data (5,7). Interestingly, the proportion of sulfur in the precursor that is removed as H_2S remains the same, irrespective of whether the coal has been cleaned or not.

Coal cleaning increases both the total (BET) surface area and the mesopore surface area of the synthesized carbons, Table 3. The bulk of the surface area is contained in the micropores. For the medium ash content coals, IBC 101 and IBC 106, the surface area is increased by 11 and 24%, respectively. However, for IBC 104, the surface areas of the carbon from the cleaned coal were about three times higher than for the carbon from the parent coal, corresponding to a major reduction in the ash content of the precursor from 39 to 4%.

The micropore, mesopore and macropore volumes are also significantly higher in the carbons from the cleaned coals, Figure 3. An exception is the macropore volume of IBC 106 which actually decreases after cleaning. The last observation may signify that, for this particular coal, the ash in the carbon made an appreciable contribution to the macroporosity.

One reason for the increased surface area and porosity in carbons from cleaned coals is considered to be that more of the phosphoric acid is available to react with the organic structure, since less will be consumed by reaction with coal mineral matter, as discussed. In the case of IBC 104, the high ash content of the parent coal could severely restrict the amount of available acid. Previous work has shown that acid concentration can be important to the development of porosity. By increasing the acid concentration from 15 to 50%, for the carbonization of coal IBC 101 at 550°C, the micropore volume was increased by a factor of four while the meso- and macropore volumes increased by a factor of two (6).

Mineral matter and ash constituents can also block the pore structure of coals and chars, which may also help to explain why coal cleaning prior to carbonization enhances porosity. Mahajan and Walker (8) examined the effects on pore structure of a number of coals by removing soluble inorganic constituents by acid washing of coals before carbonization, or the resulting chars. The results were apparently random with the surface area being increased in some cases and decreased in others, suggesting that the distribution of the mineral matter in the coal is an important parameter.

Ehrburger et al. (9) found that the micropore volume of chars was increased after demineralization of the parent coal. In these experiments, demineralization was effected by chemical treatment with HCl/HF prior to carbonization. Some of the increase in microporosity in these cases may well be due to the action of the acid on the organic structure of the coal, rather than simply the removal of mineral matter. The same authors found that acid pretreatment increased the carbonization yield which is indicative of the acid promoting crosslinking reactions. Similar phenomena may also account for some of the results obtained by Mahajan and Walker (8), where the coal structure is modified during acid washing, or during subsequent heat treatment in the presence of residual acid. It is known that acid treatment with HCl and HCl/HF modifies coal thermoplasticity and eliminates swelling during pyrolysis, Lee and Jenkins (10), Lu (11), and leads to increased microporosity in the carbon products.

It is supposed that the role of phosphoric and other acids is to initiate the cleavage of weak connecting bridges between coal structural units at sub-pyrolysis temperatures. Subsequently, bond cleavage reactions are followed by the re-combination of radical fragments to form stronger linkages or larger structural units, leading to the formation of a rigid crosslinked solid. This modified structure will be less susceptible to volume contraction upon heat treatment. Restricted shrinkage and limited volatile loss may facilitate the development, or perhaps more accurately, conservation of the elements of porosity that are present in the starting material. Consequently, factors that influence the availability of the reagent to the precursor will impact upon the pore structure of the carbon.

Summary

It has been shown that high mineral matter content can adversely influence the process of carbonization and the properties of carbons produced by chemical activation of coals. In thermal processing, it is desirable to keep the coal mineral matter content low as carbon is removed during carbonization and activation, thereby increasing the ash content. Around 8-10% ash in the activate is probably an acceptable maximum for many applications; higher concentrations can adversely affect the physical strength of the carbon and specific adsorption capacity. Ash constituents may also catalyze unwanted reactions when the carbon is in service and could reduce its ignition point.

In chemical activation with phosphoric acid, there are additional disadvantages in that acid is consumed by reaction with mineral matter. This leads to: reduced availability of acid for reaction with the organic structure, which may severely limit the extent of porosity development; the loss of recoverable acid for recycle; and an increase in the ash content of the carbon. Lowering the mineral matter content of the carbon precursor by coal cleaning techniques can provide a solution to these problems.

Acknowledgement

The authors wish to acknowledge the assistance of Jack Groppo and Danny Turner of the CAER, and the State of Kentucky and the Illinois Center for Research on Sulfur in Coal for financial support.

References

1) F. J. Derbyshire, M. Jagtoyen, B. McEnaney, S. M. Rimmer, J. M. Stencel and M. W. Thwaites, "Activated Carbon Preparation by Reaction of Subbituminous Coal with Phosphoric Acid", Proc. 20th Biennial Conference on Carbon, 23-28 June, 1991, Santa Barbara, CA, p52-53.

2) F. J. Derbyshire, M. Jagtoyen, B. McEnaney, J. M. Stencel and M. W. Thwaites, "The Adsorptive Properties of Activated Carbons Prepared by Phosphoric Acid Treatment of Subbituminous Coal", Proc. 20th Biennial Conference on Carbon, 23-28 June, 1991, Santa Barbara, CA, p2-3.

3) F.J.Derbyshire, M. Jagtoyen, B. McEnaney, S. M. Rimmer, J. M. Stencel, M. W. Thwaites, "Adsorbent Carbons form Coals by Chemical Activation", Proceedings 1991 ICCS Conference, 16-20 September, 1991, Newcastle, England, Butterworth-Heinemann Ltd.p480-483.

4) F. J. Derbyshire, M. Jagtoyen, B. McEnaney, A. R. Sethuraman, J. M. Stencel, D. Taulbee and M. W. Thwaites, "The Production of Activated Carbons from Coals by Chemical Activation", American Chemical Society, Fuel Division Preprints, 36 (3), 1072-1080, 1991.

5) F.J.Derbyshire, J. M. Stencel, B. McEnaney, M. W. Thwaites and M. Jagtoyen, "An Investigation of the Conversion of Illinois Coals to Activated Carbons". Final technical report to the Illinois Center for Research on Sulfur in Coal. Period 1st Sept. 1990 to 3rd Sept, 1991.

6) M. Jagtoyen, M. Thwaites, J. Stencel, B. McEnaney, and F. J. Derbyshire, "Adsorbent Carbon Synthesis from Coals by Phosphoric Acid Activation". Paper in preparation for Carbon.

7) Khan, M. R., "Prediction of Sulphur Distribution in Products during Low Temperature Coal Pyrolysis and Gasification", 1989, Fuel, **68**, 1439-1449.

8) Mahajan, O.P. and Walker, P.L., "Effect of Inorganic Matter Removal from Coals and Chars on their Surface Areas", 1979, Fuel, **58**, 333-337.

9) Ehrburger, P., Addoun, F. and Donnet, J.P., " Effect of Mineral Matter of Coals on the Microporosity of Charcoals", 1988, Fuel, **67**, 1228-1231.

10) Lee, C. W. and Jenkins, R.G.," Effect of Acid Treatment Atmosphere on the Thermoplasticity of a Low-Volatile Bituminous Coal", 1989, Energy Fuels, **3**, 703.

11) Lu, G.Q. and Do, D.D, "Structure Changes of Coal Reject Char during Pyrolysis at Low Heating Rates", Fuel Processing Technology, **28** , 1991, 247-258.

Table 1. Composition of parent and cleaned coals (wt.%).

Coal	ash	Fe	Si	Al	Pyr.S	Org.S	S
101	10.5	1.4	2.5	0.9	1.6	4.0	5.7
101 clean	4.1	0.8	2.5	1.2	0.8	3.6	4.4
104	39.3	3.2	10.8	3.6	4.4	3.0	7.5
104 clean	3.9	0.7	1.5	0.8	0.9	3.1	4.0
106	8.9	1.7	1.9	0.9	2.4	2.4	4.8
106 clean	3.7	0.8	1.1	1.3	1.0	2.4	3.4

Table 2: Composition of carbons from parent and cleaned coals (wt.%).
(Carbons produced at HTT=550°C, 50% phosphoric acid)

Sample	ash	P	Fe	Si	Al	Pyr.S	Org.S	S
101	20.8	3.2	0.1	10.9	4.0	0.3	0.9	1.2
101 clean	7.0	1.3	0.3	0.1	0.2	0.1	0.8	0.9
104	67.0	8.7	2.5	34.8	8.8	2.3	2.0	4.4
104 clean	8.9	1.5	0.1	0.2	0.1	0.0	0.8	0.9
106	22.7	3.2	1.2	9.8	3.7	0.5	0.3	0.8
106 clean	9.2	1.7	0.2	0.3	0.1	0.1	0.3	0.5

Table 3: Surface areas of carbons from parent and clean coals.
(Carbons produced at HTT=550°C, 50% phosphoric acid)

Sample	BET s.a. (m^2/g)	Mesopore s.a. (m^2/g)
101	575	87
101 clean	638	82
104	155	24
104 clean	652	98
106	660	92
106 clean	820	113

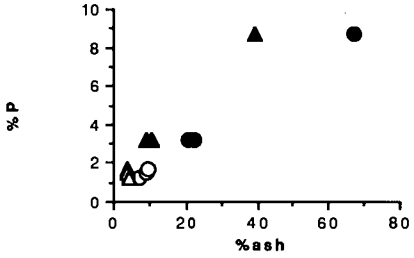

Figure 1: Correlation of P with mineral matter (parent coals) and ash (derived carbons).
(Carbons produced at 550°C, 50% phosphoric acid.)

△ clean coal
▲ carbon from clean coal
○ parent coal
● carbon from parent coal

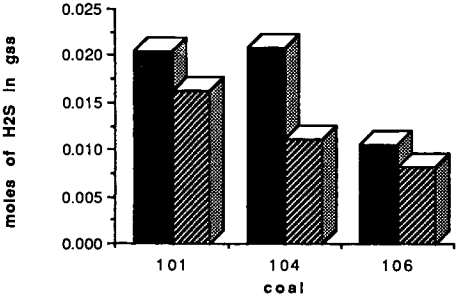

Figure 2: Moles of H2S released during heat treatment (HTT=550°C, 50% acid).

■ carbon from parent coal
▨ carbon from clean coal

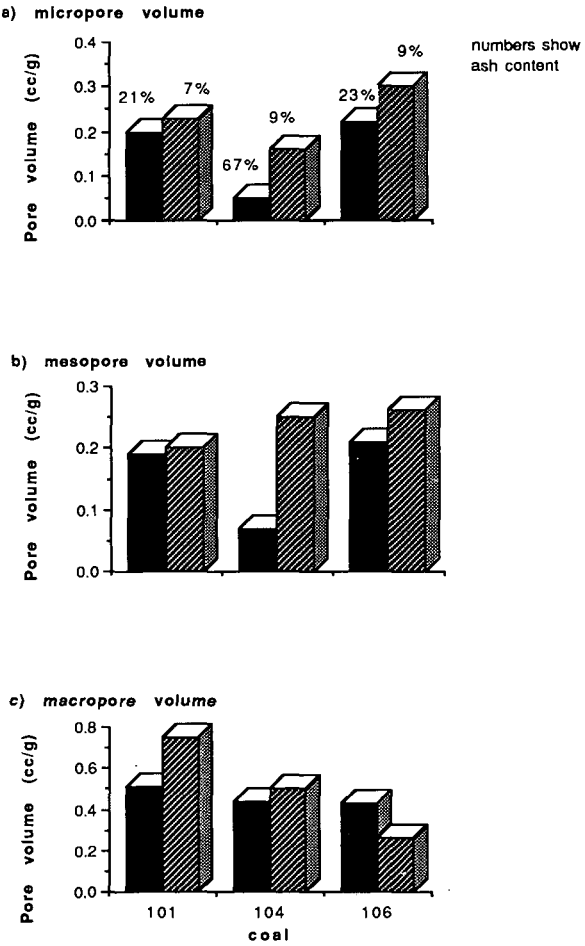

Figure 3: Pore volumes for carbons heat treated to 550°C, 50% acid.

PRODUCTION OF CARBON MOLECULAR SIEVES FROM ILLINOIS COAL

Anthony A. Lizzio and Massoud Rostam-Abadi

Illinois State Geological Survey
615 E. Peabody Drive
Champaign, IL 61820

Keywords: coal, carbon molecular sieve, adsorption, gas separation

INTRODUCTION

Gas separations are a major production cost in the chemical industry today. Production of industrial gases by noncryogenic methods, e.g., pressure swing adsorption (PSA), is expected to grow much faster than by the conventional method, cryogenic distillation [1]. Although there is room for improvement in the design and operation of PSA processes for gas separation, most gains in process efficiency will likely come about from the development of new and improved adsorbent materials [2,3].

Carbon molecular sieves (CMS) have become an increasingly important class of adsorbents for application in the separation of gas molecules that vary in size and shape [1-6]. CMS are microporous materials with average pore dimensions similar to the critical dimensions of an adsorbate molecule. Selectivity for gas uptake by CMS is controlled by the relative rates of diffusion of the adsorbing gaseous species, as opposed to zeolites, which have separation efficiencies based primarily on their chemical affinity for a specific component in the gas mixture [6]. Gas molecules with only slightly varying critical dimensions, e.g., 0.2 Å, may be adsorbed by CMS at rates that vary by several orders of magnitude [7]. Thus, a small change in the average pore size can significantly affect the rate of diffusion of a gas molecule through the pore structure. Under controlled conditions of heat treatment [8-13] and activation [11-13], it has been possible to prepare carbonaceous adsorbents (chars) from coal which exihibit molecular sieve behavior. Pore structure modification can also be achieved by carbon deposition, i.e, the cracking of a suitable hydrocarbon gas within the pores of a carbon substrate [13-17].

The coal research program at the Illinois State Geological Survey has recently initiated a project to determine whether Illinois Basin coals are suitable feedstocks for the production of CMS and to evaluate the potential application of these products in gas separation processes. Data generated in this study will be used to design and engineer CMS with a proper pore size which will resolve a specific gas separation problem. This paper reports data on the kinetics of adsorption of oxygen, nitrogen, carbon dioxide, methane and hydrogen at 25°C on a series of chars prepared from an Illinois Basin coal under various pyrolysis and activation conditions. The effects of coal and char pretreatments such as preoxidation, demineralization, addition of potassium salt and carbon deposition on the molecular sieve properties of the char are also being investigated.

EXPERIMENTAL

Char Preparation: Chars were prepared from a Colchester (Illinois No. 2) hvC bituminous coal (sample IBC-102 of the Illinois Basin Coal Sample Program [18]). The coal is from a western Illinois preparation plant and is relatively low in organic and high in pyritic sulfur. The proximate and ultimate analyses for the coal and for the size fraction (12x40 mesh) used in this study are given in Table 1.

A microbalance reactor (Cahn RG) was used initially to prepare chars. Typically, 500 mg of coal was placed in a wire mesh basket and heated at 20°C/min in flowing N_2 (500 cm^3/min) to a temperature between 600 and 1000°C and held for 0.5 h. The char was cooled in N_2, ground to -200 mesh and stored under N_2 for future characterization. A horizontal fixed-bed reactor was used to prepare larger quantities of char (up to 15 g) under similar conditions.

To enhance surface area development and increase the adsorption capacity of the char, both "physical" and "chemical" activation methods [19] were employed. Physical activation of the char was done in 1 atm CO_2 at 850°C. Upon reaching the desired conversion level, the reactant gas was switched to N_2 and the char sample cooled to 25°C. Chemical activation involved the addition of an alkali salt to the raw coal and subsequent heat treatment in inert gas. More specifically, the coal was physically mixed with potassium hydroxide (KOH) in a 1:1 ratio (by weight), ground with a mortar and pestle to -200 mesh, and pyrolyzed in N_2 at 800°C for 0.5 h. The char was cooled in N_2 to room temperature and washed with distilled water to remove the residual potassium. Since this char became noticeably warm upon removal from the furnace following pyrolysis, the char was submerged in water (quenched) to prevent any further oxidation.

Some chars were prepared by preoxidizing the coal at various O_2 partial pressures (0.2-1.0) and temperatures (130-220°C) prior to pyrolysis. In order to study the influence of mineral matter present in the coal on the molecular sieve properties of the char, a portion of the coal was acid-washed with 5 N HCl (60°C, 3 h); the ash yield was reduced from 3.2 to 1.2%.

The adsorption properties of the char were also modified by carbon deposition (CD). The char sample (1-3 g), placed in the horizontal tube furnace, was heated in flowing N_2 to 800 or 1000°C and held at this temperature for 0.5 h before switching to either 10% (balance N_2) or 100% CH_4 (300 cm^3/min). After a given CD time, N_2 was reintroduced to flush out any residual CH_4 before cooling to 25°C.

Char Characterization: Total surface areas of selected chars were determined from the amount of N_2 and CO_2 adsorbed at 77 and 195 K using a dynamic sorption method in conjunction with a single-point BET adsorption equation [20]. For comparison, a volumetric adsorption apparatus (Autosorb-1, Quantachrome Corp.) was used to obtain equilibrium adsorption data over the entire range of relative pressure. The N_2 (77 K) and CO_2 (273 K) surface areas, in this case, were determined using the multi-point BET and Dubinin-Radushkivich (DR) equations, respectively.

An experimental procedure was developed using the volumetric adsorption apparatus to determine the kinetics of adsorption (volume adsorbed vs. time) of a single gas, e.g., O_2, N_2, CO_2, CH_4, or H_2, at 25°C. A typical run proceeded as follows: 0.3-1.5 g char was placed in a sample cell and outgassed ($1x10^{-5}$ torr) at 180°C for 8 h. Helium was used to determine the dead volume of the sample cell. After outgassing again for several minutes, a known volume of gas was introduced into the sample cell (initial pressure of 350-500 torr) and the subsequent decrease in pressure monitored at 6 s intervals by a pressure transducer accurate to within ± 1 torr. After 10-30 min adsorption time, the sample was outgassed under vacuum at 25°C for 10 min and the same experiment repeated to ensure experimental reproducibility. Volumes adsorbed were calculated using the ideal gas law.

RESULTS AND DISCUSSION

Previously in this study [21], only values of N_2 and CO_2 equilibrium adsorption capacities were reported for our prepared chars. Differences in the N_2 and CO_2 surface area of each were attributed to the molecular sieving nature of the char; however, questions concerning how these materials would behave in an actual gas separation process remained. A knowledge of the kinetics of adsorption of select gases should allow us to better assess the potential usefulness of these materials in specific gas separation processes. In this section, three gas separation processes of commercial importance, N_2/O_2, CO_2/CH_4 and CH_4/H_2, are examined. Kinetic data obtained at 25°C for adsorption of these gases on selected chars are presented and discussed.

Oxygen/Nitrogen Separation: The demand for the two major industrial gases, oxygen and nitrogen, is on the rise due to their increased use in the combustion and gasification of coal [22] and in the steel and electronics manufacturing industries [23]. High purity N_2 can be produced using CMS in a PSA process. Nitrogen is the high pressure product and oxygen (35-50%) is produced as the low pressure product [2,3]. Air separation using microporous carbons relies on the fact that O_2 (kinetic diameter, 3.46 Å) diffuses into the carbon more rapidly than N_2 (3.68 Å) [24]. The kinetics of O_2 and N_2 adsorption at 25°C on the IBC-102 chars prepared at 600, 800, 900 and 950°C are shown in Figure 1. All chars adsorb more O_2 than N_2 and, thus, have some molecular sieving capability for air separation. Table 2 presents the O_2 and N_2 adsorption capacities of each char measured after 5 min and the ratio of both, or O_2/N_2 selectivity. Analysis of Figure 1 reveals that the O_2/N_2 selectivity decreases with time of adsorption, e.g., for the 800 and 900°C chars, the O_2/N_2 selectivities after only 30 s were 2.98 and 4.81, respectively, compared to 1.34 and 3.46 after 5 min. To be effective as a molecular sieve, the product should have a high selectivity ratio as well as a high adsorption capacity. A high selectivity indicates that the sieve readily discriminates between components in the gas mixture. A high adsorption capacity, of course, indicates that the molecular sieve will adsorb a large volume of gas. Table 2 shows that both the O_2 and N_2 adsorption capacities of the 800-1000°C chars decrease with increasing heat treatment temperature (HTT) while the O_2/N_2 selectivity increases from 1.34 to 4.10. Nandi and Walker [9] reported O_2/N_2 adsorption data (measured at 0.8 atm and 25°C) for several chars derived from lower rank coals. The extent of O_2 and N_2 adsorption showed a similar trend with HTT; however, their O_2/N_2 selectivities were substantially lower than those of the IBC-102 chars at any given HTT.

The IBC-102 char produced at 900°C seems to possess optimum molecular sieve properties for O_2/N_2 separation. A comparison of the the O_2/N_2 adsorption properties of this char with those of a coal-based carbon molecular sieve (CMS-A) used in air separation [12,17], a commercial CMS manufactured by Takeda Chem. Ind., Co. (measured at 1 atm and 25°C) [25] and a standard Linde type 4A zeolite is shown in Figure 1. The ability of each material to separate O_2 from N_2 is remarkably similar (except, of course, for the zeolite), suggesting that IBC-102 coal may, indeed, be a suitable feedstock for the production of CMS. No U.S. company currently manufactures CMS for commercial gas separation processes. Air

Products uses a coconut char-based CMS imported from overseas in its recently developed PSA process for production of N_2 from air [26,27]. A European patent [28] describes a process developed to manufacture CMS from coconut char. Typical values of O_2 adsorption capacity and O_2/N_2 selectivity obtained for a series of coconut char-based CMS were 4-6 cm^3/g and 6.5-8.5, respectively. In order to be competitive with currently available coconut char-based CMS, chars derived from coal should have comparable molecular sieve properties. Table 2 shows that our best product (900°C char) has an O_2 adsorption capacity of 4.46 cm^3/g and a selectivity of 3.46.

Table 2 presents O_2/N_2 adsorption capacities for two chars prepared from demineralized IBC-102 coal. For the 800°C char, acid-washing leads to a 1 cm^3/g decrease in the O_2 adsorption capacity, but a 40% increase in O_2/N_2 selectivity. For the 900°C char, there is a slight increase in the O_2 adsorption capacity, but the O_2/N_2 selectivity decreases by 18%. It seems there is no clear advantage in acid-washing this coal before pyrolysis. Table 2 presents O_2/N_2 adsorption data for two chars prepared from preoxidized IBC-102 coal. (Particle agglomeration, an eventual consideration in process scale-up, was not observed with these two chars, unlike the chars that were prepared from non-oxidized coal.) In both cases, the O_2 and N_2 adsorption capacities increase and O_2/N_2 selectivity decreases compared to the chars prepared from non-oxidized coal. The char yield from coal preoxidized at 220°C was about 35% compared to about 45% from coal preoxidized at 180°C. The more severely oxidized coal produces a char with less favorable O_2/N_2 molecular sieve properties. Table 2 also presents O_2/N_2 adsorption data for the 900 and 950°C chars activated to 14 and 10% conversion (X_c), respectively, in 1 atm CO_2 at 850°C. The O_2 adsorption capacity of both chars increases; however, this is offset by a substantial decrease in O_2/N_2 selectivity. Further work is needed to optimize coal preoxidation and char activation process conditions.

Table 2 presents O_2/N_2 adsorption data and Figure 2 shows the kinetics of O_2/N_2 adsorption for Carbosieve, a CMS used in chromatographic applications. This material adsorbs slightly more N_2 than O_2. Although Carbosieve's (CO_2-DR) surface area is about four times greater than that of the 800°C char, its O_2 adsorption capacity is only 40% greater; suggesting that total surface areas are not a good indicator of char adsorption capacity at room temperature. The closeness in value of the N_2 and CO_2 surface areas for Carbosieve, however, does suggest their utility as a preliminary indicator of molecular sieving behavior. That is, carbons which do not exhibit large differences in CO_2 and N_2 surface areas do not make good sieves for the separation of N_2 and O_2 [9,24].

In another attempt to improve the molecular sieve properties of char made from IBC-102 coal, the coal was mixed with an alkali salt (KOH) prior to pyrolysis. Table 2 shows that there is a five-fold increase in the CO_2-DR surface area of this char as compared to chars prepared without addition of KOH. The mesopore and total pore volumes of this "high-surface-area" (HSA) material were determined to be 0.20 and 0.80 cm^3/g, respectively. (Commercial CMS having 5-10 Å pores typically have total pore volumes no greater than 0.25 cm^3/g and surface areas which do not exceed 500 m^2/g [29].) Wennerberg and O'Grady [30] produced HSA carbons by mixing KOH with various carbon substrates, including petroleum coke and coal, and heat treating in inert gas. The physical and chemical properties of these materials have since been extensively studied by those investigators and others (see, for example, refs. 31-33). Whether these materials exhibit molecular sieving behavior, however, remains to be determined. Figure 2 shows that the HSA char adsorbs more N_2 than O_2 and its O_2/N_2 selectivity is quite low (0.40) compared to the chars prepared from untreated coal. Note that, although the CO_2-DR surface area of the HSA char is five times greater than that of the char prepared at 800°C from untreated coal, its O_2 adsorption capacity is about the same. Figure 2 shows the kinetics of O_2 and N_2 adsorption to be very similar for Carbosieve and the HSA char; neither appear to be a suitable adsorbent for air separation. It is interesting to note that the N_2 adsorption capacity (14.87) and N_2/O_2 selectivity (2.51) of the HSA char compare quite favorably with those of the commercial zeolite (8.26, 3.84).

In an attempt to improve the molecular sieve properties of the HSA char, carbon deposition was used to narrow the pores. Figure 2 shows the kinetics of O_2 and N_2 adsorption on the HSA char exposed to 10% CH_4 at 1000°C for 6 min. Depositing carbon in the pores of the HSA char is seen to have a significant effect on the kinetics and extent of O_2 and N_2 adsorption. The O_2 adsorption capacity nearly doubles while that of N_2 decreases by about one third. Table 2 lists the value of O_2/N_2 selectivity after 5 min adsorption time as 1.12, which is still lower than that of any of the chars prepared at 600-1000°C. Figure 2 shows the kinetics of O_2 and N_2 adsorption on the HSA char exposed to 10% CH_4 at 1000°C for 15 min. The rate of both O_2 and N_2 adsorption is considerably slower and the adsorption capacities less than those of the HSA char exposed to 10% CH_4 at 1000°C for 6 min. The O_2/N_2 selectivity, however, increases to 1.85 which is comparable to that of the untreated 800°C char. It is interesting to note that the O_2 and N_2 adsorption capacity of the 800°C char is about twice that of the HSA char (10% CH_4, 1000°C, 0.25 h) even though they have similar surface areas. Further work is needed to optimize the carbon deposition conditions, most notably, the CD temperature, time and methane concentration (see, for example, ref. 34).

Figure 2 is also interesting in that it may help explain the unexpectedly low value of O_2 adsorption capacity obtained for the HSA char (see also Table 2). It shows the kinetics of O_2 and N_2 adsorption for the HSA

char produced by quenching the sample in H_2O upon removal from the furnace following pyrolysis. The quenched HSA char is seen to have adsorbed more than twice the amount of O_2 as the unquenched HSA char; its O_2/N_2 selectivity of 0.93 is similar to that of Carbosieve (see Table 2) and also some highly activated carbons tested by Nandi and Walker [9]. The reason for the higher O_2 uptake could be that the quenched char does not have a chance to chemisorb oxygen after its removal from the furnace since it is immediately quenched in water. The unquenched HSA char, on the other hand, was observed to chemisorb a considerable amount of oxygen upon exposure to air (i.e., it became noticeably warm) and, thus, most of the sites were already occupied by oxygen prior to an O_2 adsorption experiment at 25°C. This results in an apparently lower value of O_2 adsorption capacity being measured for the unquenched char. It is interesting to note that the O_2 adsorption capacity of the HSA char increases after CD (see Table 2) even though some of the pores were undoubtedly blocked by deposits of carbon formed by the cracking of methane at 1000°C. Recall that the HSA char sample was heated in N_2 at 1000°C for 0.5 h prior to a CD experiment, which would have removed most, if not all, of the oxygen present on the char surface as CO and CO_2.

Carbon Dioxide/Methane Separation: The incentive for developing more efficient CO_2/CH_4 separation processes, in particular, PSA using CMS, has increased with the recent advent of several innovative technologies [3]. The adsorption of CH_4 and CO_2 on CMS and activated carbon has been investigated by Schollner [35] for separation of CH_4 from fermentation gas via a PSA process. Methane is also found in combination with CO_2 and N_2 in some natural gas reservoirs (50% CH_4, 50% CO_2), in the effluent gas from oil wells undergoing CO_2 flooding for enhanced oil recovery (20-80% CO_2) and in municipal and industrial landfill gases (40-60% CO_2) [3]. Recovering methane as a medium- or high-BTU gas would be the primary aim of a CO_2/CH_4 PSA process. Significant progress in this area has been realized; both zeolites and CMS have been used as adsorbents [3,36].

The chars produced in this study were tested for their ability to separate CO_2 from CH_4, which have kinetic diameters of 3.3 and 4.0 Å, respectively. Figure 3 shows the kinetics of CO_2 and CH_4 adsorption and Table 3 lists the CO_2 and CH_4 adsorption capacities and CO_2/CH_4 selectivities of the chars prepared at 600-1000°C. The CH_4 adsorption capacity decreases significantly with increasing HTT, while the CO_2 adsorption capacity exhibits a maximum at a HTT of 800°C. Note that the CO_2 adsorption capacities of these chars are about one order of magnitude greater than the corresponding O_2 and N_2 adsorption capacities listed in Table 2. Also, the CO_2/CH_4 selectivity of the char is optimized at a HTT of 900°C and is quite high compared to its corresponding O_2/N_2 selectivity, 66.40 vs. 3.46. The CO_2 adsorption capacity of this char, however, is considerably less than that of the char prepared at 600 or 800°C; so, in effect, there is a tradeoff between high CO_2 adsorption capacity and high CO_2/CH_4 selectivity, i.e., one cannot achieve both by varying just the HTT. Due to the paucity of CO_2/CH_4 separation data in the literature, a comparison with other work is not possible at the present time. However, it is thought that these chars would show good potential for application in a commercial CH_4/CO_2 separation process.

Figure 4 presents the kinetics of CO_2/CH_4 adsorption and Table 3 lists CO_2 and CH_4 adsorption capacities and the CO_2/CH_4 selectivity for Carbosieve and the HSA char. It is interesting to note the similarity in the CO_2/CH_4 (as well as in the O_2/N_2) adsorption properties of these two materials. Both materials adsorb about the same amount of CO_2 at 25°C as the 800°C char even though their CO_2-DR surface areas (measured at 0°C) are greater by a factor of four. The CO_2/CH_4 selectivities of Carbosieve and the HSA char are only 2.86 and 2.57 compared to 13.50 and 66.40 for the 800 and 900°C chars. Apparently, the former two are not nearly as efficient as the latter two chars in separating CO_2 from CH_4. The high CO_2 adsorption capacity of the HSA char is desirable; however, its relatively low CO_2/CH_4 selectivity does not lend itself to being used in a commercial CO_2/CH_4 separation process.

Table 3 lists the CO_2 and CH_4 adsorption capacities and CO_2/CH_4 selectivity and Figure 4 also shows the kinetics of CO_2/CH_4 adsorption for the HSA char exposed to 10% CH_4 at 1000°C for 6 and 15 min. There is a slight increase in the CO_2/CH_4 selectivity (2.57 to 2.98) of the 6 min char while there is considerably more improvement in the CO_2/CH_4 selectivity of the 15 min char (2.57 to 7.09), but its CO_2 adsorption capacity decreases to one sixth its original value. The CO_2/CH_4 molecular sieve properties of these two chars still do not match those of the 600-950°C chars prepared from coal without added KOH.

Methane/Hydrogen Separation: Hydrogen is utilized in a variety of chemical and petrochemical processes. The demand for H_2 would be better met if an adsorbent material could be developed to more efficiently recover it from coke oven, steam reforming, or other coal utilization process gases. In general, all the gases produced in these processes have similar compositions, i.e., they contain principally H_2, along with N_2, O_2, CO, CH_4 and CO_2 in various proportions. The efficient removal of H_2 from this mixture is of considerable commerical importance [37].

Figure 5 shows the kinetics of adsorption of H_2 and CH_4 on the chars prepared at 600-1000°C. The diffusion rate of H_2 is quite high for the 600, 800 and 900°C chars and equilibrium is reached after only 20 seconds. Only the 1000°C char restricts, to some extent, entry of H_2 into its pore structure, i.e., equilibrium

is not reached even after 5 min. The H_2 adsorption capacities of the 600-1000°C chars are quite low and are essentially unaffected by HTT, contrary to the behavior previously observed (in most cases) for CH_4, O_2, N_2 and CO_2 adsorption. The CH_4 diffusion rate is highest for the 600°C char and monotonically decreases with HTT. The pore structure of the 900 and 1000°C chars has sufficiently closed to the point where the char now adsorbs more H_2 than CH_4. For adsorbing CH_4 from a CH_4/H_2 mixture, Table 3 shows that the 600°C char would probably be the best choice with both its relatively high CH_4 adsorption capacity and CH_4/H_2 selectivity. Jüntgen et al. [38] observed similar trends in the kinetics of H_2 and CH_4 adsorption on a "wide pore" CMS, "narrow pore" CMS, activated coal and a Type 5A zeolite. Hydrogen uptake by all four materials was essentially the same, i.e., a relatively high H_2 diffusion rate and low H_2 adsorption capacity were measured. Methane adsorption, on the other hand, varied according to the pore structure of the material. Their "narrow pore" CMS showed similar molecular sieving behavior to that of our 900 and 1000°C chars, whereas their "open pore" CMS displayed behavior similar to that of our 600 and 800°C chars.

Figure 6 presents the kinetics of CH_4 and H_2 adsorption on the HSA char at 25°C. Equilibrium for H_2 is reached within seconds. Table 3 shows that the extent of CH_4 and H_2 adsorption on this char is about three times greater than that on the 600°C char. The CH_4/H_2 selectivity of the HSA char was 39.5, highest among all the chars studied. For the HSA chars upon which carbon was deposited, Figure 6 and Table 3 show that the extent of both CH_4 and H_2 adsorption and the CH_4/H_2 selectivity decrease with increasing CD time. It is interesting to note the similarity in the kinetics of CH_4 and H_2 adsorption on the 800°C and the HSA (10% CH_4, 1000°C, 0.25 h) char (see Figures 5 and 6).

CONCLUSIONS

Chars were prepared from IBC-102 coal under various pyrolysis and activation conditions in a horizontal tube fixed-bed reactor. Chars having commercially significant BET surface areas of 1200-1700 m^2/g were produced using select additives and heat treatment conditions. These high-surface-area (HSA) chars had more than twice the surface area of commercial molecular sieves. Experimental techniques were developed to study, at ambient temperature, the kinetics of adsorption of selected gases, e.g., N_2, O_2, CO_2, CH_4 and H_2, on these chars. The results were intriguing. A char prepared at 900°C was found to have similar N_2 and O_2 adsorption properties to those of commercial CMS used in air separation processes. On the other hand, the HSA char was found to adsorb more N_2 than O_2 and, therefore, was not considered a viable candidate (as is) for separating N_2 from O_2. Carbon deposition, using methane as the cracking gas, increased the O_2/N_2 selectivity of the HSA char; however, this was somewhat offset by a decrease in its O_2 adsorption capacity. Other gas separations of commercial interest studied included CO_2/CH_4 and CH_4/H_2. A char prepared at 800°C showed excellent molecular sieving properties for separating CO_2 from CH_4, i.e., both a relatively high CO_2 adsorption capacity and CO_2/CH_4 selectivity were achieved. The CO_2/CH_4 sieving ability of the HSA char was questionable. That is, although the CO_2 adsorption capacity of the HSA char was slightly greater than that of the 800°C char, its CO_2/CH_4 selectivity was lower by a factor of ten. With regard to CH_4/H_2 separation, the CH_4 adsorption capacity and CH_4/H_2 selectivity decreased with increasing HTT and CD time; H_2 adsorption was minimal and essentially independent of HTT. Future work will focus on optimizing the molecular sieve properties of the most promising chars for a given gas separation process using the char activation and carbon deposition methods employed in this study. Processing conditions will be sought which optimize molecular sieving behavior and minimize loss of adsorption capacity.

ACKNOWLEDGEMENTS

This work was funded in part by the Illinois Department of Energy and Natural Resources through its Coal Development Board and the Center for Research on Sulfur in Coal.

REFERENCES

1. Keller, G.E., in *Industrial Gas Separations* (ACS Symposium Series), (T.E. Whyte Jr., C.M. Yon and E.H. Wagner, eds.), American Chemical Society, Washington D.C., 1983, p. 223.
2. Ray, M.S., *Sep. Sci. Tech.* **21**, 1 (1986).
3. Jasra, R.V., Choudary, N.V. and Bhat, S.G.T., *Sep. Sci. Tech.* **26**, 885 (1991).
4. Jüngten, H., *Carbon* **15**, 273 (1977).
5. Jüntgen, H., Knoblauch, K. and Harder, K., *Fuel* **60**, 817 (1981).
6. Walker, P.L., Jr., Austin, L.G. and Nandi, S.P., *Chem. Phys. Carbon* **2**, 257 (1966).
7. Koresh, J. and Soffer, A., *J. Chem. Soc. Farad. I* **76**, 2457 (1980).
8. Toda, Y., Yuki, N. and Toyoda, S., *Carbon* **10**, 13 (1972).
9. Nandi, S.P. and Walker, P.L., Jr., *Fuel* **54**, 169 (1975).
10. Miura, K. and Hayashi, J., *Carbon* **29**, 653 (1991).
11. Patel, R.L., Nandi, S.P. and Walker, P.L., Jr., *Fuel* **51**, 47 (1972).
12. Verma, S.K. and Walker, P.L., Jr., *Carbon* **28**, 175 (1990).

13. Guo, S., Li, L. and Wang, A., *Fuel Sci. Tech. Conv.* **8**, 545 (1990).
14. Moore, S.V. and Trimm, D.L., *Carbon* **15**, 177 (1977).
15. Kamishita, M., Mahajan, O.P. and Walker, P.L., Jr., *Fuel* **56**, 444 (1977).
16. Chihara, K. and Suzuki, M., *Carbon* **17**, 339 (1979).
17. Verma, S.K., *Carbon* **29**, 793 (1991).
18. Harvey, R.D. and Kruse, C.W., *J. Coal Qual.* **7**, 109 (1988).
19. Rodriguez-Reinoso, F., in *Fundamental Issues in Control of Carbon Gasification Reactivity*, (J. Lahaye and P. Ehrburger, eds.), NATO ASI Series 192, Kluwer Academic, New York, 1991, p. 533.
20. Nelson, F.M. and Eggersten, F.T., *Anal. Chem.* **30**, 30 (1958).
21. Lizzio, A.A. and Rostam-Abadi, M., Proc. Twentieth Biennial Conf. on Carbon, Santa Barbara, CA, 1991, p. 106.
22. Tsang, A.C., Dow Chemical, Private Communication to A.A. Lizzio, 1991.
23. Greek, B.F., *Chem. and Eng. News*, December 2, 1991, p. 13.
24. Nandi, S.P. and Walker, P.L., Jr., *Sep. Sci.* **2**, (1976).
25. Schalles, D.G. and Danner, R.P., *AIChE Symp. Ser.* **84** (264), 83 (1988).
26. Armour, J., Air Products, Private Communication to A.A. Lizzio, 1991.
27. Armour, J., Proc. Twentieth Biennial Conf. on Carbon, Santa Barbara, CA, 1991, p. 40.
28. Sutt, R.F., Jr., Eur. Pat. 102, 902 (1983).
29. Vyas, S.N., Patwarthan, S.R. and Natraj, H.B., *J. Chem. Soc. Farad. Trans.* **86**, 3455 (1991).
30. Wennerberg, A.N. and O'Grady, T.M., U.S. Patent 4,082,694, 1978.
31. Marsh, H. and Walker, P.L., Jr., *Fuel Proc. Technol.* **2**, 61 (1979).
32. Marsh, H., Crawford, D., O'Grady, T.M. and Wennerberg, A.N., *Carbon* **20**, 419 (1982).
33. Ehrburger, P., Addoun, A., Addoun, F. and Donnet, J.-B., *Fuel* **65**, 1447 (1986).
34. Ismail, I.M.K., Rose, M.M. and Mahowald, M.A., *Carbon* **29**, 575 (1991).
35. Schnoller, R., Franke, T. and Kluge, G., Proc. Fifth Conf. Appl. Chem., Balatonfuered, Hungary, Vol. 1, 1989, p. 123.
36. Sircar, S., *Sep. Sci. Tech.* **23**, 519 (1988).
37. Kratz, W.C., Rarig, D.L. and Pietrantonio, J.M., *AIChE Symp. Ser.* **84** (264), 36 (1988).
38. Jüngten, H., Knoblauch, K., Münzner, H., Schröter, H.J. and Zündorf, D., Proc. Fourth London Inter. Carbon and Graphite Conf., 1974, p. 441.

Table 1. Proximate and Ultimate Analyses of IBC-102 Coal.

Proximate Analysis (wt%)	As-received	12x40 mesh
Moisture	13.9	10.6
Volatile Matter	35.3	37.8
Fixed Carbon	45.5	48.3
Ash	5.3	3.2
Ultimate Analysis (wt%)	**As-received**	**12x40 mesh**
Carbon	65.40	70.54
Hydrogen	6.03	6.05
Nitrogen	1.26	1.36
Oxygen	19.17	16.93
Sulfur	2.84	1.92
Sulfate	0.29	0.16
Pyritic	1.45	0.80
Organic	1.09	0.96

Table 2. O_2 and N_2 Adsorption Capacities, O_2/N_2 Selectivity and N_2-BET and CO_2-DR Surface Areas of Chars Prepared from IBC-102 Coal.

Sample	V_{O2} (cm^3/g)	V_{N2} (cm^3/g)	V_{O2}/V_{N2}	N_2-BET (m^2/g)	CO_2-DR (m^2/g)
Linde Type 4A Zeolite	2.15	8.26	0.26	35	316
CMS-A [12,17]	4.27	0.98	4.36	1	575
Takeda Type 3A CMS [25]	5.58	3.85	1.45	----	----
IBC-102, 600°C, 0.5 h	6.00	3.71	1.62	12	375
IBC-102, 800°C, 0.5 h	7.02	5.22	1.34	5	290
IBC-102, 900°C, 0.5 h	4.46	1.29	3.46	----	----
IBC-102, 950°C, 0.5 h	2.38	0.58	4.10	----	----
IBC-102, 1000°C, 0.5 h	0.17	0.00	----	2	5
IBC-102 Dem, 800°C, 0.5 h	6.17	3.21	1.92	----	----
IBC-102 Dem, 900°C, 0.5 h	4.67	1.62	2.84	----	----
IBC-102, 800°C, Preox., 220°C, 1 h, 100% O_2	7.53	6.97	1.08	----	----
IBC-102, 800°C, Preox., 180°C, 2 h, 50% O_2	10.05	8.27	1.21	----	----
IBC-102, 900°C, CO_2, X_c = 0.14	7.84	6.12	1.28	----	----
IBC-102, 950°C, CO_2, X_c = 0.10	6.12	3.80	1.61	----	----
Carbosieve	9.76	10.49	0.93	1040	1220
IBC-102 + KOH (1:1), 800°C, 0.5 h (HSA char)	5.93	14.87	0.40	1400	1690
HSA char, 10% CH_4, 1000°C, 0.10 h	11.40	10.19	1.12	710	980
HSA char, 10% CH_4, 1000°C, 0.25 h	3.39	1.83	1.85	15	240
HSA char, H_2O quench	13.75	14.74	0.93	1330	1550

Table 3. CO_2, CH_4 and H_2 Adsorption Capacities and CO_2/CH_4 and CH_4/H_2 Selectivities of Chars Prepared from IBC-102 Coal.

Sample	V_{CO2} (cm^3/g)	V_{CH4} (cm^3/g)	V_{CO2}/V_{CH4}	V_{H2} (cm^3/g)	V_{CH4}/V_{H2}
IBC-102, 600°C, 0.5 h	78.42	19.22	4.08	0.56	34.32
IBC-102, 800°C, 0.5 h	93.85	6.95	13.50	0.64	10.86
IBC-102, 900°C, 0.5 h	29.88	0.45	66.40	0.56	0.80
IBC-102, 950°C, 0.5 h	12.68	0.30	42.27	0.62	0.48
IBC-102, 1000°C, 0.5 h	0.96	0.03	32.00	1.04	0.03
IBC-102 Dem, 800°C, 0.5 h	80.53	2.66	30.27	0.52	5.11
IBC-102 Dem, 900°C, 0.5 h	39.21	0.83	47.24	0.55	1.51
IBC-102, 900°C, CO_2, X_c = 0.14	111.05	8.64	12.85	0.60	14.40
IBC-102, 950°C, CO_2, X_c = 0.10	55.15	4.98	11.07	0.60	8.30
Carbosieve	118.41	41.40	2.86	----	----
IBC-102 + KOH (1:1), 800°C, 0.5 h (HSA char)	147.10	57.27	2.57	1.45	39.50
HSA char, 10% CH_4, 1000°C, 0.10 h	96.00	32.20	2.98	1.30	24.77
HSA char, 10% CH_4, 1000°C, 0.25 h	24.07	3.40	7.09	0.96	3.54
HSA char, H_2O quench	137.06	58.73	2.33	----	----

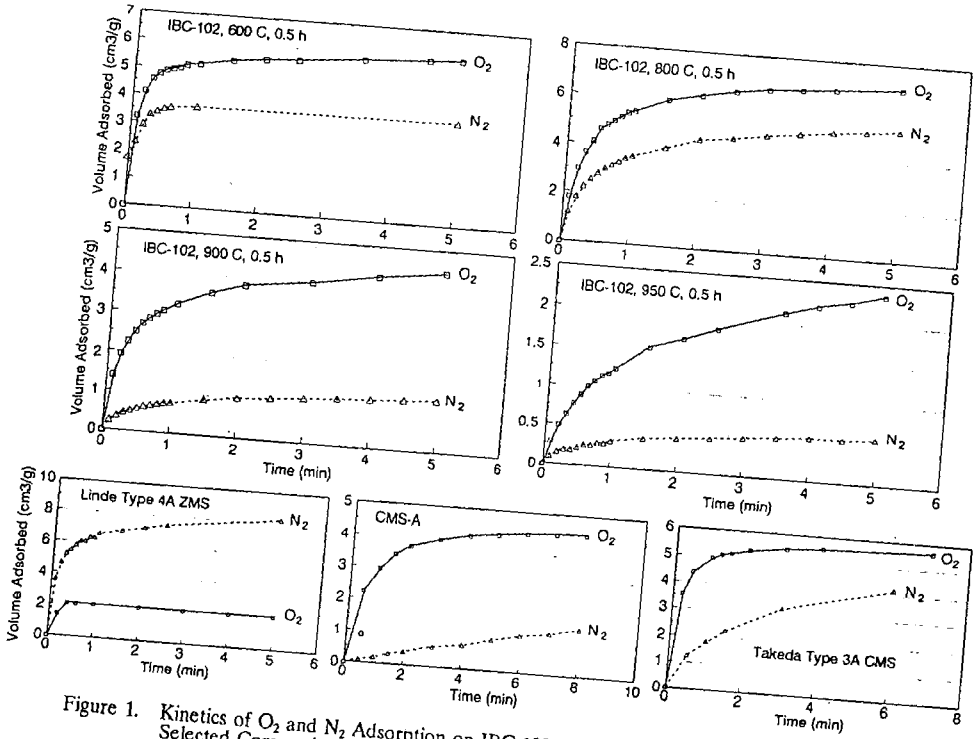

Figure 1. Kinetics of O_2 and N_2 Adsorption on IBC-102 Chars Prepared at 600-950°C and on Selected Commerical Molecular Sieves Used in Air Separation.

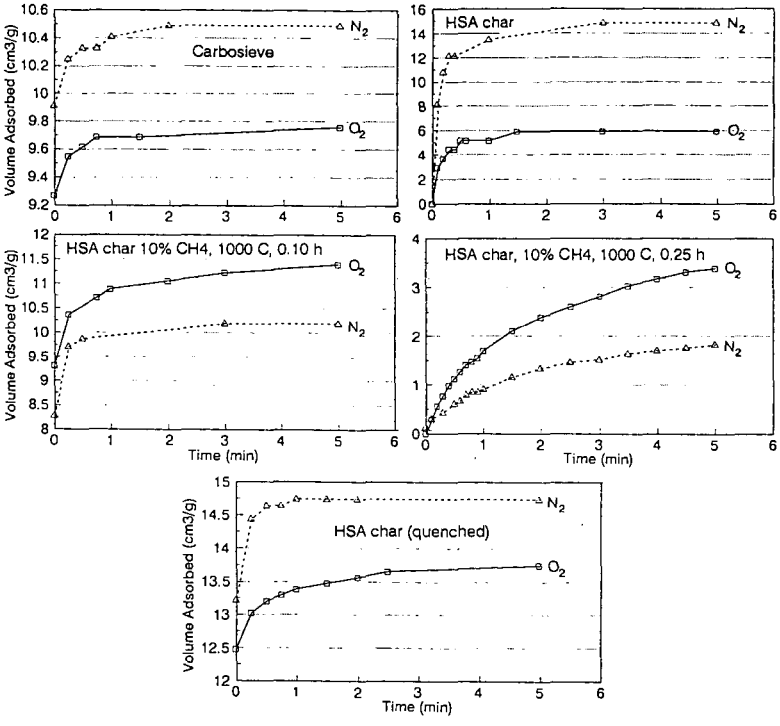

Figure 2. Kinetics of O_2 and N_2 Adsorption on Carbosieve and Selected HSA Chars.

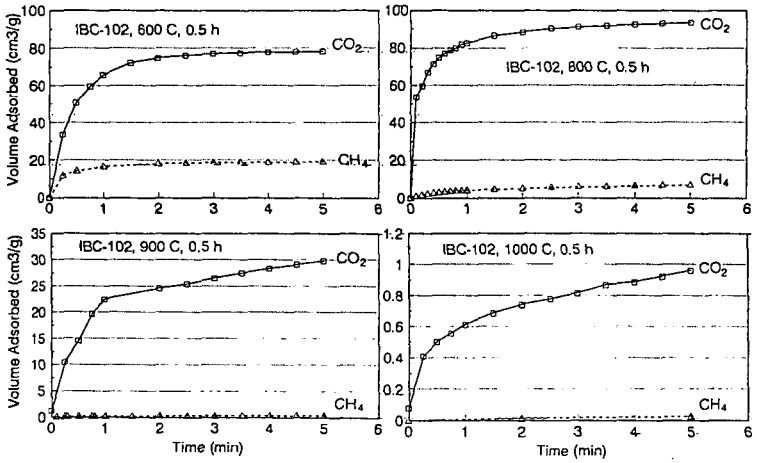

Figure 3. Kinetics of CO_2 and CH_4 Adsorption on IBC-102 Chars Prepared at 600-1000°C.

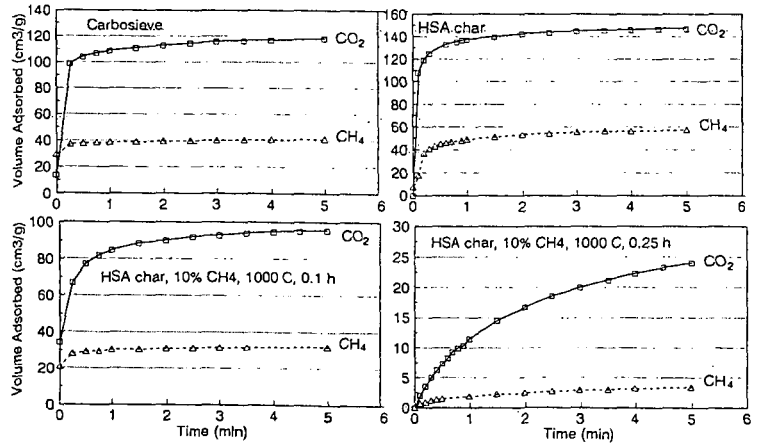

Figure 4. Kinetics of CO_2 and CH_4 Adsorption on Carbosieve and Selected HSA Chars.

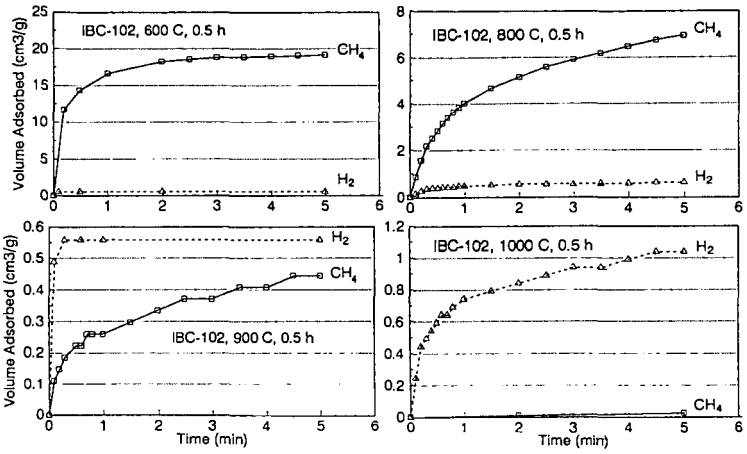

Figure 5. Kinetics of CH_4 and H_2 Adsorption on IBC-102 Chars Prepared at 600-1000°C.

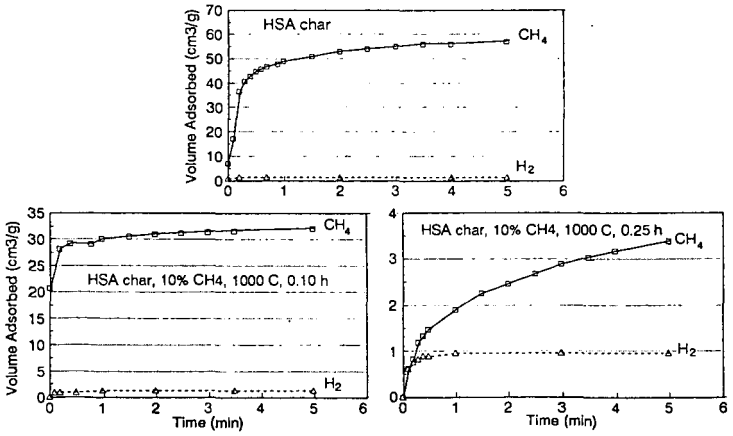

Figure 6. Kinetics of CH_4 and H_2 Adsorption on Selected HSA Chars.

SPECIALTY CHEMICALS AND ADVANCED MATERIALS FROM COALS: RESEARCH NEEDS AND OPPORTUNITIES

Chunshan SONG and Harold H. SCHOBERT

Fuel Science Program, Department of Materials Science and Engineering, 209 Academic Projects Bldg,
The Pennsylvania State University, University Park, PA 16802

Keywords: Coal Chemicals, Specialty Chemicals, Advanced Materials

1. Introduction

To use coals more efficiently as we move into the 21st century, it is important to explore the potentials and possible ways to develop high-value chemicals and materials from coals and coal liquids. This paper reports on our survey study, based mainly on literature and in part on our own experience. Our emphasis was placed on both the current status, including the applications and production level, and the future trends/growth rate of relevant chemicals and materials. The present study was guided bythe following questions: What are the major problems and the future of industrial coal utilization ? Is it necessary to develop coal chemicals now ? What kinds of coal chemicals are more useful and competitive ? Are there large-volume demands for coal chemicals ? Is it really important to develop specialty chemicals and advanced materials ? Are there large-volume applications of aromatic polymeric materials ? How the aromatic specialty chemicals can be derived from coals and coal liquids ? Are there new and better strategies for developing coal chemicals ?

Discussed in this paper are 1) major problems facing the industrial utilization of coals such as carbonization, combustion and liquefaction, 2) the importance of developing coal chemicals, 3) new strategies for developing useful and competitive coal chemicals, and 4) some possible methods for developing several specialty chemicals such as 2,6-naphthalene dicarboxylic acid, and 5) some future research areas related to coal structural chemistry. Because units and pricing systems vary for different chemicals, both SI and English units are used but the conversion factors are given in appendix. Numerous abbreviations for long names were used, and they are listed in the appendix.

2. Worldwide Sources of Aromatic Chemicals

Petroleum and natural gas presently account for probably more than 90% of the organic chemicals [Sheldon, 1983; Speight, 1991]. They are the principal sources of the seven basic building blocks: ethylene, propylene, butadiene, benzene, toluene, xylenes and methanol. The principal sources of aromatic chemicals, however, include both petroleum and coal tar. About 3-4 % coal tars are produced as by-products from carbonization of coals in coke oven at about 1200 °C. In 1987 approximately 15-17 million tons (Mt) of coal tar and about 5 Mt of benzol were produced worldwide [Murakami, 1987; Mikami, 1988].

The annual consumption of aromatics in the world is about 25 Mt for BTX and 5 Mt for naphthalene, anthracene and other two- to four-ring aromatic compounds [Collin, 1985; Murakami, 1987]. About 95% of 2- to 4-ring polyaromatic and heterocyclic chemicals and about 15-25 % BTX chemicals come from coal tar (plus benzol) [Collin, 1985, Mikami, 1988]. In 1989, 7.5 Mt of coal tars was processed worldwide by distillation; about 950 thousand tons (Kt) naphthalene, 20 Kt anthracene, 10 Kt of methylnaphthalene, phenanthrene, acenaphthene, and pyrene were isolated for use in chemical industry; the remains were used as feedstocks for carbon blacks and for carbon materials [Kikuchi et al., 1989]. In Japan, about 2.5 Mt of coal tars are produced annually and 2 Mt tars are processed by distillation; and in Nippon Steel, about 0.6 Mt tars are processed annually [Okazaki and Nozaki, 1986]. With the rapidly growing engineering applications of aromatic polymer materials (Section 6), the demands for a number of 1-4 ring aromatic compounds will increase.

3. Current Status and Problems Facing Industrial Coal Utilization

Because of the 1990 1990 Clean Air Act, switching of coal for combustion in electric utility boilers is expected and in the near future, more low rank coals, which have lower S and N contents, will be burned [Sondreal, 1991]. That humans are increasing the concentration of CO_2 in the atmosphere by burning fossil fuels, and the increased concern worldwide about global warming will certainly lead to pressure on use of all fossil fuels [Kasting, 1991]. Coal is by far the worst in terms of CO_2 production per unit energy production upon combustion. Coal is also a problem regarding NOx, SOx, and particulate emissions. It is likely that new laws will continue to mandate stricter controls on emissions of NOx and SOx, and in the near future, the control of CO_2 emission. Recent reserve estimates of natural gas suggest the reserve is much larger than heretofore thought. Natural gas produces half as much as CO_2 per J of energy as coal, and essentially no NOx, SOx or particulate. Thus natural gas is likely to be the fuel of choice for power generation in the future.

Another major industrial coal utilization is carbonization to produce metallurgical coke [Gray, 1989]. According to the data in 1987-1988, there are about 400 sets of coke ovens worldwide and approximately 450 Mt of bituminous caking coals are carbonized annually to produce about 350 Mt metallurgical coke (about 29 Mt in the USA in 1988); this coke production level account for the reduction of 800 Mt iron ores to produce approximately 450 Mt raw steel [Murakami, 1987; Patrick, 1991]. Coke production has been markedly reduced in recent years, and it appears this trend will continue. Reduced coke demand has come from reduced steel demand, which is largely due to competition from polymer materials, especially engineering plastics, and new technology of direct coal injection into blast-furnaces. By the end of 1989, 32 of Western Europe's 104 blast furnaces, and 23 out of 35 Japan's working blast furnaces were equiped for coal injection [Patrick, 1991].

It will become necessary to produce synthetic liquids from coals for transportation fuels and for chemicals. However, despite enormous strides in coal liquefaction research, and great effort at Wilsonville to reduce cost of coal-derived syncrudes, coal-derived liquid fuels are still not cost-effective with petroleum, and do not seem to be likely to compete with petroleum in near future. Moreover, the liquid fuels from coal must meet with the 1990 Clean Air Act Amendments. For this reason, the transportation fuels will be hydrogen-rich, highly aliphatic fuels. We need to realize that production of such fuels from coal-derived syncrudes will be considerably higher than those from petroleum crudes. This is because petroleum are originally aliphatic in nature, but coal-derived syncrudes are highly aromatic and contain primarily two- to four-ring polyaromatics; conversion to aliphatic transportation fuels would require extensive hydrotreating [Song et al., 1991a, 1991b].

4. Importance and Opportunities for Developing Coal Chemicals and Materials

The question why it is necessary to develop chemicals and materials from coals may be answered with respect to what is happening in the world around coal. The overall picture of the situation that emerges from the above is as follows: Significantly reduced coke demand will reduce the demand for bituminous coking coals and substantially reduce the production of by-product coal tar. However, coal tars are the sources of most polyaromatic and heterocyclic chemicals, which are the chemicals of great interest as feedstocks for specialty chemicals and advanced materials (Sections 2 and 6), and currently coal tar pitch is the major raw materials for coal-based carbon fibers and other carbon materials (Section 8). The demands for aromatic chemicals, aromatic polymer materials, engineering plastics, carbon-fibers and other carbon materials are remarkable and are rapidly increasing. Increased environmental concern about the greenhouse effects will result in significant environmental pressure on the use of coals as boiler fuels. Abundant supplies of cheap and clean natural gas will compete with coal-fired power generation.. Synthetic fuels from coals do not seem likely to be competitive with petroleum for transportation fuels until 2010 or beyond.

From this situation, it is clear that we now need to explore other ways of using coals. We need to recognize that, primarily, coal is a hydrocarbon source, and this apparently has been often overlooked. As a hydrocarbon source, coal can also be used as feedstock for chemicals and materials, in addition to its use as fuel. The 70's and 80's have brought an explosive developments and applications of various organic materials, and the 90's and 21st century will definitely see the significant growth of these materials including aromatic polymers such as engineering plastics, liquid crystalline polymers, and high-temperature heat-resistant polymers, polymer blends, polymer membranes, carbon fibers, carbon-plastic composite materials, and other carbon materials.

A major shift in emphasis of developing new polymer materials is taking place, from aliphatic polymers to the polymers with benzene ring in the chains, and from benzene ring to naphthalene ring or from benzene ring to biphenyl ring. The incorporation of aromatic ring structures has led to higher melting polymers. Future use of polymer materials will involve a significant shift to polymers with two-ring aromatic groups in the chain. These significant developments will give rise to large-volume industrial demands in the 90's and 21st century for a number of 1-4 ring aromatic chemicals and specialty chemicals (Sections 6-7) such as 2,6-dialkylnaphthalene (**2,6-DAN**) and 4,4'-dialkylbiphenyl (**4,4'-DAB**), and high-quality pitch feedstocks for carbon fibers and other carbon materials.

By developing the critical chemicals and substances for the advanced materials, coal chemical research could contribute significantly to high-technology development. The commercial and military importance of advanced polymer materials such as liquid crystalline polymers (**LCP**) resides in their unique properties. However, their commercial future and availability is intimately tied to lowering their cost. In turn, this is largely determined by the cost of the aromatic monomers [NRC, 1990]. Many of the aromatic monomers for newly developed high-performance materials are not readily available from petroleum.

This situation provides an excellent opportunity for starting to explore the potentials and possible ways to develop high-value chemicals and materials from coals and coal liquids. The coal liquids-to-coal chemicals research can be viewed

as an extension of, or product development part, of coal liquefaction research. Development of high-value chemicals from coal liquids could not only increase significantly the economic viability of coal liquefaction process, but also make coal liquids more competitive with petroleum because the former contains many chemicals which are not found in the latter [Song et al., 1991a]. For example, WI-MD contains many two- to four-ring aromatics, which can be converted into high-value specialty chemicals (Section 7). Heavier coal liquids can be transformed to fuels, chemicals, and carbon materials. The direct coal-to-chemical conversion is a new concept (Section 5) and has not been studied. The ideal target of the direct coal-to-chemical conversion research is to allow the structural units in various coals be transformed directly to useful chemicals. Research toward this end will contribute greatly to exploring new coal chemistry.

5. Chemicals from Coals - Old but New Approach

5.1 What Kinds of Chemicals from Coals ?

Several decades ago, the change from acetylene to ethylene brought about an explosive change from coal-based chemical technology to petroleum technology. Petrochemical industry based on ethylene and propylene is still a major industry, and there is no need for coal to be competitive for producing the basic chemicals. Our idea on coal-to-chemicals is to develop more valuable aromatic chemicals from coals, including those which are not not readily available from petroleum but will be needed in relatively large volumes, and those which can be obtained both from coal and petroleum such as BTX and phenollic compounds. The "aromatization" trend of materials development and applications described in Sections 6 and 7 strongly supports this idea. In this way, both petrochemicals and coal-chemicals can find their uses, and this will contribute to the highly efficient utilization of these valuable resources.

5.2 How to Derive Chemicals from Coal ?

5.2.1 Traditional Approaches

The state-of-the-art of chemicals from coal has been reviewed recently by Schlosberg (1990). Among two general approaches to making chemicals from coal, in the first case, by-products such as carbonization tar could be subjected to some appropriate sequence of separation operations to produce eventually pure compounds of interest. The principal drawback is that the starting materials are often extremely complex mixtures. In tar from gasification of lignite, the most predominant compound type accounted for only 4.3% of one fraction. Thus, the sequence of separation steps needed to extract a particular compound becomes enormous. In the other approach, coal could be gasified to synthesis gas, the synthesis gas is converted via Fischer-Tropsch process to liquids, the liquids degraded to ethylene, and the ethylene used to synthesize desired chemical products. The technology for each of these processes is well known. Unfortunately, this route involves significant investment in plant equipment to manufacture what should ideally be a cheap commodity. Also, the overall procedure involves a degradation (gasification), followed by a synthesis (Fischer-Tropsch), followed by another degradation (cracking), followed by another synthesis (chemical manufacture). If one looks at the forest rather than the trees, this laborious tearing down and building up seems slightly crazy.

5.2.2 New Approaches

In regard to aromatic specialty chemicals, the liquids from advanced coal liquefaction, which retain mostly the original molecular components or ring structures of coals, may be theoretically more attractive as feedstocks for aromatic chemicals as compared to Fischer-Tropsch synthesis. This approach lead to aromatics, phenols, and heterocyclic compounds as chemicals. As compared to the distillate fractions of coal tars from coke oven which contain relatively simple and non-substituted aromatics, the disadvantage of chemicals from liquefaction is the presence of many, but not necessarily desirable, alkylsubstituents on the ring systems. Two approaches can be taken to overcome this problem. The first is to use a simple liquefaction method followed by catalytic dealkylation of the coal liquids. The second approach is catalytic or thermal liquefaction at lower temperature to derive the aromatic compounds, followed by thermal dealkylation via hydropyrolysis at higher temperature to take off the alkyl substituents, producing relatively simple aromatics. The key factors are the conversion efficiency and the product separation. These approaches may become promising with the large-volume demands for aromatic chemicals, and can be economically competitive if improved separation methods emerge.

All the above-mentioned methods can be viewed as "indirect" coal-to-chemical conversion. An alternative is to explore introducing a reagent into the coal to cleave only a certain well-defined set of bonds, carefully cutting out the structures of interest. It is generally thought that a significant number of the aromatic systems in low rank coals such as lignites and subbituminous coals contain only 1- to 2-ring. Low rank coals therefore offer promise for production of phenol and catechol type chemicals as well as BTX (benzene, toluene, xylenes) and naphthalene. A careful oxidation should be able to produce large yields of benzene carboxylic acids. If long chain aliphatic units exist, as some investigators believe, neatly clipping the ends of the aliphatic chains may allow useful materials based on aliphatic carbon to be recovered.

5.3 Supporting Research in Fundamental Coal Chemistry

In the past ten years, there has been an accelerated development of our understanding of coal structures, reactivity, and reactions. What is needed more in order to assess the potential of this approach to chemicals from coals ? First, more knowledge of the principal organic structural features is needed. Average parameters such as aromaticity are not very useful. To selectively obtain specialty chemicals, especially important knowledge is the number and specific position of substituents on aromatic rings in coals. When such knowledge is available, it should be possible to select specific coals and to select those types of bonds which are desired to cleave; and then knowledge is needed on the kinetics, mechanism, and the thermochemistry of the cleavage processes. Finally, better ways are needed of selecting appropriate solvents and adjusting the molecular size and polarity.

6. Aromatic Polymer Materials & Engineering Plastics Related to Coal Chemicals

We will review briefly the recent developments and applications of aromatic polymer materials and engineering plastic related to coal chemicals, namely, the polymers synthesized from aromatic monomers that can be made from coal and coal liquids. The world-wide consumption of synthetic polymers is now in the order of 70 Mt/yr, about 56% of which are plastics, 18% are fibers, and 11% synthetic rubber. The balance is made up of coatings and adhesives [Stevens, 1990]. The production of plastics is growing fast while the others are not. Assuming the industrial production indexes for synthetic polymer materials to be 100 in 1987, such indexes in 1990 are 115.8 for plastic materials, 92.7 for man-made fibers, and 88.6 for synthetic rubber [News-CI, 1991]. Numerous reviews on polymer materials have been published in recent years [Hall, 1981; Critchley et al., 1983; MacDermott, 1984; Bowden and Turner, 1987; Seymour, 1987; Stevens, 1990; Dyson, 1990; NRC, 1990; Weiss and Ober, 1990; Kroschwitz, 1991; Mark et al., 1992].

Engineering plastics are relatively higher in cost but have superior mechanical properties and greater durability, which make them competitive with metals, ceramics, and glass in a variety of applications. Engineering plastics is now a $2 billion business in USA [Schlosberg, 1990]. More importantly, engineering plastics are rapidly growing market with consumption projected to increase up to 10% annually [Stevens, 1990]. The following are principal engineering plastics: polyamide / nylon (**PA**), polyacetal (**PAL**), polycarbonate (**PC**), polyphenylene oxides (**PPO**), thermoplastic polyester including polyethylene butylate (**PBT**) and polyethylene terephthalate (**PET**), polyarylate (**PAR**), polysulfone (**PS**); polyphenylene ether ether ketone (**PEEK**); and high-temperature heat-resistant polymers such as polyimdes (**PI**) and polyamideimide (**PAI**). The top five are PA, PC, PPO, PAL, and PBT [Stevens, 1990]. The selling prices for the family of the 5 products was in the $1.40-$2.00 per pound (lb) range in 1985. It is forecast that consumption of thermoplastic polyester in North America will increase by 7.5% per year from 1.945 billion lb in 1990 to 2.79 billion lb in 1995, in which PET is the major player (from 1.73 to 3.425 billion lb) and the second is PBT (from 180 Mlb to 370 Mlb) [Vervalin, 1991].

Polyimide-type heat-resistant polymers, as well as carbon fibers (Section 8) were developed initially for aerospace industry as better light-weight heat-resistant materials. They now have found wide commercial applications. Polyimides have experienced extremely rapid developments in recent years, the major emphasis being on engineering applications [Stevens, 1990].

The liquid crystalline polymers (**LCPs**) containing naphthalene or biphenyl ring are capable of replacing metals and ceramics in many applications. Moldings of these rigid, rod-like, heat-resistant engineering polymers may be used in place of metals and ceramics for electronics, aerospace, and transportation applications [Seymour, 1987]. In 1989 worldwide production of LCP fibers is about 94 Mlb with an average market value of nearly $10/lb; thermotropic LCPs about 10 Mlb (valued at about $10/lb) of which about 5 Mlb was used in cookware [Weiss and Ober, 1990].

Most polymers are good insulators. However, some polymers such as poly-N-vinylcarbazole (PVCA) are photoconducting [Penwell et al., 1978]. Recently Hara and Toshima (1990) reported that the conductive and heat-resistant polymer films can be prepared by electrochemical polymerization of aromatic hydrocarbons such as naphthalene. Otani and co-workers reported that polyaromaties such as pyrene and phenanthrene can be used to make condensed polynuclear aromatics (COPNA) resin (Otani et al., 1986, Ota et al., 1988). In addition, cyclic and short-chain linear phosphazenes with biphenyl as side chain [Allcock, 1991] may be viewed as biphenyl type organic-inorganic macromolecules.

7. Monomers for High-Performance Polymers

Many aromatic and heteroatom-containing compounds can be converted into monomers for various polymers. **Scheme 1** presents a list of important monomers for aromatic engineering plastics, liquid crystalline polymers (monomers in first 3 rows), and heat-resistant resins (monomers in the 4th row in Scheme 1). Because alkyl chains on aromatic rings can be readily oxidized to COOH or OH groups by using oxidizing agents or by heterogeneous catalytic oxidation, an

Scheme 1. Some Important Monomers for Aromatic Polymer Materials

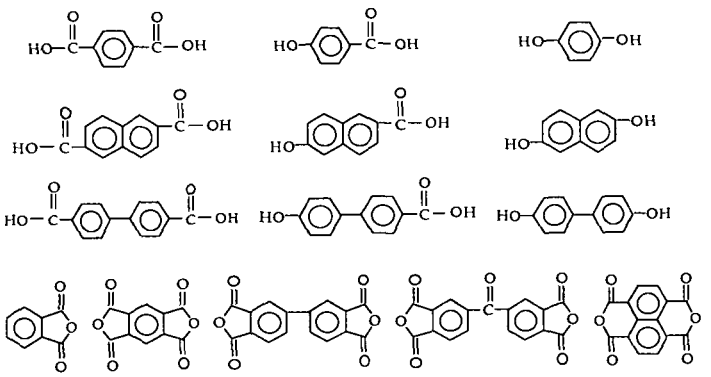

Scheme 2. Possible Routes for Synthesis of 2,6-NDCA

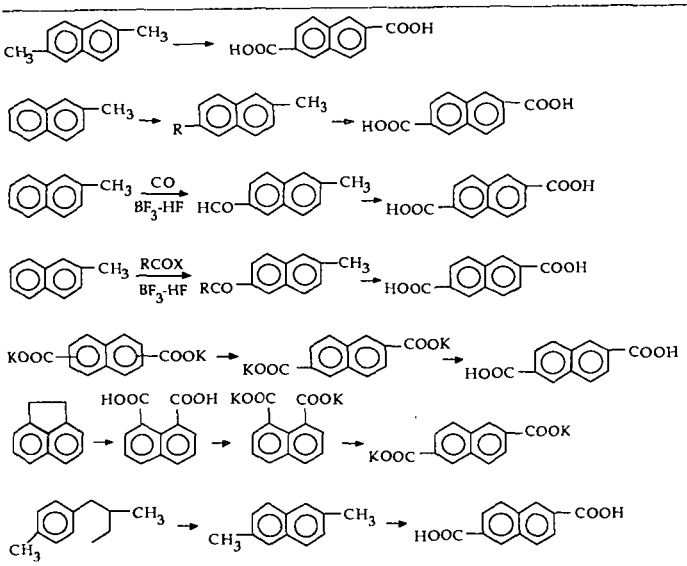

important research subject is how to prepare the needed aromatics. For example, the oxidation of 2,6-DAN and 4,4'-DAB can readily give 2,6-naphthalene dicarboxylic acid (**2,6-NDCA**) and 4,4'-biphenyl dicarboxylic acid (**4,4'-BDCA**), respectively. **Scheme 2** shows the possible routes for synthesis of 2,6-NDCA based on the chemicals that can be obtained from coal. By extending the methods used in catalytic synthesis of 1,4-xylene, terephthalic acid, and p-hydroxybenzoic acid, various methods seem to be available for the research and laboratory-scale synthesis of 2,6-disubstituted naphthalene and 4,4'-disubstituted biphenyl chemicals. However, because of the increase in the peripheral positions on the rings, the steroselectivity is much more important, and in practice more difficult to control as compared to the situation of alkylbenzene.

Some of the coal-related important monomers for polyimides are pyromellitic anhydride (**PMDA**) and 1,4,5,8-naphthalene tetracarboxylic acid (NTCA) and its dianhydride (**NTCADA**) as well as the well known phthalic anhydride. Oxidation of pyrene produces NTCADA, which can be used for making some high-temperature heat-resistant resins. Phenanthrene and its derivatives are rich in coal-derived liquids, and can be obtained in relatively high yields from pyrolysis and carbonization tars. Considerable efforts have been devoted to finding the uses for it in the past decades, but its use is still very limited [Kurata, 1986]. During the Lewis acid-catalyzed hydrogenation of anthracene, sym-octahydrophenanthrene (sym-OHP) and phenanthrene were produced [Song et al., 1991c, 1989b]. sym-Octahydroanthracene (sym-OHA) was produced from phenanthrene over some acidic catalysts [Song et al., 1991 unpublished]. It is possible that sym-OHA can be formed from sym-OHP. Because sym-OHP can be obtained in considerably high yields by using supported NiW/Al_2O_3 or $NiMo/Al_2O_3$ catalysts [Shabtai, 1978; Song et al., 1988, 1991b; Ueda et al., 1990], it seems that one can hydrogenate phenanthrene and then isomerize sym-OHP to sym-OHA. The oxidation of sym-OHA and subsequent dehydration could produce PMDA, and dehydrogenation of sym-OHA can readily produce anthracene which is one of the most valuable chemicals and has found large-volume uses in dye industry as intermediate and in pulp industry as pulping agent (anthraquinone).

Biphenyl compounds are not as rich as naphthalene compounds in coal liquids. However, coal liquids contain phenanthrenes, fluorenes, dibenzofurans, and dibenzothiophenes. The latter three compounds can be converted to biphenyl type compounds by catalytic hydrocracking. Phenanthrene, may be used to produce diphenic acid and 4,4'-BDCA. Oxidation of phenanthrene can produce either phenanthrquinone or diphenic acid (biphenyl-2,2'-dicarboxylic acid). Diphenic acid may also be used for heat-resistant resins.

8. Advanced Carbon Materials from Coals and Coal Liquids

It is now well known that various useful carbon materials and composite materials can be made from coals, coal tars, coal liquids from liquefaction, and petroleum. It has been indicated in several recent reviews by Marsh [1989, 1991] and by Walker [1986, 1991] that the following are advanced or "old but new" carbon materials based on coal-derived feedstocks:

- o Pitch-based carbon fibers
- o Mesophase-based carbon fiberso
- o Carbon fiber reinforced plastic
- o Carbon whiskers or fillament
- o Graphite and graphite-based materials
- o Electrodes
- o Composite materials
- o Molecular sieving carbons
- o Mesocarbon microbeads
- o Activated adsorbent carbons
- o Activated carbon fibers
- o Metallurgical cokes
- o Intercalation Materials
- o Fullerenes or bucky-balls
- o Diamond-like films

Currently, coal tar pitch and bituminous coals (for making coke) are the major feedstocks of coal-based carbon materials. Coals ranging from low-rank coals to anthracites, and heavy liquids from coal liquefaction and tars from low temperature pyrolysis may be used for carbon materials in the future. The large-volume uses of coals for carbon materials can be stimulated significantly by the development of molecular sieving carbons (MSC) for gas separartion and the adsorbent carbons for purifying water, air and medical and environmental applications. The application of MSC for air separation by PSA method is now comercially viable (Large-scale separation of CO from coal-derived gases may be carried out using COSORB method, provided care is taken to remove moisture and oxygen [Song et al., 1987, unpublished]). There are several recent review and original articles on coal-based carbon molecular sieves [Walker, 1986, 1990; Verma, 1991; Hashimoto, 1991] and adsobent carbons [Marsh, 1989, 1991; Verheyen et al, 1991; Derbyshire and McEnaney, 1991a, 1991b].

The large-volume uses of coal liquids including those from carbonization and liquefaction may depend mainly on the development of technologies for producing general-purpose and mesophase-based carbon fibers, including activated carbon fibers for environmental protection uses, graphite electrodes, and mesophase microbeads-based materials. Several

reviews on carbon fibers are now available [Johnson 1989; Dorey, 1987; Anderson, 1987; Donnett, 1984]. Coal tar pitch-based carbon fibers are still in the development stage. Recently, commercialization of coal tar pitch carbon fibers has been announced by Mitsubishi Chemical (500 tons/yr) and Osaka Gas (300 tons/yr) through its subsidary [Matsumura, 1989].

Coal-derived materials have higher N and O contents than petroleum feedstocks. Application of catalytic hydroprocessing for structural modification and heteroatom (especially N) removal of coal-derived carbonization feedstocks may become increasingly important for making mesophase-based carbon materials such as carbon fibers and graphite electrodes. Moderate hydrogenation and hydrodenitrogenation (HDN) of pitch feedstocks using large-pore [Song et al., 1991f, 1992f] hydrotreating catalysts can improve carbonization process; and perhaps more importantly, HDN of the feedstocks may significantly improve the properties of the coal-based mesophase carbon materials upon graphitization.

9. End of Begining

Can we build a new basis in coal science for advanced and viable coal chemical industry ? Would liquefaction of coals be commercialized in 21st century ? Can we make break-through in coal-to-chemicals research to match the demands arising from rapidly developing polymer industry and carbon industry in the forseeable future ? Will it ever be possible to produce specific chemicals directly from coals ? The future is not certain, particularly if the word "produce" carries the implication of a commercially viable process. Nevertheless, the potential exists, and the future may show handsome dividends from relatively modest investments in research on organic coal structures, reactivity, catalytic conversions, new pretreatments, novel reactions, supercritical extraction for the conversion processes such as direct coal-to-chemicals and coal liquids-to-chemicals tests coupled with advanced liquefaction method. While it may seem to be beyond the scope of "coal" science, the conversion of the coal aromatic chemicals to specialty chemicals such as 2,6-dialkylnaphthalene is also important part, which determines the potential of coal chemicals as monomers for polymer materials.

Relevant Literature
(Due to space limit, some of the relevant references cited below were not mentioned in the text).

Allcock, H.R.; Ngo, D.C.; Parvez, M.; Whittle, R.R.; Birdsall, W.J. , J. Am. Chem. Soc. 1991, 113, 2628-2634.
Anderson, B.W., J. Phys. D: Appl. Phys. 1987, 20, 311-314.
Bacon, R. "Carbon Fibres from Rayon Precursors" in "Chemistry and Physics of Carbon", Vol. 9, (Eds. Walker, P.L. and Thrower, P.A.), Marcel Dekker, New York, 1975, pp.1-101.
Bowden, M.J.; Turner, R.S. "Polymers for High Technology". ACS Sym Ser. 1987, No. 364, 466 pp.
Borman, S., C & EN, 1992, Jan 6, p.26
Chapoy, L.L. "Recent Advances in Liquid Crystal Polymers". Elsevier Appl. Sci. Pub: New York, 1985
Chiba, K.; Tagaya, H., Kagaku Kogaku 1988, 52 (7), 520-525.
Collin, G. Erdol und Kohle - Erdgas Petrochem. 1985, 38 (11), 489-496
Critchley, J.P.; Knight, G.J.; Wright, W.W., "Heat-Resistant Polymers", Plenum Press:New York, 1983, 462 pp.
Derbyshire, F.; McEnaney, B., Energia, University of Kentucky, 1991a, 2 (1), p.1-6.
Derbyshire, F.; McEnaney, B., 1991 Int. Conf. Coal Sci., 1991b, Newcastle upon Tyne, pp.480-483.
Donnett, J.B.; Bansal, R.P., "Carbon Fibers", Marcel Dekker: New York, 1984.
Dorey, G., J. Phys. D: Appl. Phys. 1987, 20, 245-256.
Dyson, R.W. "Engineering Polymers". Blackie (Chapman and Hall): New York, 1990
Economy, J., Mol. Cryst. Liq. Cryst. 1989, 169, 1-22.
Finkelmann, H., Angew. Chem. Int. Ed. 1987, 26 (9), 816-824.
Gray, R.J., "Coal to Coke Conversion", *in "Introduction to Carbon Science"*, H. Marsh Ed., Butterworths : London, 1989, pp.285-321.
Hall, C., "Polymer Materials". John Wiley & Sons: New York, 1981, 198 pp.
Haggin, J., C&EN, 1990, Aug. 6, p.29
Hara, S.; Toshima, N., Chemistry Letters 1990, pp.269-272.
Hirota; Nomura, M.; Song, C., "A Method for Manufacture of Aromatic Chemicals from Coals", Japan Patent Appl., 1989
Jackson, W.J., Jr., Mol. Cryst. Liq. Cryst. 1989, 169, 23-49.
Johnson, D.J. "Carbon Fibers: Manufacture, Properties, Structure and Applications". in "Introduction to Carbon Science", H. Marsh, Ed., Butterworths, London, 1989, pp. 198-228.
Kamiya, T., Aromatics (Japan) 1988, 40, No.3-4, p.52-55.
Kasahara, T.; Takamizawa, Y., Kagaku Kogaku 1988, 52 (6), 416-420.
Kasting, J., Paper presented at Information Transfer Session, Cooperative Program in Coal Research, November 18-19,

1991, Pennsylvania State University, University Park, PA.
Kikuchi, E.; Ariyoshi, J.; Sugi, Y.; Horida, Z.; Iwasaki, M., Petrotech 1989, 12 (2), 78-85.
Komatsu, M., Kagaku Kogaku 1986, 50, (9), 614-618.
Kroschwitz, J. Ed. "High Performance Polymers and Composits". Wiley : New York, 1991, 922 pp.
Kurata, N., Kagaku to Kogyo 1988, 41 (1), 33-36.
Kurata, N., Kagaku to Kogyo 1986, 60 (7), 274-280.
MacDermott, C.P. "Selecting Thermoplastics for Engineering Applications". Dekker:New York, 1984.
Margolis, J.M. (Ed.), "Engineering Thermoplastics: Properties and Applications". Dekker:New York, 1985.
Mark, J.E.; Allcock, H.R.; West, R. "Inorganic Polymers". Prentice Hall, Englewood Cliffs, NJ, 1992.
Marsh, H. "New and Traditional Carbon Materials from Petroleum and Coal Sources". Paper presented at Information Transfer Session, Cooperative Program in Coal Research, November 18-19, 1991, Pennsylvania State University, University Park, PA.
Marsh, H. (Ed.), "Introduction to Carbon Science", Butterworths:London, 1989, 321 pp.
Marsh, H.; Menendez, R., Butterworths:London, 1989, pp.38-73.
Matsumura, Y., Kagaku Keizai 1989a, No.9, 33-41
Matsumura, Y., JETI 1989b, 37 (No.9), 223-226.
Mittal, K.L. Ed. "Polyimides". Plenum Press : New York, 1982.
Mikami, K., Aromatics 1988, 40 (1-2), 26-29.
Miura, K.; Hayashi, J.; Hashimoto, K., 1991 Int. Conf. Coal Sci., 1991, Newcastle upon Tyne, pp.560-563.
Murakami, H., Nenryo Kyokai-Shi 1987, 66(5), 448.
News-CI, C&EN, 1991, June 24, pp.28-69.
News-CO, C&EN, 1992, Jan 6, p.12.
News-LCP, Speciality Chemicals 1987, 11 (6), 12-19.
News-LCP, Speciality Chemicals 1988, 12 (8), 17-22.
News-NDCA, Petrotech 1989, 12 (7), p.513.
News-PC, C&EN 1991, Dec. 23, p.8.
News-PAR, Kagaku Gijutsu-Shi MOL 1988, No.3, p.20
News-PBT, Kagaku Gijutsu-Shi MOL 1987, No.11, p.20-21
News-PET, Speciality Chemicals 1988; 12 (10), 17-22.
News-PET, C&EN 1991, Sept. 9, p.15.
News-PS, C&EN, 1991, Dec.16, p.8.
Nomura, M., Kagaku, 1986, 41 (7), 442-448.
NRC National Materials Advisory Board. "Liquid Crystalline Polymers". National Academy Press, 1990, 106 pp.
Okuda, K., Petrotech (Japan) 1982, 5 (1), 37-42.
Ota, M.; Otani, S.; Iizuka, S.; Sawada, T.; Ota, E.; Kojima, A., Nippon Kagaku Kaishi 1988, No.3, 343-350
Otani, S.; Raskovic, V.; Oya, A.; Kojima, A. J. Mater. Sci. 1986, 21, 2027.
Okazaki, H.; Nozaki, M., Fine Chemicals 1986.6.15, 5-17.
Patrick, J.W., Energia, University of Kentucky, 1991, 2 (5), p.1-6.
Penwell, R.C.; Ganguly, B.N.; Smith, T.W., Macromol. Rev. 1978, 13, 63.
Samulski, E.T. "Polymeric Liquid-Crystals". Physics Today 1982, 35 (5), 40-46.
Sato, K., Kagaku Keizai 1987, No.11, 28-36.
Schlosberg, R.H., "Chemicals from Coal", Chap. 24 in "Fuel Science and Technology Handbook", J.G. Speight Ed., Marcel Dekker: New York, 1990a, pp.763-773.
Schlosberg, R.H., "Chemicals from Petroleum", Chap. 11 in "Fuel Science and Technology Handbook", J.G. Speight Ed., Marcel Dekker: New York, 1990b, pp.277-306.
Schobert, H.H., Paper presented at the Twelfth Biennial Lignite Symposium, Grand Forks, North Dakota, May 18-19, 1983.
Scobert, H.H.; Bartle, K.D.; Lynch, L.L. (Eds.), "Coal Science II", ACS Sym. Ser. 461, 1991, 337 pp.
Schobert, H.H., "The Chemistry of Hydrocarbon Fuels", Butterworths: London, 1990, 348 pp.
Seymour, R.B. "Polymers for Engineering Applications". ASM International, 1987, 198 pp.
Shabtai, J.; Veluswamy, L.; Oblad, A.G., Am. Chem. Soc. Div. Fuel. Chem. Prepr. 1978, 23 (1), 107-113.
Sheldon, R.A. "Chemicals from Synthesis Gas", Reidel Pub. Co.: Boston, 1983
Shindo, A. Osaka Kogyo Gijutsu Shikenjo Koho, 1961, 12, 110-119.
Song, C.; Hanaoka, K.; Ono, T.; Nomura, M., Bull. Chem. Soc. Japan 1988, 61, 3788.
Song, C.; Hanaoka, K.; Nomura, M., Fuel 1989a, 68 (3), 287-292.
Song, C.; Ono, T.; Nomura, M., Bull. Chem. Soc. Japan 1989b, 62 (2), 630-632.
Song, C., Eser, S.; Schobert, H.H. et al., "Compositional Factors Affecting Thermal Degradation of Jet Fuels", Annual Progress Report for the Period July 1990 - July 1991, DOE/Sandia National Laboratory, 78-0899-TPR-4, 1991a, 181 pp.
Song, C., Schobert, H.H.; Matsui, H., Prepr. Pap.-Am. Chem. Soc., Div. Fuel Chem. 1991b, 36 (4), 1892-1899.

Song, C., Nomura, M.; Ono, T., Prepr. Pap.-Am. Chem. Soc., Div. Fuel Chem. 1991c, 36 (2), 586-596.
Song, C.; Schobert, H.H.; Hatcher, P.G., Proc. 1991 Int. Con. on Coal Sci., UK, 1991d, p.664-667.
Song, C.; Nihonmatsu, T.; Hanaoka, K.; Nomura, M., Prepr. Pap.-Am. Chem. Soc., Div. Fuel Chem. 1991e, 36 (2), 542-550.
Song, C.; Nihonmatsu, T.; Nomura, M., Ind. Eng. Chem. Res. 1991f, 30, 1726-1734.
Song, C.; Schobert, H.H.; Hatcher, P.G., Energy & Fuels 1992a, in press.
Song, C.; Schobert, H.H.; Hatcher, P.G., Prepr. Pap.-Am. Chem. Soc., Div. Fuel Chem. 1992b, 37, in press.
Song, C.; Hatcher, P.G., Prepr. Pap.-Am. Chem. Soc., Div. Petrol. Chem. 1992c, 37, in press.
Song, C.; Schobert, H.H., Prepr. Pap.-Am. Chem. Soc., Div. Fuel Chem. 1992d, 37, in press.
Song, C.; Peng, Y.; Jiang, H.; Schobert, H.H., Prepr. Pap.-Am. Chem. Soc., Div. Petrol. Chem. 1992e, in press.
Song, C.; Hanaoka, K.; Nomura, M., Prepr. Pap.-Am. Chem. Soc., Div. Fuel Chem. 1992f, 37, in press.
Speight, J.G. (Ed.), "Fuel Science and Technology Handbook", Marcel Dekker: New York, 1990,1193 pp.
SRI International "1990 Directory of Chemical Products - United States of America", 1990, 1203 pp.
Stevens, M.P., "Polymer Chemistry", Oxford University Press: New York, 1990, 633 pp.
Sugi, Y.; Matsuzaki, T.; Hanaoka, T.; Takeuchi, K.; Arakawa, H., Shokubai 1989, 31 (6), 373-376.
Sugi, Y., Kagaku Gijutsu Kenkyusho Hokoku 1990, 85 (8), 263-274.
Taniguchi, K., Methods for Preparation of Dimethylnaphthalene", Japan Patent 49-86350, 1974, pp.323-327.
Ueda, K.; Matsui, H.; Song, H.; Xu, W., J. Japan Petrol Inst. 1990, 33 (6), 413-417.
Verheyen, T.V.; Guy, P.J.; Felber, M.D.; Perry, G.J., Energia, University of Kentucky, 1991, 2 (3), p.1-4.
Verma, S.K., Carbon 1991, 29 (6), 793-803.
Vervalin, C.H., Hydrocarbon Processing 1991, 70 (11), p.35
Vogel, H.; Marvel, C.S., J. Polym. Sci. 1961, 50, 511.
Vogel, H.; Marvel, C.S., J. Polym. Sci. 1963, A 1, 1531.
Walker, P.L., Jr. "Review Article: Coal Derived Carbons". Carbon 1986, 24 (4), 379-386.
Walker, P.L., Jr. "Carbon: An Old but New Material Revisited". Carbon, 1990, 28, 261-279.
Weiss, R.A.; Ober, C.K. (Eds.) "Liquid-Crystalline Polymers". Am. Chem. Sym. Ser., 1990, No. 435, 32 chapters, 510 pp.
Yokono, T.; Obara, T.; Sanada, Y.; Shimomura, S.; Imamura, T., Carbon 1986, 24, 29.

Abbreviations

BPL:	4,4'-Biphenol (p,p'-biphenol)
4,4'-BDCA:	4,4'-Biphenyl dicarboxylic acid
4,4'-DAB:	4,4'-Dialkylbiphenyl
2,6-DAN:	2,6-Dialkylnaphthalene
ICI:	Imperial Chemical Industries
Lb:	Pounds (1 lb = 454 g)
LCP:	Liquid crystalline polymer
Kt:	Thousand tons (1 tons = 2204.6 pounds (lb))
Mlb:	Million pounds (1 Mlb = 453.59 tons)
MSC:	Molecular sieving carbon or CMS (carbon molecular sieves)
Mt:	Million tons (1 kg = 2.2046 lb)
2,6-NDCA:	2,6-Naphthalene dicarboxylic acid
sym-OHA:	1,2,3,4,5,6,7,8-Octahydroanthracene
sym-OHP:	1,2,3,4,5,6,7,8-Octahydrophenanthrene
PPO:	Polyphenylene oxide
PAR:	Polyarylate
PC:	Polycarbonate
PEEK:	Polyether ether ketone
PEN:	Polyethylene naphthalate
PET:	Polyethylene terephthalate
PBT:	Polybutylene terephthalate
p-HBA:	para-Hydroxy benzoic acid
PPTA:	Poly-p-phenylene terephthalamide (Du Pont's Kevlar LCP super-fibers)
PS:	Polysulfone
PSA:	Pressure-swing adsorption
PVCA:	Poly-N-vinylcarbazole
TPA:	Terephthalic acid
WI-MD:	Wilsonville middle distillates from catalytic two-stage coal liquefaction
3M:	Minesota Mining and Manufacturing

REPROCESSING OF USED TIRES INTO ACTIVATED CARBON AND OTHER PRODUCTS

Hsisheng Teng, Michael A. Serio, Rosemary Bassilakis,
Philip W. Morrison, Jr. and Peter R. Solomon

Advanced Fuel Research, Inc.,
87 Church Street
East Hartford, CT 06108

Keywords: Used Tires, Activated Carbon, Pyrolysis

ABSTRACT

The disposal of used tires generated each year in the U.S. by landfill is increasingly becoming an unacceptable solution. A better solution from an environmental and economic standpoint is to thermally reprocess the tires into valuable products such as activated carbon, other solid carbon forms (carbon black, graphite, and carbon fibers), and liquid fuels. In this study, a high surface area activated carbon (> 800 m^2/g solid product) was produced in relatively high yields from pyrolysis of tires up to 900°C, followed by activation in CO_2 at the same temperature. The surface area of this carbon is comparable with that of commercial activated carbon. The efficiency of the activation process (gain in specific surface area/loss in mass) was greatest when the pyrolysis was done on unground pieces of tire. This approach was found to give the best results for the preparation of activated carbon from used tires, with a total surface area production as high as 138 $m^2/(g$ original tire). Oxygen pretreatment of tires appears to increase both the yield and surface area of carbon produced from this system. High pressure treatment of tires at low temperatures (< 400°C) is an alternative approach if recovery of carbon black or fuel oils is the primary objective.

INTRODUCTION

The disposal of 280 million tires generated each year in the U.S. by landfill is increasingly becoming an unacceptable solution [1]. The tires take up large amounts of valuable landfill space and also represent a fire hazard. Recently, a large mountain of tires caught on fire in Canada with widespread environmental consequences due to the oils and gases generated from the decomposing tires. A better solution from an environmental and economic standpoint is to thermally reprocess the tires into valuable products [2]. The largest scale efforts employ tires either as a fuel [3] or as a filler for asphalt [4]. These two technologies consume about 5-6 million tires annually. However, tire burning has had repeated problems with feeding the tires and slagging, while the rubber asphalt costs 40% more than conventional material. An alternative is to reprocess the used tires into activated carbon and other solid carbon forms (carbon black, graphite, and carbon fibers), and liquid fuels. The key to producing such a product is controlling the chemistry of low temperature carbonization, which is the subject of this paper.

Pyrolysis has been widely used for converting solid fossil fuels, e.g. coal, into liquid and gaseous hydrocarbons, a process which results in a solid char residue. Coal pyrolysis has been extensively studied [5-7]. Used automotive tires contain polymeric aromatic structures which are similar to those of coal in some respects. Therefore, pyrolysis of waste tires to produce valuable products is currently receiving some attention. However, investigations of tire pyrolysis are rarely reported in the open literature.

The most commonly used vulcanized tire rubber is a styrene-butadiene-copolymer (SBR) containing about 25 wt.% styrene [8]. A typical composition for tire rubber is shown in Table 1. Also, a comparison of the structure and composition of tire rubber with that of a bituminous coal is shown

in Fig. 1. In most cases, tire pyrolysis studies were performed under inert conditions [8,9,10]. However, pyrolysis may be carried out in mildly oxidizing atmospheres, such as steam and carbon dioxide, to improve the quality of pyrolytic products [11,12,13].

Tire pyrolysis experiments have been conducted in the 500-900 C° range [8,9,11]. Similar to coal pyrolysis, the principal products from tire pyrolysis are gases, liquid oils and solid carbon residues. The following yields (as-received basis) of tire pyrolysis are typical: 33-38 wt.% char, 38-55 wt.% oil, and 10-30 wt.% gas. The product yields are affected by the pyrolysis conditions, such as pyrolysis temperature and heating rate. The literature work on the analysis of products from tire pyrolysis is summarized as follows:

Gas Analysis - Gases produced from tire pyrolysis are mainly hydrogen, carbon dioxide, carbon monoxide, methane, ethane and butadiene, with lower concentrations of propane, propene, butane and other hydrocarbon gases [8]. The temperature for the maximum evolution rate of each gas shifts to higher temperature levels as heating rate is increased. There was an increase in the total gas emission with heating rate and a corresponding decrease in oil yield [8]. Pyrolysis carried out in the presence of water increases the production of hydrogen and carbon monoxide [11]. This is thought to result from the occurrence of carbon gasification by steam, i.e., $C + H_2O \rightarrow CO + H_2$.

Oil Analysis - The yield of oil from tire pyrolysis is high (~50 wt % of initial tire rubber), reflecting the potential of tire rubber as a substitute for fossil fuel and chemical feedstocks. The oils have high aromaticity, low sulfur content, and are considered relatively good fuels [13]. The molecular weight range of the oils was up to 1600 with an average molecular weight in the 300-400 range [8]. The average molecular weight increases with increasing pyrolysis temperature and with decreasing heating rate. Infrared analysis of the oils indicated the presence of alkanes, alkenes, ketones or aldehydes, aromatic, polyaromatic and substituted aromatic groups [8]. An increase in pyrolysis temperature produced a decrease in the aliphatic fraction and an increase in the aromatic fraction [8]. Aliphatic hydrocarbons and alkylbenzenes are the major components of the oil if the pyrolysis is performed in the presence of water [11], and the average molecular weight of the aliphatic hydrocarbons was 164 and that of alkylbenzenes was 180. These average molecular weights are lower than the values for the oils from tire pyrolysis under an inert environment. This may indicate that the cracking of oil molecules during pyrolysis is promoted by the introduction of water.

The oil product from tire pyrolysis is a potential source of energy and chemicals. The oils may be used directly as fuel or added to petroleum refinery feedstocks [8]. The composition of the gasoline boiling fraction was reported to be comparable to that of petroleum gasoline [13]. The derived oils may also be an important source of refined chemicals, because it has been reported that they contain high concentrations of valuable chemical feedstocks, such as benzene, toluene and xylene [8].

Carbon Residue Analysis - The carbon residue would become a marketable product if its properties are similar to those of manufactured carbons. The simultaneous production of valuable solid products and gaseous and/or liquid fuels from what is currently a waste material would make tire pyrolysis economical if a large supply is readily available. This situation exists in many regions of the U.S.

Tire pyrolysis performed in an inert environment can produce 33-38 wt. % of carbon residue, as mentioned previously. It has been reported that the char yield increases with decreasing pyrolysis temperature and decreasing heating rate [8]. The surface area of the tire char also depends on pyrolysis temperature and heating rate. Williams et al. [8] reported that the surface area of the tire chars increases with both pyrolysis temperature and heating rate. However, Petrich [9] claims that chars prepared at too low of a temperature retain a large fraction of volatile material, resulting in lower surface areas, and those prepared at too high of a temperature tend to sinter and lose surface area. The surface area of a tire char produced by pyrolysis in an inert gas usually ranges from 30 to 90 m^2/g [8,9,11].

Basically, there are two uses of tire chars: as a reinforcing filler and an adsorbent. Usually commercial carbon black is used for filling polymers and vulcanizates. Use of the tire char as an end product for the tire and printing ink industries has been reported to be unsatisfactory [8,9]. This is due to the high ash content of the tire char. Chars from tire pyrolysis contain as much as 15 wt. % of ash, with the majority of this ash being zinc oxide [9]. A means of removing the ash from tire char is an important issue in the process of producing useful carbon black from waste tires.

Carbon as an adsorbent is usually evaluated by its surface area. Measurement of surface area can be obtained by a gas adsorption method, for example nitrogen BET. Tire chars which had not been activated served well in removing mercury compounds from aqueous solution [13]. As mentioned above, the surface area of tire char is in the range of 30-90 m^2/g, which is comparable with those of carbon blacks used in rubber products [8]. However, these values are too low for use of the char as activated carbon since commercial activated carbons have surface areas of around 1000 m^2/g [8,9,11]. Therefore, an activation process is required to produce activated carbon from tire char. Carbons can be activated by mild oxidation with steam or carbon dioxide at high temperatures to develop internal surface area. The slow gasification kinetics of carbons in steam or carbon dioxide allows gas molecules diffusing into the carbon micropores to create or enlarge micropores. The activation process usually follows hydrocarbon pyrolysis performed in an inert environment, but it is possible to accomplish pyrolysis and activation in one stage by pyrolyzing under mildly oxidizing conditions [11].

Torikai et al. [10] pyrolyzed tires at 550°C for 30 minutes and activated the granulated char with CO_2 at 900°C. They found linear relationships between activation time and burn-off, burn-off and surface area, and burn-off and Methylene Blue value (an adsorption test). This activated carbon had a surface area up to 400 m^2/g.

Ogasawara et al. [11] carried out the pyrolysis and activation of tires in one stage. In their study, water was continuously introduced to the sample with helium. The carbon residue from 1 hour steam activation at 900°C had a surface area of 1260 m^2/g, while pyrolysis in helium gave a char with a surface area of 87 m^2/g. The carbon residue produced from this "wet method" is as good as the commercial activated carbon in terms of surface area, but the carbon yield was only 9 wt. % of the starting tire.

In studies on coal liquefaction and pyrolysis [14,15], it has been found that oxygen functional groups, such as carboxyl and hydroxyl appear to play a major role in promoting the crosslinking reactions between molecules in coal. These crosslinking reactions are usually encountered at low temperatures (< 200°C) prior to the occurrence of bond cleavage in liquefaction or pyrolysis. A lot of effort has been devoted to the reduction of oxygen functions of coal in order to increase the liquid yield for coal liquefaction. Conversely, an increase of the oxygen functional group content would be expected to result in an increased char yield from pyrolysis of coal.

In the study of tire pyrolysis, some workers [10,11] have already produced high surface activated carbons from tire chars. However, the product yields of their systems were very low, and this is a serious drawback from economic point of view. Therefore, a method to increase the char yield from tire pyrolysis is one of the most important issues in making activated carbon from waste tires. Since the chemical structures in the tire rubber are similar to structures found in the coal, an increase of the oxygen functional group content in tires would be expected to promote the crosslinking reactions between tire molecules, and thus enhance the char yield in pyrolysis. In this study, oxygen pretreatment of tires was carried out prior to pyrolysis, and the results were compared to those without oxygen pretreatment.

High pressure treatment of coal under wet (steam) conditions, has been reported to allow the breaking of hydrogen bonds, loosening of the coal matrix and stabilization of some of the reactive components of the coal [16]. The extraction of oils from tires by supercritical or subcritical water was

studied by Funazukuri et al. [12]. Under the current study, a limited number of runs was done on low temperature, high pressure treatment of tires under wet or dry conditions to study the "self-liquefaction" of tires to recover the carbon black and provide liquid fuels simultaneously.

EXPERIMENTAL

There were two tire samples used in this investigation: granulated and non-granulated. The granulated sample was prepared by crushing and grinding a large piece of frozen tire under cryogenic conditions. The particle size of the sample was -50 mesh. The non-granulated sample was prepared by cutting the tire rubber into a fixed size of 170 $\pm$ 5 mg, unless otherwise specified.

Most of the tire pyrolyses were carried out in a TG-FTIR system under an inert (helium) or a mildly oxidizing (carbon dioxide) environment [17]. Tire char produced from a fixed-bed reactor under an inert environment was prepared to compare with that produced from the TG-FTIR system. Flash pyrolysis of tire was also performed in a wire-grid reactor with direct electrical resistance heating in helium. The heating rate was as high as 20,000°C/min.

Various treatments of the tires were investigated in order to improve the quality of products. The granulated sample was used for these treatments. The tire treatment procedures are briefly described as follows: 1) Oxygen pretreatment: Sample was kept in the air at 140°C for 15 days; 2) Wet high pressure treatment: Sample was treated with water in an autoclave at 4000 psig and 400°C for 30 min.; 3) Dry high pressure treatment: Sample was enclosed in a 3500 psig helium filled autoclave at 400°C for 30 min.

The gases evolved during pyrolysis can be quantitatively measured in the TG-FTIR system [17]. The liquid oil product was analyzed as KBr pellets in a Nicolet FT-IR. For quantitative analysis of the oil FT-IR spectra, a curve analysis program is employed to synthesize the IR spectra [18-21]. The quantitative data derived from the spectral synthesis gives a good quantitative determination for aliphatic, aromatic, ether, carboxyl and hydroxyl functional groups and a qualitative determination of alkanes and alkenes [18-21].

The solid residues produced under various pretreatment and pyrolysis conditions were subject to surface area measurements. The measurements were carried out using a dynamic, continuous method. A commercial instrument (Quantasorb, Quantachrome Corp.) was used to determine N_2 BET surface areas. Prior to surface area analysis, all samples were outgassed in a flow of nitrogen at 300°C for 1 hour. The N_2 surface area was determined at 77 K.

A scanning electron micrograph (SEM) with an x-ray analysis instrument was used in this study to investigate the surface structure and sulfur content of different samples.

Tire chars produced from pyrolysis were activated in a flow of CO_2/He mixture at 900°C. The CO_2 partial pressure during activation was fixed at 0.08 atmosphere, unless otherwise specified. The activated chars with various burn-offs were prepared and subject to surface area analysis.

RESULTS AND DISCUSSION

1. Tire Sample Analysis

The results of proximate and ultimate analyses of the granulated tire are shown in Table 2. Since the ash content shown in Table 2 is higher than for the unground sample and those reported in the literature [8,11], it was concluded that the granulated tire sample was accidentally contaminated in the grinding and/or sieving process. By SEM/x-ray analysis, the contamination was found to be mainly iron. The non-granulated tire sample, which was not contaminated, has an ash content around 2.9 wt.%. This

is similar to what has been reported previously for tires [8,11]. The ash free composition of the non-granulated tire sample is the same as that of granulated sample shown in Table 2. The samples were supplied by Prof. Mark Petrich of Northwestern University from a batch of shredded (used) truck tires.

2. Product Composition from Tire Pyrolysis

Gas Products - The typical product evolution data during granulated tire pyrolysis, starting from room temperature with a heating rate of 30°C/min up to 900°C, are shown in Fig. 2. The principal gases evolved are H_2O, CH_4, CO_2, CO, SO_2, C_2H_4, and NH_3. The total yield of gases and tars increases with temperature up to 650°C, after which there is no significant change in product yield. Tar is the major product of tire pyrolysis. It evolves mainly between 350 and 500°C.

The product evolution during the pyrolysis of the oxygen treated sample is shown in Fig. 3. It is of interest to notice, by comparison of Fig. 3 with Fig. 2, that the gas yields during pyrolysis were significantly increased by oxygen pretreatment, whereas the tar yields were reduced. The comparison of the product yields of these two samples is shown in Table 2. There was no surprise to see the enhanced evolution of H_2O, CO, CO_2 and SO_2 due to oxygen pretreatment, since oxygen would react with the components in the tire, and result in the increase of oxygen containing products from pyrolysis. However, the interpretation of the observations of the increased evolution of CH_4 and C_2H_2 and the reduced production of tars resulting from oxygen pretreatment is not as straightforward. It has been reported that oxygen plays a major role in crosslinking and cleavage of the network structure of coals [14,15]. Our results obviously revealed that oxygen pretreatment promoted the cleavage reactions for producing small molecules, such as CH_4 and C_2H_2, and the crosslinking between macromolecules in tires to reduce tar evolution, with a corresponding increased char yield (see below). This is a very beneficial result for tire carbonization process, since the char yield is significantly raised (see Table 3) due to the crosslinking between macromolecules, whereas the production of gaseous fuels, CH_4 and C_2H_2, is also promoted.

Liquid Products - The condensable liquid products (tars) are the major products of tire pyrolysis. The compounds found in tire pyrolysis oils have been identified as largely consisting of benzene, toluene, xylene, styrene, indane, indene, naphthalene, methyl naphthalenes, biphenyl, fluorene, pyrene, anthracene, phenanthrene and various other 3, 4, 5 and 6 ring polyaromatic hydrocarbons and aliphatic compounds, including alkanes and alkenes [8]. Since the compounds in the oil are too numerous and diverse to recognize quantitatively, functional group compositional analysis was used to more clearly reveal the properties of the oil. The FT-IR absorbance spectrum of the tire oil is shown in Fig. 4. As shown in Fig. 4, the aliphatic C-H stretching vibrations at 2930 and 2850 cm^{-1} and C-H deformation vibrations at 1350-1470 cm^{-1} indicate the presence of alkanes. The C-H stretching at 3000-3100 cm^{-1}, 1600 and 1500 cm^{-1} carbon-carbon stretching vibrations, C-H in-plane bending in the 1000-1100 cm^{-1} region, and 700-900 cm^{-1} (C-H out of plane bending) peaks indicate the presence of aromatic compounds. The C=O stretching vibrations at 1700 cm^{-1} indicate the presence of ketones or aldehydes. The 1630 and 990 cm^{-1} absorbance peaks are indicative of alkenes. The O-H stretching vibrations between 3200 and 3600 cm^{-1} indicate the presence of hydrogen-bonded alcohols or phenols. The C-O stretching in the 1060- 1300 cm^{-1} range indicates the presence of alcohols, ethers, and carboxylic acids. The quantitative functional group analysis of the oil based upon the absorbance spectra in Fig. 4 is summarized in Table 4. It is indicated in Table 4 that the oils formed are mostly aliphatic.

Solid Products - The solid residue yield varied with pyrolysis conditions. The product yields of tire pyrolysis in helium under different pyrolysis conditions are shown in Table 5. These results show that the char yield increases with decreasing pyrolysis temperature. This is consistent with the results of other workers [8,11,12]. Table 5 also shows an increasing char yield with increasing heating rate, and this trend is opposite to that reported by Williams et al. [8]. This disagreement is probably due to the absence of a holding period at the final pyrolysis temperature in our study, whereas there was at least two hours of holding time at final temperature in the work of Williams et al. [8].

Tire pyrolysis performed in a fixed bed reactor shows no effect in promoting char yield. However, it is of interest to note that the char yield from pyrolysis of granulated tires was enhanced roughly 26% by oxygen pretreatment, as revealed in Table 5. As mentioned previously, this char yield enhancement may be attributable to the crosslinking between macromolecules in tire rubber due to the formation of oxygen functional groups during oxygen pretreatment. Oxygen pretreatment (at 140°C for 88 hours) of non-granulated tires shows little effect in increasing char yield. This may be due to the fact that oxygen cannot access the interior part of a large size tire rubber to promote the crosslinking between the molecules of the tire, or the pretreatment time was not long enough.

Tire pyrolysis performed under a mildly oxidizing (CO_2) condition was investigated. The comparison of char yields of tire pyrolysis in helium and CO_2 is shown in Fig. 5. These results show that char yields were higher when pyrolysis is carried out under a mildly oxidizing condition. Again, the existence of CO_2 during pyrolysis may provide oxygen to enhance the crosslinking reactions between tire molecules, and, therefore, increase the char yield. Since crosslinking enhancement has been mainly accomplished in the period of oxygen pretreatment, therefore pyrolysis carried out in CO_2 gives much less effect in the promotion of char yield for oxygen pretreated tires. Pyrolysis of non-granulated tires in CO_2 shows no effect in promoting char yield. This may also be due to the fact that CO_2 cannot easily diffuse into the interior part of a large piece of tire rubber to enhance the crosslinking reactions.

Zinc and sulfur have been reported to be the major components of the ash in tire chars [8,11]. Fig. 6 shows zinc and sulfur in the internal section of the solid residue from the pyrolysis of non-granulated tires in CO_2, as measured by a SEM/X-ray microanalyzer. It shows, from the micrographs in Fig. 6, that zinc and sulfur grains are widely spread in the char and exist at the same locations, suggesting they are in a compound of zinc sulfide. Zinc sulfide is thought to be produced by the reaction between zinc oxide and the sulfur contained in tires [11].

Sulfur Distribution - Sulfur is used to cross link the polymer chains within the rubber. Therefore, due to environmental concerns, the emission of sulfur compounds from waste tire use has to be taken into account in the assessment of processes, such as tire pyrolysis, tire oil combustion, ..., etc. The distribution of sulfur in products after pyrolysis was investigated in this study. The sulfur contents of the gas and char from pyrolysis were determined by TG-FTIR and SEM/x-ray microanalysis, respectively. The quantity of sulfur contained in the liquid oil can be evaluated from the overall mass balance of sulfur of the tire pyrolysis. It is found that ~13% of tire sulfur is evolved in the gas phase ~9% is contained in the liquid oil, and ~78% is retained in the solid char. The results indicate that the sulfur within tire is preferentially retained in the char product after pyrolysis, since the char yield is typically 40% of the tire mass. This would imply that the cost of sulfur pollution control would be low in tire pyrolysis and for various uses of the tire oil.

High Pressure Treatments - High pressure treatment of automotive tires may hopefully result in the liquefaction of tire rubber and the recovery of carbon black. Table 6 presents the results obtained from wet and dry high pressure treatment of granulated tires. The overall mass balance is not 100% in Table 6. This deficiency in mass balance was also observed by Funazukuri *et al.* [12] in supercritical extraction of tire with water. The mass loss may be due to the evaporation of low boiling point oils during the process of product separation (separating solid and liquid). The product composition of wet and dry high pressure treatment are similar, and it shows roughly 35.9 $\pm$ 0.8 wt% solid residue, 45.4 $\pm$ 1.7 wt% oil, and 2.44 $\pm$ 0.89 wt% gas. The gaseous product is composed of CO_2, CO, C_2H_4, C_2H_6 and CH_4, and its composition is shown in Table 7.

The results in Table 7 indicate that CO_2 is the main component of the gaseous products. The FT-IR absorbance spectra of the oils from high pressure treatment of tire are shown in Fig. 7, and the results of quantitative functional group analysis are shown in Table 8. Fig. 7 and Table 8 reveal that the property of the oils from high pressure treatment of tire is similar to that from tire pyrolysis shown in Fig. 4.

The solid residues from high pressure treatment (wet or dry) of tire contain carbon black, solid hydrocarbons and ash. The above results show that high pressure (wet or dry) pyrolysis of tires at low temperatures (<400°C) is an alternative approach if recovery of carbon black or fuel oils is the primary objective. However, additional analysis is required of the solid material recovered in order to confirm this conclusion.

3. Surface Area Analysis

Unactivated Tire Chars - Fig. 8 shows the surface areas of the chars formed from the pyrolysis of the granulated tire sample in helium up to 500 and 700°C at a heating rate of 30°C/min., and up to 900°C at various heating rates. The surface areas can be seen to increase with pyrolysis temperature. This result is in agreement with that of Williams et al. [8]. This observation says that chars prepared at lower temperatures retain a higher fraction of volatile material, resulting in lower surface areas. On the other hand, it is revealed in Fig. 8, that the surface area decreases with heating rate, and this trend is opposite to that observed in the study of Williams et al. [6]. As mentioned previously, this disagreement may be due to no holding period at final temperatures in our study.

Pyrolysis of non-granulated tires in helium up to 900°C also produced a char with a surface area of 97 m^2/g. Surface areas of tire chars produced from the pyrolysis of both granulated and non-granulated tires in CO_2 were analyzed, and it shows no effect of CO_2 on the surface areas of char products. Pyrolysis of tires in a fixed bed reactor up to 700°C gave a char having a surface area of 79 m^2/g, showing no significant improvement on creating char surface area. The surface area of char formed from the pyrolysis of O_2 pretreated tires in helium up to 900°C was measured, and it was found that the surface area of O_2 treated tire char was as high as 179 m^2/g, which is almost twice as much as that of char from tires without any pretreatment under identical pyrolysis condition. Also, in the previous section, it showed that pyrolysis of O_2 treated tire gave the highest char yield. Therefore, considering both surface area and char yield, O_2 pretreatment of tires is very beneficial in producing high total surface area (in units of m^2/(g tire)) carbon.

Fig. 9 shows the scanning electron micrographs of chars formed from pyrolysis of O_2 treated tires and tires with no pretreatment. It shows that the O_2 treated tire char has a very rough and dented surface, indicating that crosslinking or polymerization between rubber molecule and carbon black was enhanced by O_2 treatment and, therefore, the rubbers could not be totally volatilized during pyrolysis. On the other hand, the char from tires without any treatment shows a very smooth surface, indicating that most of the rubbers were volatilized during pyrolysis and the solid residue contains mainly carbon black and ash. The difference of char surfaces shown in Fig. 9 explains the higher surface area and yield of char produced from O_2 treated tires.

The above results show that the surface areas of chars formed from tire pyrolysis are comparable with the surface areas of carbon blacks in rubber products, including tires [7]. However, use of the char as activated carbon is not possible since commercial activated carbon has a higher surface area. An activation process is thus required for producing activated carbon from tire chars.

Activated Tire Chars - The surface areas of tire chars activated in CO_2 for various extents of burn-off are summarized in Table 9. It shows that the surface areas of tire chars increase monotonically with char burn-off, and pyrolysis conditions (including pyrolysis temperature, heating rate and gas environment) have little effect on the ultimate surface areas of activated tire chars. For granulated samples, similar to the results of unactivated chars, the O_2 treated tire chars gave the highest surface areas, ie., up to 370 m^2/g at 50% burn-off.

Table 9 shows that non-granulated samples gave much higher surface areas than the granulated. This can be attributable to the higher ash contents of granulated samples, since the surface area of ash is very low (8.6 m^2/g). Having the value of ash surface area and the ash content allows us to calculate the specific surface area of dry ash free (d.a.f.) char. The calculated values for d.a.f. chars are also shown in Table 9. Table 9 reveals that the surface areas of granulated samples in terms of

daf mass are comparable to those of non-granulated samples. This is reasonable, since they were all derived from the same material.

For non-granulated samples, there was little size effect on surface areas of the activated chars, as revealed in Table 9. O_2 pretreatment of tires indeed increase the surface area of activated non-granulated char, but not as significantly as in the case of the granulated sample. Table 9 also shows that the surface area of non-granulated char was increased by performing activation under a higher partial pressure of CO_2. Similar behavior was also reported for tire char activation in steam [11].

Torikai et al. [10] produced activated carbon from automotive tires by pyrolysis of the samples in an inert environment and activating the solid residue in a stream of CO_2 at 900°C. This activated carbon had surface areas of up to 400 m^2/g at 80% burn-off. Ogasawara et al. [11] prepared activated carbon from automotive tires from a wet thermal decomposition, and a 1260 m^2/g of carbon residue is obtained, however, with a yield of only 9 wt.% of the original tire sample. The total surface area of their product is 113 m^2/(g tire). In our study, 813 m^2/g of activated carbon was produced with a yield of 17 wt.% of the original tire sample. The total surface area of this activated carbon was up to 138 m^2/(g tire), a 20% increase when compared to the results of Ogasawara et al. [11]. This improvement could be partly due to differences in the starting tire samples.

The total surface area in units of m^2/(g tire) is actually a measure of activation (or burn-off) efficiency for producing activated carbon from tires. Fig. 10 shows the values of total surface area at various char burn-off. It shows no significant change with burn-off for granulated sample, indicating a low activation efficiency at higher burn-off. However, the total surface area of non-granulated sample increases significantly with carbon burn-off, indicating that the activation efficiency is high for this case. The reason for the better activation results for the char derived from larger tire pieces is not known. Since pyrolysis occurs from the outside of the particle to the center, a char layer will progressively move inward for larger pieces as the pyrolysis becomes less isothermal. This phenomenon may affect the development of the char morphology which in torn will affect how the material response to the activation process. This will be the subject of additional research.

CONCLUSIONS

1. Pyrolysis of granulated and non-granulated tires has shown recoveries of gases, liquid oils and solid char. The product yields vary with the variation of pyrolysis condition and pretreatment. The total yield of gases and tars increases with temperature up to 650°C, after which there is no significant change in product yield. The main gases evolved are H_2O, CH_4, CO_2, CO, SO_2, C_2H_4, and NH_3. The derived oils are mostly aliphatic. The char yield increases with decreasing pyrolysis temperature and increasing heating rate. The char yield was found to be increased by performing pyrolysis under mildly oxidizing conditions, especially in the case of granulated tires. Both the gas and char yields of tire pyrolysis were increased by oxygen pretreatment, whereas the oil yield was reduced.

2. The sulfur within tires is preferentially retained in the char product after pyrolysis. This is an advantage for tire pyrolysis versus tire incineration, since the cost for sulfur emission controls would be low.

3. High pressure treatment of tires at low temperatures (<400°C) is an alternative approach if recovery of carbon black or fuel oils is the primary objective.

4. The surface area of tire char is shown to increase with pyrolysis temperature and decrease with heating rate. O_2 pretreatment of tire shows beneficial results in promoting both char yield and surface area in tire pyrolysis, especially for granulated tires. The surface areas of tire chars are comparable with those of carbon blacks in rubber products, but too low if compared with that of commercial activated carbon. Therefore, an activation process is required for producing activated carbon from tire chars.

5. For production of a high specific surface area char directly from tire pyrolysis, the best results were obtained by O_2 pretreatment of granulated tires (~200 m^2/g). However, in order to produce a commercial grade activated carbon an activation process is required and the efficiency of the activation process is best when non-granulated tire pieces are used. At 50% burnoff, specific surface areas close to 1000 m^2/g (daf basis) were achieved in both cases. However, the net yield of activated carbon was significantly higher when starting with non-granulated tires. This is beneficial from an economic standpoint since the grinding costs are lower.

ACKNOWLEDGEMENTS

The financial support of the National Science Foundation under Grant No. ISI-9060297 is gratefully acknowledged. The Project Officer was Dr. Edward Bryan. The authors also acknowledge helpful discussions with Prof. Mark Petrich of Northwestern University, who supplied the tire samples, and the assistance of Prof. Eric Suuberg of Brown University with surface area analysis of the samples.

REFERENCES

1. New York Times, May 9, 1990, p. D1.
2. Schulman, B.L. and White, P.A., "Pyrolsis of Scrap Tires using the Tosco II Process -a Progress Report", Solid Wastes and Residues: Conversion by Advanced Thermal Processes, (J.L. Jones and S.B. Radding, Eds.), ACS Symposium Series #76, 1978, p. 274.
3. Oxford Energy Corporation, Modesto,CA.
4. Rubber Asphalt Producers, Phoenix,AZ.
5. Solomon, P.R., Hamblen, D.G., Carangelo, R.M., Serio, M.A., and Deshpande, G.V., Energy and Fuel, 2, 405, (1988).
6. Serio, M.A., Hamblen, D.G., Markham, J.R., and Solomon, P.R., Energy and Fuels, 1, 138 (1987).
7. Suuberg, E.M., Peters, W.A., and Howard, J.B., 17th Symp. (Int) on Combustion, The Combustion Institute, Pittsburgh, PA, 1979, p. 117.
8. Williams, P.T., Besler, S., and Taylor, D.T., Fuel, 69, 1474 (1990).
9. Petrich, M.A., "Conversion of Plastic Waste to Valuable Solid Carbons", Final Report of a Project in the Innovative Concepts Program, U.S. DOE, Jan., 1991.
10. Torikai, N., Meguro, T., and Nakamura, Y., Nippon Kagaku Kaishi, 11, 1604 (1979).
11. Ogasawara, S., Kuroda, M., and Wakao, N., Ind. Eng. Chem. Res., 26, 2552 (1987).
12. Funazukuri, T., Takanashi, T., and Wakao, N., J. Chem. Eng. Japan, 20 23 (1987).
13. Merchant, A. and Torkelson, J.M., "Pyrolysis of Scrap Tires", Chemical Engineering Dept., Northwestern U., Spring, 1990.
14. Serio, M.A., Solomon, P.R., Kroo, E., Bassilakis, R., Malhotra, R., and McMillen, D.F., ACS Div. of Fuel Chem. Prepr., 35, (1), 61, (1990).
15. Serio, M.A., Solomon, P.R., Kroo, E., and Charpenay, S., ACS Div. of Fuel Chem., Prepr., 36, (1), 7 (1991).
16. Bienkowski, P.R., Narayan, R., Greenkorm, R.A., and Choa, K.W., I&EC Res., 26, 202&206(1987).
17. Carangelo, R.M., Solomon, P.R. and Gerson, D.J., "Application of TG-FTIR to Study Hydrocarbon Structure and Kinetics", Fuel, 66, 960 (1987).
18. Solomon, P.R., Hamblen, D.G. and Carangelo, R.M., ACS Symp. Series, 205, Coal and Coal Products: Analytical Characterization Techniques, Washing., DC (1982), pg. 77.
19. Solomon, P.R., Hamblen, D.G. and Carangelo, R.M., Analytical Pyrolysis of Coal Using FT-IR, 5th Int. Symp., on Analytical Pyrolysis, Colorado (1982).
20. Solomon, P.R. and Carangelo, R.M., Fuel, 61, 663 (1982).
21. Solomon, P.R. and Carangelo, R.M., Fuel, 67, 949 (1988).

Table 1. Composition of Tire Rubber [8,11]

Component	wt.% (as-received)
SBR	60 - 65
Carbon Black	29 - 31
Zinc Oxide	1.9 - 3.3
Sulfur	1.1 - 2.1
Extender Oil	~2
Additives	~0.7

Table 2. Composition of a Granulated Tire Sample.

Proximate Analysis (wt.%) (as-received)		Ultimate Analysis	
Moisture	0.4		
Volatile Matters	63.6	C, wt.% d.a.f.	88.1
Fixed Carbon	22	H, wt.% d.a.f.	7.9
Ash	14	N, wt.% d.a.f	0.5
		S, wt.% d.a.f.	2.1
TOTAL	100	O, wt.% d.a.f.	1.4

* Supplied by Huffman Laboratories (Wheat Ridge, CO).

Table 3. Product Yields From Pyrolysis of Tires and O_2 Treated Tires in an Inert Environment.

	weight % (as received)								
	H_2O	CO_2	CO	CH_4	C_2H_4	SO_2	NH_3	Tars*	Char
Granulated Tires	3.5	0.6	1.5	0.36	0.089	0.31	0.38	57	36
O_2 Treated Granulated Tires	5.3	3.3	3.3	1.2	0.24	1.0	0.21	39	45

* Estimated from mass balance

Table 4. Functional Group Analysis of Liquid Oils Formed from Tire Pyrolysis.

weight % (dmmf)								
Hydrogen		Aromatic Hydrogen			Carbon	Oxygen		
H_{al}	H_{OH}	1 Adj	2 Adj	3 or more	(Aliphatic)	$O_{Carbonyl}$	O_{OH}	O_{ether}
13	0.045	0.44	0.44	0.40	81	0.84	0.75	0.58

Table 5. Product Yields (as-received basis) from Tire Pyrolysis in Helium Under Different Conditions

PYROLYSIS CONDITIONS								
Temp (°C)	Ramp (°C/min)	Pressure (atm)	Size	Reactor	Pretreat	Char Yield (%)	Gas (%)	Oil[+] (%)
500	30	1	granu.	TG	—	40	4.7	56
700	30	1	granu.	TG	—	38	5.6	57
900	20,000	1	granu.	Wire-Grid	—	38	—	—
900	100	1	granu.	TG	—	37	6.8	56
900	30	1	granu.	TG	—	36	7.0	57
900	3	1	granu.	TG	—	35	7.4	57
900	30	1	granu.	TG	Oxygen	45	15	39
700	30	1	granu.	Fixed Bed	—	37	—	—
900	30	1	non-granu.	TG	—	34	3.8	62
900	30	1	non-granu.	TG	Oxygen	35	—	—

[+] Estimated from mass balance.

Table 6. Product Yields (as-received basis) of High Pressure Treatment of Tires.

	Solid (%)	Liquid (%)	Gas (%)	Mass Balance (%)
Wet	36.6	43.7	3.32	83.6
Dry	35.1	47.0	1.55	83.7

Table 7. The Gaseous Product Composition (by volume) from High Pressure Treatment of Tires

	CO_2 (%)	CO (%)	C_2H_2 (%)	C_2H_6 (%)	CH_4 (%)
Wet	90.6	—	2.9	3.8	2.6
Dry	60.3	8.7	9.0	13.5	8.5

Table 8. *Functional Group Analysis of Liquid Oils Formed from High Pressure Treatments of Tires.*

	weight % (dmmf)								
	Hydrogen		Aromatic Hydrogen			Carbon	Oxygen		
	H_{al}	H_{OH}	1 Adj	2 Adj	3 or more	(Aliphatic)	$O_{Carbonyl}$	O_{OH}	O_{ether}
Wet	13	0.045	0.18	0.37	0.40	76	1.0	0.75	0.65
Dry	13	0.040	0.14	0.38	0.40	80	0.79	0.65	0.23

Table 9. Surface Areas of Tire Chars and Activated Tire Chars

SUMMARY OF RESULTS														
PYROLYSIS CONDITIONS								SURFACE AREA						
								M^2/g (as-received)			M^2/g,daf (daf)			
Temp °C	M °C/min.	Press ATM	Size	Gas	Reactor	Pretreat	Char Yield[a] (%)	0%	30%	50%	0%	30%	50%	
500	30	1	P	He	TG	—	40	41	135	—	58	261	—	
700	30	1	P	He	TG	—	38	69	134	—	104	273	—	
900	20000	1	P	He	Wire-Grid	—	38	57	—	293	85	—	1089	
900	100	1	P	He	TG	—	37	85	117	—	131	245	—	
900	30	1	P	He	TG	—	36	99	124	188	157	268	815	
900	30	1	P	CO_2	TG	—	37	78	—	185	120	—	734	
900	3	1	P	He	TG	—	35	98	125	—	158	280	—	
900	30	1	P	He	TG	O_2	45	179	252	357	256	447	930	
900	30	1	P	CO_2	TG	O_2	45	—	—	365	—	—	952	
700	30	1	P	He	Fixed Bed	—	37	79	126	—	122	264	—	
900	30	1	L	He	TG	—	34	97	—	732	105	—	882	
900	30	1	L*	CO_2	TG	—	34	113	423	703	123	481	847	
900	30	1	L	CO_2	TG	O_2	35	—	—	793	—	—	952	
900	30	1	L	CO_2+	TG	—	34	—	—	813	—	—	980	

[a] As-received basis. * Smaller piece of non-granulated tire (10 mg). + Higher CO_2 partial pressure (1 atm).

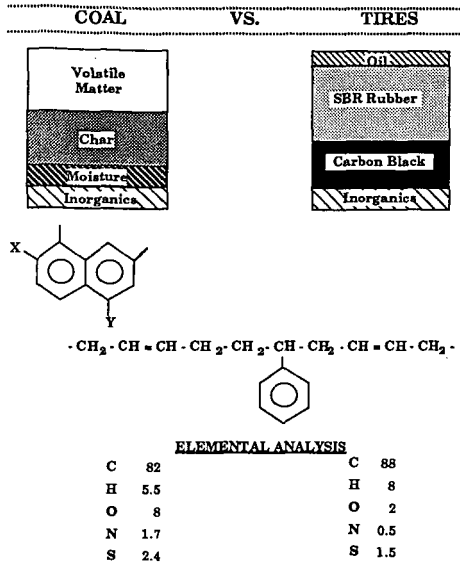

Figure 1. Comparison of Structure and Composition Between Coal and Tire Rubber.

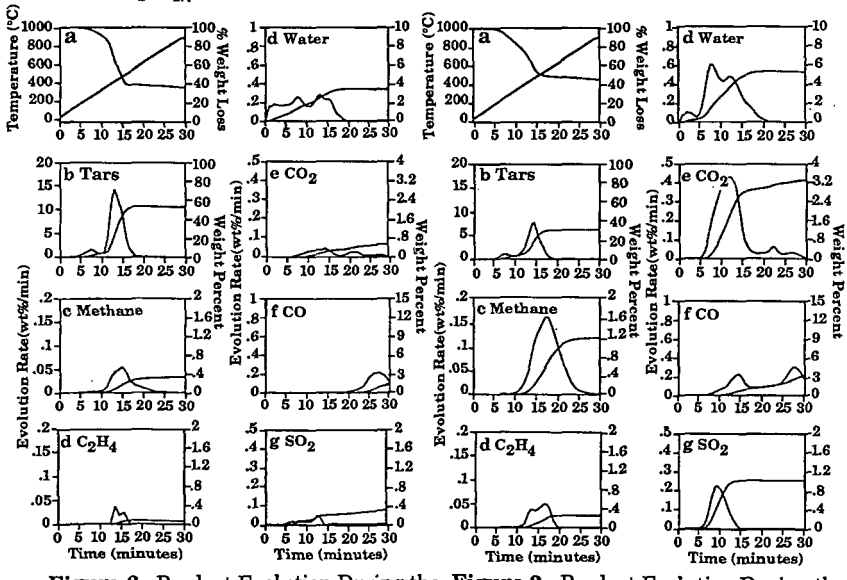

Figure 2. Product Evolution During the Pyrolysis Cycle of Granulated Tires.

Figure 3. Product Evolution During the Pyrolysis Cycle of the Oxygen Pretreated Tires.

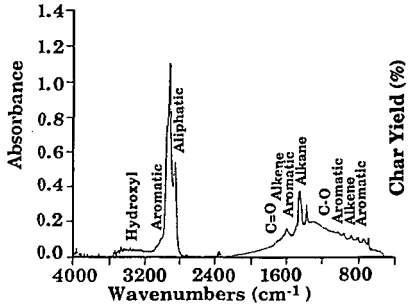

Figure 4. FT-IR Absorbance Spectrum of the Oils from Tire Pyrolysis.

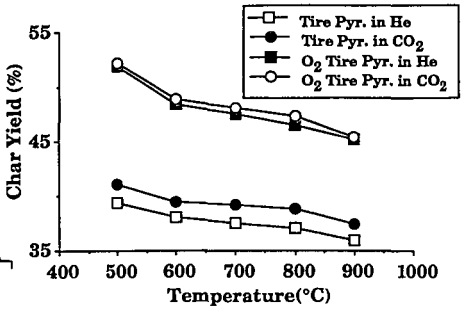

Figure 5. Comparison of Char Yields of Tire Pyrolysis in Helium and CO_2.

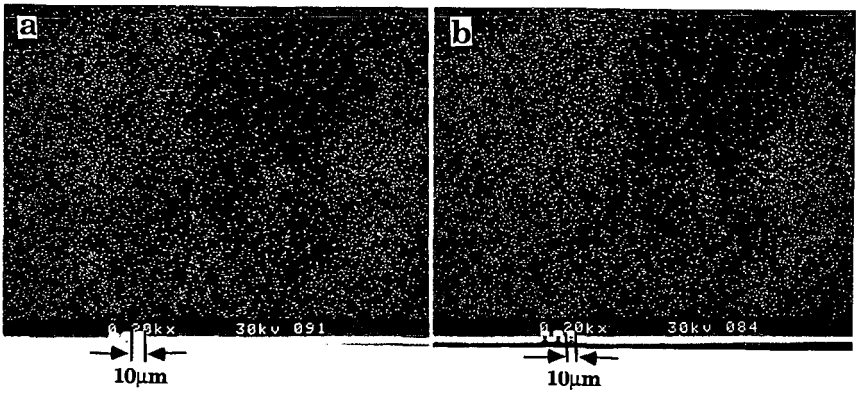

Figure 6. SEM/X-Ray Microanalysis of Zinc and Sulfur in a Carbon Residue. a) Zinc; b) Sulfur.

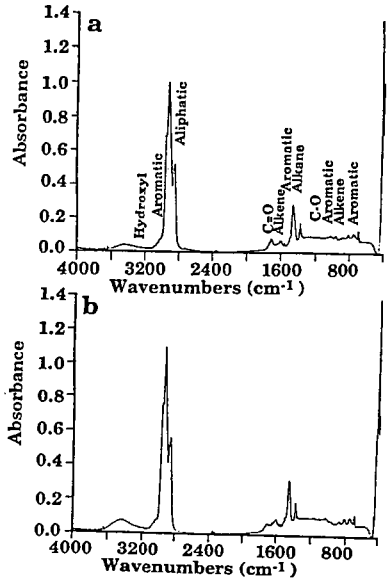

Figure 7. FT-IR Absorbance Spectra of Oils from High Pressure Treatments of Tires. a) Wet Process; b) Dry Process.

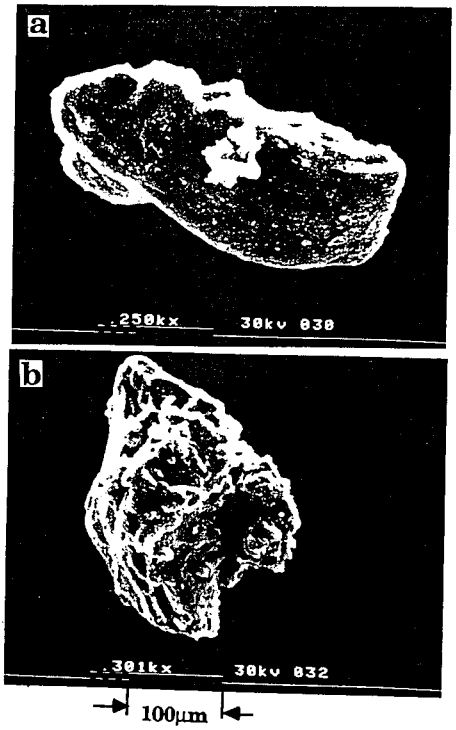

Figure 9. Scanning Electron Micrograph of 900°C Tire Chars from Tires. a) Without Pretreatment; b) Treated with Oxygen.

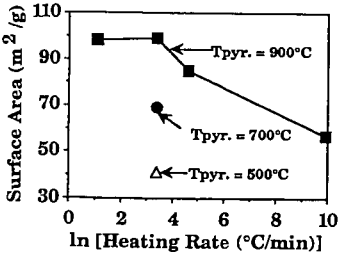

Figure 8. Surface Areas of Chars Formed from Different Pyrolysis Conditions.

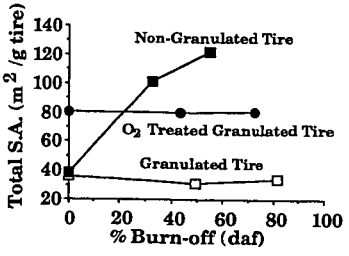

Figure 10. Total Surface Areas of Tire Chars at Various Extents of Carbon Burn-off.

ACTIVATED CARBONS FOR THE REMOVAL OF NITRIC OXIDES

S. N. Ahmed, J. Stencel, F. Derbyshire and B. Baldwin*
Center for Applied Energy Research, University of Kentucky,
3572 Iron Works Pike, Lexington, KY 40511; *Colorado School
of Mines, Golden, CO 80401.

Keywords: Activated Carbon, Nitric oxide, and Reduction

INTRODUCTION

Nitrogen oxide (NOx) emissions from stationary and mobile sources are precursors to acid precipitation, are important in the formation of ozone during interaction with hydrocarbons, and have been implicated as intermediates in greenhouse gas formation. The amount of NOx emitted is distributed nearly equally between transportation, industry and power generation (1). For stationary sources, the recent Title III federal legislation will restrict NOx emissions to levels of approximately 0.45 lb/MM Btu. As a result, it is anticipated that many coal fired power sources will be required to install some type of post combustion clean-up equipment to reduce NOx emissions.

One of the commercially available technologies that has been used to control NOx is selective catalytic reduction (SCR) using NH_3 as a reductant over oxide supported catalysts. It is called selective because with O_2 in the combustion flue gas, the following reactions are possible:

$$4\,NH_3 + 6\,NO \longrightarrow 5\,N_2 + 6\,H_2O \qquad (1)$$

$$4\,NO + 4\,NH_3 + 3\,O_2 \longrightarrow 4\,N_2 + 6\,H_2O \qquad (2)$$

$$4\,NH_3 + 5\,O_2 \longrightarrow 4\,NO + 6\,H_2O \qquad (3)$$

Reactions (1) and (2) are desired where as nonselective Reaction (3) would cause NO to be produced.

Currently, SCR technology using metal oxide catalysts has an optimum reaction temperature between 350-450^{0}C. This range places restrictions on locating the catalyst bed for flue gas treatment in coal fired units. For example, if the catalyst bed is placed before the particulate and the sulfur oxide clean-up equipment, the flue gas temperature would be within the desired range but the catalyst life would be reduced because of high concentrations of particulates and catalyst poisons (2,3). If the catalyst bed is placed after the clean-up equipment, an additional source of heating is required to reheat the flue gas to a desired temperature.

To investigate catalysts for alternative lower temperature NOx decomposition, we have initiated studies on the use of activated carbons and their modification. To date, these studies have concentrated on commercially available carbons and on comparisons with commercially available V_2O_5/TiO_2.

EXPERIMENTAL

A schematic diagram of the overall experimental setup is presented in Figure 1. Gas flow rates were controlled by Tylan model FC-280 mass flow controllers. Each stream was filtered through a 0.5 micron sintered metal filter before entering the flow controller. After passing through a block valve and a check valve, the gases entered the mixing chamber which was made up of a 2.54 cm od stainless steel pipe filled with 3 mm glass balls. This arrangement allowed a thorough mixing of gases before entering the reactor vessel. The reactor vessel was a 1.9 cm od stainless steel tube with a 1.22 cm id and was 30.45 cm in length. The catalyst bed was sandwiched between glass wool plugs which were supported by 3 mm glass beads. The reactor was enclosed in a tube furnace. After passing through the reactor, the product stream was analyzed by a non-dispersive infrared CO_2 detector, a chemiluminescence NO/NOx detector and mass spectrometer.

Four commercial samples, originating from three different precursors have been obtained for this investigation. Their origins and surface areas are presented in Table I. Three of these samples (labelled SP1, SP2 and SP3) will be discussed here. They were used in a powdered form (50 - 100 mesh) and have characteristics shown Table II.

In the test runs, the temperature was varied from 100-300°C, the total gas flow rate was 1000 SCCM, and the catalyst weight was 3 g. An emphasis was placed on using the conditions similar to that of flue gas generated from power plants; hence, the NO and NH_3 concentrations were 700 ppm and O_2 was 4%. Prior to each test run, samples were heated for four hours at 300°C under a helium flow. For comparisons, a commercially prepared V_2O_5/TiO_2 catalyst was tested under the same conditions.

The pH of the samples was obtained using a standard procedure in which 3 g of the sample was mixed with 60 ml of distilled water and heated at 100°C for three minutes. The solution was then filtered, allowed to cool to room temperature, and its pH was measured.

RESULTS AND DISCUSSION

Figure 2 shows the NO conversion for the three samples as a function of temperature. SP1, which was produced from coal, had the highest activity and SP3, which was produced from peat, had the lowest activity. All samples showed a decrease in activity between 120°C and 200°C.

The NO conversion did not correlate with BET surface area, as shown in Figure 3. SP1 showed the highest activity but had the lowest surface area. Similarly, there was no correlation between pore volume and activity. Rather, NO conversion activity correlated inversely with pH and ash content, as displayed in Figure 4 and Figure 5. SP1, which had the lowest pH, showed the highest activity. This trend implies that a more acidic surface would maximize activity. The inverse correlation obtained for activity and ash contents of the samples might complement the inverse correlation between pH and activity. However, the mineralogy of the carbons have not been examined to define the influence of the ash on pH.

To examine further whether pH affects activity, SP3 was washed with distilled water for 24 hrs to reduce its pH from 9.55 to 8.23. This washing increased its activity at temperatures above 100°C (see Figure 6); no increase occurred at 100°C. This may imply that two conversion mechanisms are operative. One dominant at low temperatures and the other prevalent at higher temperatures.

The oxygen content of the carbons also was observed to correlate with activity. For example, as shown in Figure 7, SP1, which had the highest oxygen content, showed the highest activity. Hence, oxygen plays an important role in NO conversion. Perhaps, the amount of oxygen in the sample indicates the presence of acidic surface oxides, which decrease the sample's pH. SP1, which had the highest oxygen content, also had the lowest pH.

SP1 was also tested for the nonselective formation of NO by reacting NH_3 with O_2 in the absence of reactant NO (Reaction (3)). NO was not formed, thus suggesting that activated carbons promote NO reduction. In absence of reactant or gas phase oxygen, NO conversion was negligible.

A comparison of NO conversion activity for SP1 and V_2O_5/TiO_2 is shown in Figure 8, At low temperatures around 100°C, SP1 proved to be a better catalyst than V_2O_5/TiO_2. However, at temperatures higher than 150°C, V_2O_5/TiO_2 was more active than SP1.

SP3, which had shown the lowest activity, was further treated with sulfuric acid. Initial results have shown that its activity increased considerably. This could probably be due to the oxidation of the surface thus creating acidic functional groups on the surface. This possibility is under further investigation.

CONCLUSIONS

Activated carbons are potentially good catalysts for NO reduction. Low pH, activated carbons have higher activity for NO reduction implying that activated carbons which are acidic in nature are better catalysts for NO reduction. A higher oxygen content in the activated carbons increases their activity., whereas gas phase oxygen

is needed for NO conversion. Activated carbons can have a higher activity than V_2O_5/TiO_2 at low temperatures around 100°C.

REFERENCES

1) F. P. Boer, L. L. Hegedus, T. R. Gouker, K. P. Zak, Chemtech, 312, May (1990).
2) H. Gutberlet, VGB Kraftwerkstech, 68, 287 (1988).
3) I. S. Nam, J.W. Eldridge and J. R. Kittrell, I & EC Prod. Res. Dev., 25, 192 (1985)

TABLE I. SAMPLE'S BET SURFACE AREA

SAMPLE	PRECURSOR	BET SURFACE AREA m^2/g
SP1	Coal	466
SP2	Peat	1110
SP3	Coconut Shell	739
SP4	Peat	791

TABLE II. ULTIMATE AND PROXIMATE ANALYSIS

SAMPLE	C%	O%	H%	N%	S%	ASH%
SP1	91.54	4.77	0.47	1.17	0.70	2.05
SP2	91.55	3.87	0.17	0.54	0.46	3.44
SP3	91.54	2.55	0.46	0.51	0.02	4.92

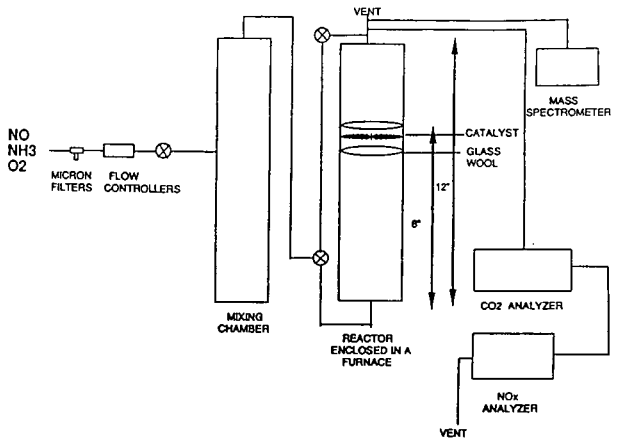

FIGURE 1. PROCESS FLOW DIAGRAM

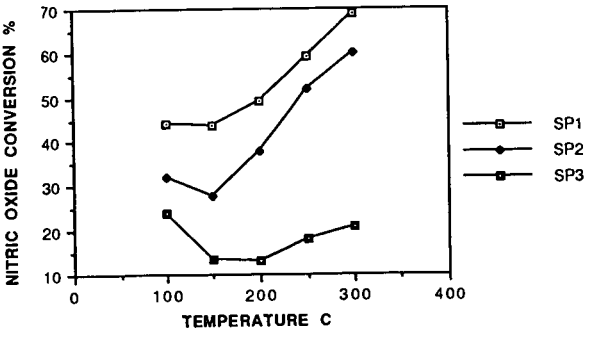

FIGURE 2. NO CONVERSION AT VARIOUS TEMPERATURES

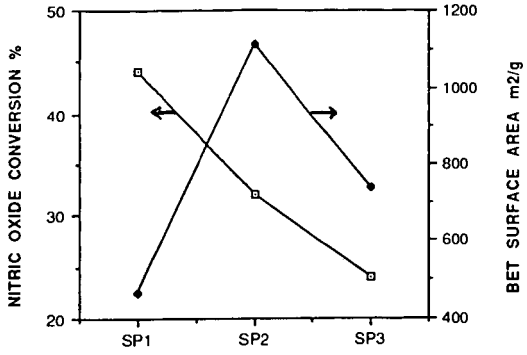

FIGURE 3. ACTIVITY (100C) VS BET SURFACE AREA

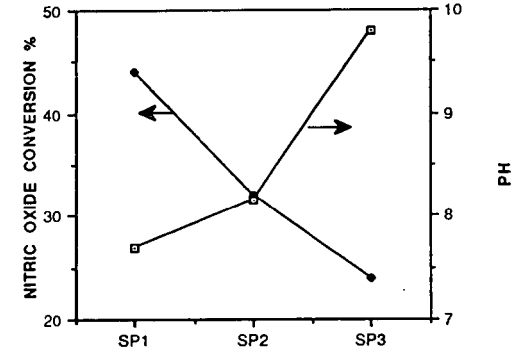

FIGURE 4. ACTIVITY (100 C) VS pH

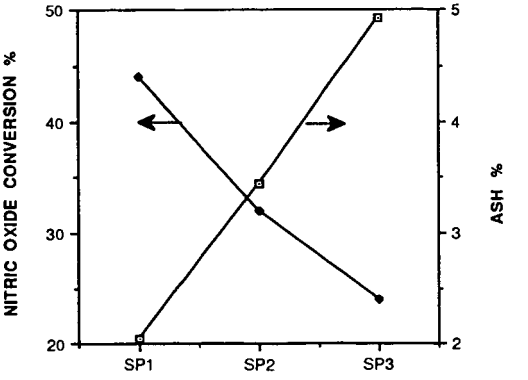

FIGURE 5. ACTIVITY (100C) VS ASH CONTENT

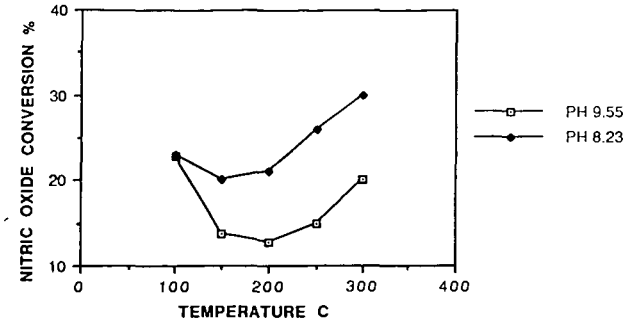

FIGURE 6. EFFECT OF pH ON THE ACTIVITY

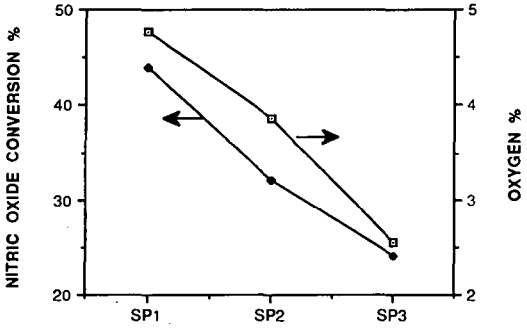

FIGURE 7. ACTIVITY (100 C) VS OXYGEN CONTENT

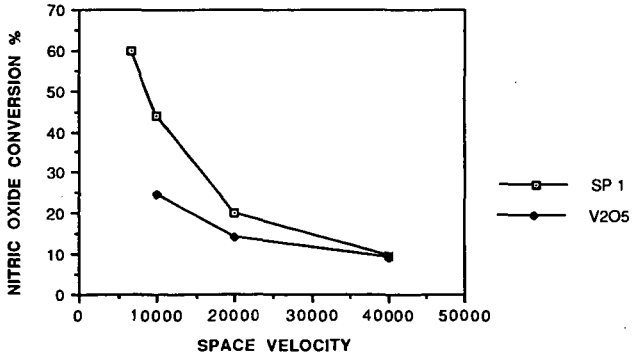

FIGURE 8. COMPARISON OF SP 1 AND V205/TiO2 (100C)

OXIDIZED COAL CHAR AS A CATALYST: I. CHARACTERIZATION

C.W. Kruse, M.I.M. Chou, C. Feizoulof
Illinois State Geological Survey, Champaign, IL 61820

M. Fatemi, P. Beaulieu, and J. Schreiner
Amoco Corporation, Amoco Research Center, P.O. Box 3011 Naperville, IL 60566-7783

Keywords: coal, mild gasification, char, oxidized char, catalyst

ABSTRACT

Oxidizing the surface of carbonaceous materials at 500° C to 700° C in air was shown in the 1960s (1-3) to produce an excellent dehydrohalogenation catalyst. One goal of the current research was to prepare this catalyst from an activated mild gasification coal char having good sorptive properties, test its activity as a catalyst for other elimination reactions, and characterize the catalyst and its precursors. The pore surface area (nitrogen adsorption/desorption, BET) of a mild gasification (MG) coal char was raised from <5 to 475-580 m^2/g by steam gasification at 870° C and the catalyst properties were imparted by controlled oxidation with 10% O_2/90% N_2 at 450° C. This material catalyzed not only dehydrochlorination but also dehydration and deamination reactions. Samples of the original coal and final oxidized activated char, as well as two intermediate samples (MG char and steam activated MG char) were fully characterized using Proximate and Ultimate Analysis, Inductively Coupled Plasma Analysis, X-Ray Diffraction, Nitrogen (BET) Surface Area, X-ray Photoelectron Spectroscopy, Diffuse Reflectance IR Spectroscopy, and Scanning Tunneling Microscopy.

INTRODUCTION

Gasification of coal under mild conditions produces char, coal-derived liquids and some gases. Economic viability of this approach to coal utilization is unquestionably dependent on the marketability of the char. To have a reasonable impact on coal utilization via mild gasification, any market considered for the char must be large and should have a projected price greater than coal's fuel value. The activated carbon market has the required price structure, more than $1000/ton for a high quality product, and a potentially large volume. Activated carbon is used not only for air and water purification but also for cleanup of nonaqueous solutions or suspensions. More than 300 chlorinated organic compounds have been identified in chlorinated potable waters, cooling waters, and sanitary effluents. Systems are needed which will trap and destroy unwanted organic compounds, both those occurring in industrial streams and those that are introduced into drinking water by chlorination.

Carbonaceous materials were converted in the 1960s to effective dehydrochlorination catalysts by heating material, like char, to 500° C to 700° C in air. Some of these catalysts produced linear olefins from chlorinated n-alkanes with little rearrangement of the carbon skeleton. Other dehydrochlorination catalysts studied later were also effective for producing olefins from alcohols and amines by elimination of water and ammonia, respectively (4-8). Oxidized activated char might have the capacity not only to adsorb waste molecules from a variety of streams, but also to catalyze chemical transformations of the unwanted adsorbed compounds into more manageable or even useful chemicals. This work was undertaken to better characterize and define the properties and methods for making the oxidized char catalyst.

MATERIALS AND METHODS

Char preparation and activation - The mild gasification char was prepared in a pilot-scale, fixed-bed reactor at United Coal Co. (UCC), Bristol, Virginia, from a Herrin (Illinois No. 6) coal, IBC-103 in the Illinois Basin Coal Sample Program. This char was from a previous study on the burning behavior of partially devolatilized coal as a function of the amount of volatile matter (VM) in the char (9). Stepwise grinding and sieving of a composite of material having 11% and 15% VM produced 13.5 pounds of 10x30 mesh

particles, a size comparable to commercial granular activated carbon. This UCC char composite was subjected to additional pyrolysis in a 2.5-cm ID, batch, fluidized-bed reactor (FBR) (200-gram increments, N_2 gas, heated to 500° C at 20 C°/min) to drive off most of the VM. The pyrolyzed product is designated MG Char.

The FBR was used both for improving the porosity by steam gasification and for activating the material as a catalyst by oxidation with 10% O_2/90% N_2. In a typical steam gasification run, the MG char was heated in nitrogen to 870° C at a rate of 20 C°/min, and the fluidizing gas was switched to a 50:50 steam-nitrogen mixture. Fourteen steam-treatment runs, designated SA01 through SA14, were made. The SA01 and SA02 were used to determine the conditions for the final oxidation. Composites of SA03 through SA09 and SA10 through SA14 are designated SA3-9 and SA10-14, respectively. The catalyst surface was produced in the same reactor by heating batches in nitrogen to 450° C, and switching to 10% O_2/90% N_2 for 15 minutes. The gas was switched back to N_2 while cooling to room temperature in runs SA01 through SA09 but the flow of 10% O_2/90% N_2 was continued for SA10 through SA14. Composites from SA3-9 and SA10-14 are designated OSA3-9 and OSA10-14, respectively.

Testing as a catalyst - A 2.5 ml quantity of redistilled Wiley 3-chloro-3-methylpentane was heated 5 minutes at reflux temperature (120° C) in a 25 ml tube fitted with a micro reflux condenser before adding 0.25 g of the activated char to be tested. The temperature was maintained for another 10 minutes before the tube was removed from the heater. The liquid was separated from the char by filtration through a 10 ml gas-tight syringe connected to a filtration apparatus. The olefins in the filtrate were then analyzed using a Perkin-Elmer 8500 GC for a preliminary determination. A Hewlett Packard 5988A GC/MS (HP GC/MS) with a fused silica capillary column and a split (ratio 1:100) injection system was used for a molecular level identification. The preceding procedure was also used to dehydrate 2,3-dimethyl-2-pentanol.

Preliminary test data indicated that there was no catalytic activity exhibited by OSA3-9 for the deamination of t-butylamine or cyclooctylamine at a temperature lower than 220° C and a residence time of <10 minutes. Evidence that deamination requires a higher temperature than dehydrochlorination with other catalysts was found in the literature (5). Tests at higher temperatures were carried out in a Perkin-Elmer 8500 Gas Chromatograph equipped with a hot wire detector and liquid nitrogen trap. Helium was used as GC carrier gas. The GC injector glass liner was packed with 0.1 g of oxidized char and used as a catalytic column. The GC injector temperature was set at 295° C, the temperature found by Lycourghiotis to work. A 6' x 1/8" packed column was used as an analytical column for product separation. Deamination products eluted from the GC analytical column were collected at the exit of the detector at liquid nitrogen temperature. The expected olefins were identified on the HP GC/MS.

Surface Areas - Total surface area, micropore area and volume, and cumulative pore volume were determined from nitrogen adsorption data obtained at 77 K using a Micromeritics (ASAP 2400) apparatus. Adsorption isotherms were analyzed using the BET equation to obtain total surface area. Micropore area and volume were obtained from t-plots using the Halsey equation (10). Adsorption/desorption isotherms were analyzed using the BJH method (11) to calculate cumulative pore volumes.

RESULTS AND DISCUSSION

Catalyst activity. The oxidized char (OSA3-9 and OSA10-14) catalyzed the production of the expected olefins (identified by GC/MS) from 3-methyl-3-chloropentane at its boiling point, 2,3-dimethyl-2-pentanol at about the same temperature (120° C), and cyclooctylamine at 295° C. The methods used showed some differences in catalytic activity among char samples made by methods not described here, but better analytical procedures will be required to quantify the differences in catalytic activity.

Proximate and Ultimate analyses - Proximate analyses (Perkin Elmer TGA 7 thermogravimetric analyzer), and Ultimate analyses (Leco CHN-600 and Leco SC-132) appear in Table 1. There are significant differences among the samples. While the percent VM decreased from about 51% to 2.5% from coal to OSA char on a dry-ash-free basis (not shown in the table), the ash and fixed carbon

contents increased. The carbon content increased from a low of 80%, on a dry-ash-free basis, for the original coal to a high of 95% for the OSA char sample and, at the same time, the hydrogen decreased tenfold. The atomic H/C ratio was decreased from 0.87 to 0.28 by mild gasification and from 0.28 to the minimum of 0.07 when the MG char was steam treated (SA3-9 or SA10-14).

As expected, as the coal is pyrolyzed and gasified, it loses oxygen functional groups. Therefore, when IBC-103 was pyrolyzed to 500°C, it lost over 40% of its oxygen (from 9.27 to 5.24%, direct analysis) and then when this char (MG char) was steam gasified at 870°C, it lost another 60% to 75% of its oxygen content (down to 1.94% and 1.23% for SA3-9 and SA10-14). When this steam treated char was oxidized in air, to make it a catalyst, its oxygen content increased significantly (up to 3.32% and 3.33%, respectively). The cooling in the presence of 10% O_2/90% N_2 for OSA10-14 did not appear to increase the oxygen over that of OSA3-9.

Inductively Coupled Plasma (ICP) analysis - ICP spectroscopy determines the inorganic elements present in the bulk of a sample. Only the elements commonly present in the coal were determined. The data are shown in Table 2. As expected, the concentration of all metallic is elements was increased as the original coal (IBC-103) was pyrolyzed to produce the MG char and even more as the char was steam treated to obtain SA3-9 or SA10-14.

X-Ray Diffraction (XRD) - All samples were found to be mostly amorphous and showed a graphite-like structure. Quartz (SiO_2) was the major crystalline phase in all samples. XRD data, like the data from ICP analysis, indicate that significant amounts of oxides of Si, Fe, Al and Ti are present in the oxidized chars (OSA3-9 and OSA10-14). In addition to phase and crystallinity information, XRD analyses provided some important correlations between the small-angle X-ray scattering (SAXS) intensity and microstructure of the samples. The SAXS intensity for the SA char was approximately 480 cps, and 550 cps for the OSA char samples OSA3-9 and OSA10-14, respectively. The conclusion one can reach solely on the basis of these two data sets is that the microporous structure in the OSA char is more fully developed than that for SA char. This is in contrast to the data on micropore volume, cumulative pore volume and average pore size radius data obtained from N_2 gas adsorption/desorption (BET) surface areas which indicated no significant differences between SA chars and the OSA chars.

Nitrogen (BET) surface area - Char activation has two purposes. One is to develop adsorption capacity, as estimated by pore surface area, and the other is to give the char the type of oxidized surface that catalyzes elimination reactions. Thermogravimetric analysis (TGA) was used for preliminary assessment of two methods for increasing surface area: 1) oxidation with 10% O_2/90% N_2 at 450°C and 2) steam gasification at 870°C. Because steam gasification generated higher nitrogen BET surface areas, steam was used. Adsorption/desorption data with N_2 at 77°K and the Brunauer, Emmett, and Teller (BET) equation were used to calculate pore surface areas and the micropore surface areas (Table 3). Due to the small surface area, the micropore area, micropore volume, cumulative pore volume and average pore radius were not measured for the original coal (IBC-103) and MG Char.

Steam activation raised the N_2 surface area from <5 m^2/g in the mild gasification char (MG char) to 460 m^2/g at 41% weight loss and to a high of 625 m^2/g at 54% weight loss as measured at the ISGS. The average weight losses and pore surface areas generated were 51% and 542 m^2/g for the 7 batches mixed to produce SA3-9 and 54% and 575 m^2/g for the composite of 5 batches designated SA10-14. Amoco's values for these composites, 473 m^2/g and 585 m^2/g, respectively, confirmed order but showed a greater difference. The oxidized steam-activated (OSA) char having catalyst properties was made by oxidation at 450°C with 10% O_2/90% N_2 for 15 minutes. The pore surface areas of the catalyst composites, OSA3-9 and OSA10-14, were about equal, 557 m^2/g and 552 m^2/g, respectively, despite the difference in the pore surface areas and micropore surface areas of their precursors (473 m^2/g and 187 m^2/g for SA3-9 and 584 m^2/g and 230 m^2/g for SA10-14). The micropore surface area of the catalyst which during preparation was cooled in 10% O_2/90% N_2 to leave more oxygen on the surface (OSA10-14) had a lower micropore surface area than the one (OSA3-9) cooled in nitrogen (207 m^2/g and 242, respectively).

Clearly the steam treatment and air oxidation steps opened up some very fine micropore structures in the MG char. This fine microstructure could account for the greatly increased surface area of the steam treated and final activated chars.

X-ray Photoelectron Spectroscopy (XPS) - Elemental surface composition (relative weight percent) and a summary of their binding energies (BE), as determined by XPS, are shown in Tables 4 and 5, respectively. Table 4 shows the concentration of several elements, including oxygen, on the surface of the samples which is typical for these types of materials. Binding energy data, Table 5, indicate the presence of hydrocarbon species such as C-C and C-H (284.6 $\pm$0.2 eV), oxidized carbon species such as C-O and C=O (286.2$\pm$0.2 eV), and carbonate/carboxylic species O-C=O (289$\pm$0.6 eV). The binding energy of 163.6 eV ($\pm$0.6 eV) is typical for elemental sulfur and/or organic sulfur species such as mercaptans (R-SH), disulfides (R-SS-R) and thiophenes, and the binding energy of 168.0 eV ($\pm$0.3 eV) is typical for species such as sulfonates (R-SO_3), alkylsulfonates (RO-SO-OR) and dialkylsulfates (RO-SO_2-OR). The nitrogen binding energies suggest the presence of amines (RNH_2) including alkylamines, aromatic (phenyl) amines and pyridine derivatives at 398.6 eV ($\pm$0.6 eV), pyrolic nitrogen species at 400.4 eV ($\pm$0.3 eV), and ammonium derivatives (RNH_3+) at 402.0 eV ($\pm$0.4 eV) with one unidentifiable species at about 404.0 eV. However, numerous nitrogen-containing organic compounds (i.e. nitrobenzene and dinitrobenzene) fall into the binding energy range of 404-405 eV ($\pm$5 eV). The presence of binding energies at approximately 711.5 eV ($\pm$0.5 eV) for Fe, 103.0 eV ($\pm$0.1 eV) for Si, and 75.0 eV ($\pm$0.6 eV) for Al is most likely due to the respective oxides.

Based on the data in Table 5, the chemical species concentrated on the surfaces of the catalytic variety of char differ from those not oxidized. For example, while the concentration of hydrocarbon species such as C-C and C-H (284.6 $\pm$0.2 eV) on the surfaces of steam activated chars (SA3-9 and SA10-14) were 75% and 65%, respectively, the concentration of the same species on the surfaces of the air oxidized chars (OSA3-9 and OSA10-14) were 66% and 60%. On the other hand, the concentration of oxidized carbon species such as C-O and C=O (286.2 $\pm$0.2 eV) on the surfaces of steam treated chars were 16% and 23%, respectively, and on the surfaces of air oxidized chars were 23% and 30%. The concentration of carbonate/carboxylic species O-C=O (289 $\pm$0.6 eV) remained constant at about 10% for both steam treated and air oxidized chars.

The surface binding energies, Table 5, obtained from the XPS studies also suggest that the surface concentration of oxidized carbon species (C-O and C=O) is lower for OSA3-9 (23%) than for OSA10-14 char (30%), the sample that was cooled in 10% O_2/90% N_2 atmosphere rather than N_2. While four types of nitrogen species were identified on the surface of OSA3-9, only two were identified on the surface of OSA10-14, and this too may be the result of the cooling regime.

Diffuse Reflectance IR Spectroscopy - Spectra were obtained on a Mattson Cygnus 100 FTIR using a Harrick Diffuse Reflectance accessory. All spectra were acquired by co-adding 1024 scans at a resolution of 8 cm^{-1}. Powdered KBr was used as a background. Bands elucidated by second derivative treatment are broadly assigned as: 1867 cm^{-1} and 1809 cm^{-1}, C=O, anhydride, probably cyclic and unconjugated; 1740 cm^{-1}, C=O, ester; 1707 cm^{-1}, C=O, possibly ketone, aldehyde, or COOH; 1655 cm^{-1}, C=O, highly conjugated, Ar-(C=O)-Ar; and 1613 cm^{-1}, highly conjugated, hydrogen bonded C=O. Mild gasification of the IBC-103 resulted in a higher ratio of aromatic C-H functional groups to aliphatic C-H functional groups which is consistent with a graphitization process. The pyrolysis process resulted in modest band shifts, which may be due to differences in electronegativity or level of conjugation in the substituents bonded to the various carbonyl groups. The spectrum obtained from the air oxidized char (OSA3-9) had features that were very faint and broad. A band centered near 1590 cm^{-1} suggests the same aromatic character along with carboxylic acid salts. The former assignment is consistent with the broad feature centered near 3150 cm^{-1} encompassing the aromatic C-H stretch region. A band near 1590 cm^{-1} along with a very broad feature centered near 1170 cm^{-1} may also be indicative of coordinated inorganic carbonate, which is consistent with the XPS results.

Scanning Tunneling Microscopy (STM) - STM and the newer technique for imaging and resolving surface detail at atomic and near atomic level, atomic force microscopy (AFM), are becoming increasingly

important in studies of molecules deposited on the surfaces of catalysts. The original coal sample (IBC-103) could not be imaged by STM, most likely because of the low intrinsic conductivity of the material. Chars had sufficient conductivity. Images were obtained with 1-2 nA tunneling current and 750 mV-1750 mV positive bias on the tip and sample at ground which is tunneling from occupied π states of the carbon to the probe tip. Images from the oxidized char (OSA3-9) suggest aggregated particles as large as several thousands of Angstroms which clearly are aggregates of still smaller particles. Particles were usually made of an aggregated state of several 200-400 Å particles. Increasing magnification indicated a further heterogeneity with smaller aggregates of size in the order of tens of Angstroms. At even higher magnification (less than 10 nm) an apparent lattice imaging became evident. The partially ordered region seen in this image was in the order 50x70 Å with a very poor registry. A well-ordered domain of size 20x40 Å was also seen at this magnification.

CONCLUSIONS

The oxidized, steam-activated (OSA) char catalyzed dehydration of an aliphatic tertiary alcohol and deamination of a primary aliphatic amine, in addition to dehydrochlorination of an alkyl halide. PS data indicated a significant amount of oxygen was in the surface of the OSA char. The ICP and XRD data indicated the presence of significant amounts of Si, Fe, Al and Ti oxides. In addition to phase and crystallinity information, XRD data provided an important correlation between the small angle X-ray scattering (SAXS) intensity and the microstructure of the samples. The strong presence of SAXS at low angles in OSA char is evidence that OSA char is a microporous material, and a comparison of intensity measurements suggests that the microporous structure becomes more fully developed during the oxidation of steam-activated (SA) char. XPS data suggest the chemical species concentrated on the surfaces of the chars are indeed different and these differences are expected to be related to variations in catalyst reactivity among samples. The surface binding energies from XPS work, and IR data supported the speculation that the cooling under N_2 atmosphere after the oxidation step causes the removal of some of the CO and C-O complexes.

Both IR and ^{13}C NMR data confirm that the ratio of aromatic C-H groups to aliphatic C-H groups increased significantly when volatile matter was removed during mild gasification. An oxidation index is defined as the ratio of the integrated area of the carbonyl region (1635-2000 cm^{-1}) to the integrated area of the region associated with the aliphatic and aromatic C-H stretches (2675-3135 cm^{-1}). The calculated oxidation index was about 0.48 and 1.09 for the coal and MG char, respectively. This index may prove useful in characterizing mild gasification chars and correlating final pore development with thermal histories.

In general, STM imaging of the samples revealed a highly aggregated hierarchical structure. A very fine sheet-like microstructure could be seen in steam-activated and oxidized steam-activated chars. STM data clearly support the BET data that the steam-activation opened up a very fine micropore structure on the originally small, several hundred Angstrom, features of MG char. Certainly, this fine microstructure could account for the greatly increased active surface area of the steam-activated char. The OSA chars have been shown to have good sorption properties and results will be reported in a subsequent publication.

ACKNOWLEDGEMENT

This work has received direct financial support from the Illinois Department of Energy and Natural Resources, through its Coal Development Board and the Center for Research on Sulfur in Coal CRSC, and from the United States Department of Energy through (CRSC). We also acknowledge in-kind contributions funded by the Alternative Feedstock Development (AFD) program of Amoco Corporation. Without this support and the encouragement of R. E. Lumkin (AFD), this work would not have been possible. The authors wish to acknowledge contributions by the following Amoco Research Center staff members in the areas specified: R. Roginski, Diffuse Reflectance IR Spectroscopy; B. Meyers, pore surface areas; G. Zajac, STM; and J. Faber, XRD. Assistance at the ISGS included Sheng-Fu J. Chou, identification of compounds by GC/MS analysis; Robert Frost, surface area measurements; and M. Rostam-Abadi, directing the char activation portion of this study.

REFERENCES

1. Kruse, C.W.; Ray, G.C., U.S. Patent 3,240,834, March 15, 1966.
2. Mahan, J.E., Reusser, R.E.; Kruse, C.W., U.S. Patent 3,352,935, Nov. 14, 1967.
3. Kruse, C.W., U.S. Patent 3,437,695, April 8, 1969.
4. Lycourghiotis, A. *React. Kinet. Catal. Lett.* **1976,** *5*(4), 453-7.
5. Lycourghiotis, A.; Vattis, D,; Katsonos, N.A.; *Z. Phis. Chem. (Wiesbaden),* **1981,** *126*(2), 259-67.
6. Suarez, A.R.; Mazzieri, M.R. *J. Org. Chem.* **1987**, *52*(6), 1145-7.
7. Mochida, I.; Watanabe, H.; Uchino, A; Fujitsu, H.; Takeshita, K.; Furuno, M,; Sakura, T.; Nakajima, H. *J. Mol. Catal.* **1981,** *12*(3), 359-64.
8. Misono, M. *J. Catal.* **1973,** *30*(2), 226-34.
9. Rostam-Abadi, M.; DeBarr, J.A.; Chen, W.T. *Prepr. Pap.--Am. Chem. Soc., Div. Fuel Chem.* **1989**, *35*(4), 1264-71.
10. Halsey, G.D. *J. Chem. Phys.* **1948**, *16*, 931.
11. Barrett, E.P.; Joyner, L.G.; Halenda, P.P. *J. Am. Chem. Soc.* **1951**, *75*, 373-380.

Table 1. Proximate and Ultimate Analyses

	IBC-103 Coal	MG Char	SA3-9 Char	OSA3-9 Char	SA10-14 Char	OSA10-14 Char
Proximate Analysis (wt%, as-received)						
Moisture	3.35	1.01	2.28	0.93	2.01	1.62
Ash	5.92	10.42	19.81	21.81	21.43	24.58
V. Matter	49.2	16.02	12.36	2.44	11.38	2.72
Fixed C	41.53	72.55	65.55	74.82	63.18	71.08
Proximate Analysis (wt%, dry)						
Ash	6.12	10.53	20.27	22.02	21.87	24.98
V. Matter	50.91	16.18	12.65	2.46	11.61	2.76
Fixed C	42.97	73.29	67.08	75.52	66.52	72.26
Ultimate Analysis (wt%, as-received)						
%C	71.82	80.06	69.61	72.14	69.82	70.48
%H	5.63	1.98	0.65	0.53	0.67	0.58
%N	1.69	2.22	1.58	1.47	1.43	1.37
%S	2.2	1.84	1.23	1.21	1.19	1.24
%O[a]	11.39	5.54	3.54	3.39	2.73	3.9
Ultimate Analysis (wt%, dry)						
%C	79.16	90.39	89.35	93.37	91.2	95.5
%H	5.79	2.11	0.51	0.55	0.58	0.54
%N	1.86	2.51	2.03	1.9	1.87	1.86
%S	2.42	2.08	1.58	1.57	1.55	1.68
%O[b]	10.77	2.91	6.53	2.61	4.8	0.42
%O[a]	9.27	5.24	1.94	3.32	1.23	3.33
H/C	0.87	0.28	0.07	0.07	0.07	0.07

[a]Oxygen values were obtained by direct analysis.
[b]Oxygen values were obtained by difference (100 - (%C + %H + %N + %S) = %O).

Table 2. Metal Composition (Wt.%) Data from ICP Analyses

Sample I.D.	IBC-103 Coal	MG Char	SA3-9 Char	OSA3-9 Char	SA10-14 Char	OSA10-14 Char
Fe	1.04	1.59	4.1	2.85	3.14	3.27
Si	0.67	1.31	2.13	4.30	4.80	4.3
Al	0.74	1.38	2.72	2.45	2.95	2.92
Na	0.30	0.04	0.11	0.10	0.08	0.08
K	0.14	0.25	0.5	0.46	0.46	0.45
Ca	0.07	0.14	0.26	0.27	0.27	0.21
Mg	0.04	0.06	0.13	0.13	0.16	0.14
Ti	0.04	0.06	0.12	0.16	0.16	0.16

Table 3. Nitrogen Surface Area Data (Adsorption/Desorption)

		IBC-103 Coal	MG Char	SA3-9 Char	OSA3-9 Char	SA10-14 Char	OSA10-14 Char
N_2 - BET Surface Area (m^2/g)		1.3	1.1	473	557	584	552
Micropore Area (m^2/g)		N.D.[a]	N.D.[a]	187	242	230	207
Micropore Vol (cc/g)		N.D.	N.D.	0.08	0.11	0.11	0.10
Cumulative Pore Vol (cc/g)	Ad.	N.D.	N.D.	0.17	0.19	0.22	0.22
	De.	N.D.	N.D.	0.18	0.20	0.23	0.23
Average Pore Radius (Å)	Ad.	N.D.	N.D.	20	20	20	20
	De.	N.D.	N.D.	18	18	19	19

[a] Not Determined. Surface areas are too small to measure pore volumes by this technique.

Table 4. Surface Composition (Wt.%, Relative) Data from XPS Analyses

	IBC-103 Coal	MG Char	SA3-9 Char	OSA3-9 Char	SA10-14 Char	OSA10-14 Char
C	71.3	74.1	78.7	78.8	80.	80.
O	17.6	15.7	12.9	13.3	10.4	10.2
N	1.6	1.6	0.9	0.9	0.5	0.8
S	1.4	1.2	0.7	0.7	3.7	3.9
Al	2.8	2.4	2.1	2.3	1.6	1.6
Si	4.6	3.6	3.4	3.0	2.6	2.3
Fe	0.4	0.8	0.9	0.4	0.8	0.8
Mg	0.2	0.2	0.2	0.2	Tr.	Tr.
Ca	---	0.3	0.3	0.3	0.3	0.3

Table 5. Binding Energies (eV) Data from XPS Analyses

Sample Identification	C 1s	%	O 1s	Si 2p	Al 2p	S 2p	%	N 1s	%	Fe 2p	Ca 2p
IBC-103	284.5	84	533.0	103.5	75.0	163.8	88	398.5	38	712.0	-------
(coal)	286.2	14				168.9	12	400.2	57		
	289.2	2						402.1	5		
MG Char	284.5	81	533.2	103.6	75.7	163.7	100	398.6	28	712.1	349.0
(United Coal Company)	286.4	16						400.4	62		
	288.8	3						402.4	10		
SA3-9	284.6	75	533.2	104.0	75.7	163.8	100	398.6	19	711.7	347.7
	286.3	16						400.7	68		
	288.7	9						402.3	13		
OSA3-9	284.6	66	533.2	104.1	75.7	163.9	100	398.4	13	711.2	347.7
	286.1	23						400.7	56		
	289.7	10						402.3	23		
								403.9	9		
SA10-14	284.6	65	533.2	103.6	75.4	163.9	100	398.6	22	711.6	348.2
	286.3	23						401.2	78		
	289.7	12									
OSA10-14	284.6	60	533.2	103.9	75.7	163.9	100	398.7	22	711.9	347.9
	286.0	30						402.3	78		
	290.0	10									

COAL AS A FEEDSTOCK FOR FULLERENE PRODUCTION AND PURIFICATION

Louis S.K. Pang, Anthony M. Vassallo and Michael A. Wilson
CSIRO Division of Coal and Energy Technology,
P.O. Box 136, North Ryde, NSW 2113, Australia

Keywords: fullerenes, coal, preparation, chromatography.

INTRODUCTION

Since the first availability of fullerenes in bulk,[1,2] research on these materials has fluorished rapidly. There is implication that these molecules are potentially useful[3] as lubricants, superconductors, rechargable batteries, diamond nucleators,[4] catalysts and chemical feedstocks. Fullerenes are commonly produced by the electrical arcing of graphite in helium,[1] but can also form from benzene combustion in an Ar/O_2 mixture.[5] Purification is usually performed by chromatography on silica.[6] We have recently demonstrated that fullerenes can be produced by the electrical arcing of coke derived from coking coals.[7] We have now extended the study using different Australian coals including brown coal and semi-anthracite and prepared coke from these coals by a number of different methods. Coal was also demonstrated to be a useful chromatographic material to purify C_{60}.

EXPERIMENTAL

Preparation of conductive coke rods

The primary requirement for production of fullerene from coal in this work is the preparation of conductive coke rods. Three methods of coke preparation were used.

1) laboratory coke. A finely ground coking coal was heated in an aluminium mould in an argon flow at 395°C for 24 h to form a semi-coke rod. This rod was carbonised at 1200°C in argon for 5h.

2) Coal-pitch composite. This method is suitable for both coking and non-coking coals. Finely ground coal and pitch (20 wt. %) mixtures were placed in a Swage-lok type stainless steel tube and sealed. The system was heated to 500°C for 24 h. A semi-coke rod was formed, which was carbonised at 1200°C in argon for 5 h. Additional carbonisation conditions (1200°C for 10 h, 1300°C for 1 h) was used for brown coal and neat pitch to induce electrical conductivity.

3) Oven coke. Finely ground coking coals were heated in a wall oven (0.42 m^3) under sealed condition at 1010°C for 16-19 h. Samples of coke were cut into rods for electrical arcing.

Fullerene production

Fullerene was produced by electrically arcing the coke rods in a 250 torr helium atmosphere at 23-30 V and 80-130 A a.c. or d.c. in a stainless steel chamber. The soot produced by this process was Soxhlet extracted with toluene to give crude fullerenes.

Purification of C_{60} on coal

For purification of C_{60} on coal, Yarrabee semi-anthracite (H/C 0.74, O/C 0.013) was ground and size separated. The 63-125 um size fraction was pre-washed in a Soxhlet extractor for 3 days with toluene to remove any soluble materials. A glass column was packed with this pre-washed coal (1.2 cm by 58 cm) using hexane, and crude fullerene (15 mg) was dissolved in toluene (3 ml) and loaded on the head of the column. After elution with hexane (800 ml) at a flow-rate of 2 ml/min, 8.7 mg of solid pure C_{60} was obtained from the eluate.

RESULTS AND DISCUSSION

Table 1 lists the carbon contents and ash yields for the different cokes, and fullerene yields. Infrared spectroscopy showed absorption peaks characteristic of C_{60} and C_{70} fullerenes in similar ratios (ca. 10:1 for C_{60} : C_{70}) reported for graphite as a source material[1]. The ratios have been confirmed by solid-state ^{13}C nuclear magnetic resonance spectroscopy.

All cokes tested so far produced fullerenes. Thus it appears that other conductive carbonaceous materials may also be able to produce fullerenes. An optimum fullerene yield of 8.6% was obtained from superclean Goonyella coke. This compares favourably with the yield of 9.3% obtained from graphite under identical conditions. Pitch (neat) yielded only 2% fullerenes, therefore, in the composite with coal in which pitch was present at a level 20%, the fullerenes were predominantly produced from the coal, since much higher yields were obtained from these

composites. Also, the use of d.c. current rather than a.c. appears to markedly increase the yield of fullerenes from both graphite and coal.

Although coking occurs readily at 1200°C, graphitisation does not usually occur below 2500°C on these time scales[8]. The results presented here show that graphitisation is not a requirement for fullerene production by the electrical arc method.

The presence of mineral matter (ash yield) in the coal does not inhibit fullerene formation from coke, however, its presence does result in a reduced yield of fullerene. Data in Table 1 indicate that poorer fullerene yield (around 3% or less) was obtained from the oven cokes and Coalcliff composite which have over 10% mineral matter. On the other hand, Loy Yang composite, Newvale composite and superclean Goonyella coke each has under 4% mineral matter and produces 6% or more fullerene yield. The electrical resistivities of the cokes do not appear to be directly related to mineral matter contents and no clear trend can be drawn between the electrical resistivities and fullerene yield.

It appears that the method of coke preparation may also affect fullerene yield. The data are scattered, but Table 1 shows that laboratory cokes (2.3-8.6%) produce comparable fullerene yield to carbonised coal-pitch composites (2-7.7%) while oven cokes (2-3.3%) give the poorest yield.

The presence of a small amount (below 4%, Table 1) of hydrogen and heteroatoms (O, S and N) in the coke does not inhibit fullerene formation. In addition, there is no simple relationship between the coal rank and fullerene yield. Semi-anthracite (Yarrabee coal) derived composite produced 5.0% fullerene, while Loy Yang brown coal composite produced 7.7% yield, which on a coal basis is at least equivalent to, if not higher than graphite at 5.8%.

A number of reports have appeared on fullerene generation by the laser ablation of coal, graphite and mesophase in an ion cyclotron resonance (ICR) spectrometer[9-11]. These results showed that the laser power required to generate fullerenes increased from mesophase < brown coal < high rank coal < graphite. Higher laser power may be needed to break down some of the regular hexagonal structure in graphite, which then rearranges to form the five and six membered ring structure in C_{60}. On the other hand, the breakdown of the more disordered structure present in brown coal and mesophase may be accomplished with relative ease. Moreover, five and six membered rings are already present in these materials, which may assist in the formation of fullerenes. For comparison, a lower laser power requirement in the ICR experiment may relate to a higher fullerene yield in the electrical arc experiment. However, in our electrical arc experiment, a definite correlation between fullerene yield and coal rank or graphite could not be made.

CONCLUSIONS

The results presented here clearly show that a suite of coals of different ranks are capable of producing fullerenes. Moreover, for Yarrabee semi-anthracite a self-consistent process for producing fullerenes is possible. The coal can be used to produce fullerenes and also to separate pure C_{60}. The presence of mineral matter and heteroatoms does not inhibit fullerene formation but does reduce fullerene yield. The regular hexagonal carbon structure present in graphite is not a requirement for fullerene formation. In fact, a disordered carbon structure may be favourable. With the present cost of coal at $100 per tonne or less, its use as an industrial material for fullerene may greatly improve the economics of large scale production.

REFERENECES

1. Kratschmer, W.; Lamb, L.D.; Fostiropoulos, K.; Huffman, D.R. *Nature* **1990**, *347*, 354-358.

2. Taylor, R.; Hare, J.P.; Abdul-Sada, A.K.; Kroto, H.W. *J.C.S. Chem. Commun.* **1990**, 1423-1425.

3. Stoddart, J.F. *Angew Chem. Int. Ed. Engl.* **1991**, *30*, 70-71.

4. Meilunas, R.; Chang, R.P.H.; Liu, S.; Kappes, M.M. *Nature* **1991**, *354*, 271.

5. Howard, J.B.; McKinnon, J.T.; Makarovsky, Y.; Lafleur, A.; Johnson, M.E.; *Nature* **1991**, *352*, 139-141.

6. Ajie, H.; Alvarez, M.M.; Anz, S.J.; Beck, R.D.; Diederich, F.; Fostiropoulos, K.; Huffman, D.R.; Kratschmer, W.; Rubin, Y.; Schriver, K.E.; Sensharma, D.; Whetten, R.L. *J. Phys. Chem.* **1990**, *94*, 8630.

7. Pang, L.S.K.; Vassallo, A.M.; Wilson, M.A. *Nature* **1991**, *352*, 480.

8. Brooks, J.D.; Taylor, G.H. in *"Chemistry and Physics of Carbon"*, Ed. Walker, P.H. Jr. p282, Marcel Dekker, N.Y., 1968.

9. Greenwood, P.F.; Strachan, M.G.; Willett, G.D.; Wilson, M.A. *Org. Mass Spec.* **1990**, *25*, 353-362.

10. Greenwood, P.F.; Strachan, M.G.; El-Nakat, H.J.; Willett, G.D.; Wilson, M.A.; Attalla, M.I. *Fuel* **1990**, *69*, 257-260.

11. Dance, I.G.; Fisher, K.J.; Willett, G.D.; Wilson, M.A. *J. Phys. Chem.* **1991**, *95*, 8425-8428.

Table 1. Electrical conductivities, fullerene yields, carbon contents and ash yields for coke[a] and graphite.

source carbon	electrical resistivity ohm/cm	fullerene yield (wt. %)	%C	%ash yield	%O+H+S+N[b]
I. Laboratory coke					
Goonyella[c,d]	.53	5.6	95.8	2.1	2.1
Goonyella[c,e]	.38	8.6	94.8	3.8	1.4
Goonyella[c,f]	.33	2.3	91.0	7.6	1.4
graphite[c]	.009	9.3			
graphite	.009	16.2			
II. Carbonised coal and pitch composite					
Coalcliff[c]	.07	2.0	85.2	14.5	0.3
Coalcliff	.07	3.2			
Newvale	.12	6.0	95.1	1.6	3.3
graphite[g]	.009	5.8			
Loy Yang	.38	7.7	96.5	1.8	1.7
Yarrabee	.26	5.0	95.7	4.2	0.1
pitch	.26	2.0	96.9	2.0	1.1
III. Oven coke					
Norwich Park	.10	3.3	84.2	12.1	3.7
Riverside	.09	2.5	85.4	12.0	2.6
Blackwater	.09	2.2	86.3	10.7	3.0
Goonyella	.46	2.3	85.3	11.0	3.7
Gregory	.12	2.8	85.4	11.5	3.1

a wt. % dry basis

b by difference

c electrical arcing was induced by a.c.; d.c. was used for the other experiments.

d from ultraclean coal

e from superclean coal

f from as received coal

g The fullerene generator was modified for these experiments, and the yield of fullerenes reduced significantly but consistently. Yield data for cokes below this column should be compared to this value.

EVIDENCE FOR ENTRAPMENT OF C_{60} AND C_{70}

F. Hopwood, K.J. Fisher, I.G. Dance, G.D. Willett
Chemistry Department, University of New South Wales
PO Box 1, Kensington NSW 2033, Australia

M.A. Wilson*, L.S.K. Pang and J.V. Hanna
CSIRO Division of Coal and Energy Technology
PO Box 136, Ryde NSW 2113, Australia

Keywords: buckminsterfullerene, mass spectrometry, fullertubes

ABSTRACT

The carbon arc soot from coal produced in a fullerene generator has been exhaustively extracted with toluene and pyridine. Complete extraction of C_{60} and C_{70} was not fully achieved with toluene since the residue was shown to contain pockets of C_{60} and C_{70} some of which could subsequently be extracted by pyridine as demonstrated by negative ion laser desorption mass spectrometry, infra-red spectrometry and solid state nuclear magnetic resonance spectrometry. Threshold laser power experiments also indicated the presence of fullerenes to m/z 1800. These results clearly indicated the entrapment of C_{60} by other fullerenes or fullertubes of higher molecular weight. When laser ablation techniques were used odd numbered cluster ions were observed indicating the presence of ruptured or chain substituted fullerenes.

INTRODUCTION

The isolation of stable carbon clusters including C_{60} and C_{70} fullerenes from carbon arc soot produced via the vaporisation of graphite in an inert gas atmosphere has recently been reported[1-6]. For example, Diederich et al.[4] and Ettl et al.[5] have extracted arc soot with toluene and separated and identified C_{76}, C_{78}, C_{84} and C_{94} fullerenes. It is expected that a range of other fullerenes may be present in the soot and little is known about how C_{60} and C_{70} are formed and whether any are entrapped in the soot with other fullerenes. In this work we report the use of pyridine to extract the soot residue after toluene extraction. Both pyridine soluble and pyridine insoluble fractions have been characterised by FTICR mass spectrometry and FTIR spectrometry and in some cases also by solid state ^{13}C NMR spectrometry.

EXPERIMENTAL

Preparation of fractions

The preparation of the fullerene soot from graphite and coal was carried out in a modified fullerene generator as reported elsewhere[7].

The soot was generated from coal or graphitic rods using 25V and 100A d.c. We observed that holes drilled in the graphite rods increased the yield of soot for a given time and current.

Use of an inner water cooled chamber for the arcing process was designed to limit the penetration of the soot into the main chamber and thence its pumping system. The removal of the inner chamber also facilitated the easy recovery of the soot after each run for quantitative analysis and to limit the 'possible' health hazards that may arise handling this light fluffy material.

The resulting soot (3 g) was divided equally into two portions. One portion was Soxhlet extracted with toluene for 6 h. This yielded 85 mg of fullerene extract after solvent removal. After drying, the soot residue was Soxhlet extracted exhaustively with pyridine for 12 h (under nitrogen to prevent solvent decomposition). A clear brownish yellow solution was obtained. This yielded 65 mg of solid extract after solvent removal. This was dried in a vacuum oven at 80°C for 2 h to remove residual pyridine.

The second portion was Soxhlet extracted with pyridine for 11 h under nitrogen to yield a brownish yellow solution which gave 150 mg solid extract after solvent removal. After drying, the soot residue was Soxhlet extracted with toluene. A faint reddish solution was obtained which yielded a negligible amount (<5 mg) of solid fullerene residue.

Analysis

Details of the laser desorption FTICR mass spectrometry technique have been described previously[8]. Mass spectrometric studies were carried out using the fundamental frequency of a Nd YAG laser (1064 nm) and a Spectrospin CMS-47 Fourier transform ICR mass spectrometer. Careful variation of the laser power was carried out with neutral filters which allowed the determination of the threshold energies for laser desorption of the fullerenes. The laser power was determined using a Scientec power meter. Pressed samples of the soot were ablated in the ICR cell and the ions directly observed.

Fourier transform infra-red spectra (FTIR) were obtained on a Digilabs FTS 80 instrument. The soot was carefully pressed into KBr plates before observation. A sample of the material was mixed with KBr and then pressed in a 13 mm die at 9 t for 5 min.

Solid state nuclear magnetic resonance (n.m.r.) spectra were obtained on a Bruker CXP 100 instrument at 22.5 MHz for ^{13}C. Spectra were obtained by single pulse (Bloch decay) techniques using a 4 μs pulse and 5 s recycle time[9]

RESULTS AND DISCUSSION

The total amount of toluene extract and pyridine extract from the first portion of soot is identical to the total amount of pyridine extract and toluene extract from the second portion of soot. This shows that an equal amount of material can be extracted from the soot with these solvents irrespective of the sequence. Of this total, 57 wt. %

can be first extracted by toluene and a further 43 wt. % can be extracted by pyridine afterwards.

The soot and soot residue after solvent extraction have been examined by FTIR spectroscopy. Adsorptions from C_{60} can clearly be seen in the infra-red spectrum of the raw soot at 527 and 577 cm^{-1}. When the soot is extracted with toluene, the toluene extract contains C_{60} and C_{70} in the ratio of about 10:1 as reported previously by us and others[1,3,7]. However when the extracted soot was examined by FTIR C_{60} resonances were still found to be present even though the soot had been exhaustively extracted with toluene. This result shows that much of the C_{60} is trapped in the soot in some way, so that it becomes unextractable. Pyridine extracts C_{60}. However after pyridine extraction the soot still contained C_{60} adsorptions showing that even pyridine cannot remove all C_{60}.

The pyridine extracted toluene insoluble material was studied in more detail. Its solid state n.m.r. spectrum showed a large resonance at 143 ppm and smaller resonances between 147 and 133 ppm with a small shoulder at 128 ppm. C_{60} resonates at 143 ppm in the solid state[10] and hence this resonance can be ascribed to C_{60}. The other resonances although not fully resolved may be ascribed to C_{70}[1-3].

Laser desorption studies at low laser powers (2 kW cm^{-1}) were in full agreement with the FTIR and N.M.R. results. Initial FTICR spectra of the residue from toluene extraction indicated the presence of C_{60} and C_{70} and smaller amounts of higher fullerenes on laser desorption. However when the experiment was repeated continually, the amount of C_{60} and C_{70} observed was found to be quite variable. This suggests successive desorption through the surface of the extract indicating that C_{60} and C_{70} were entrapped in various layers.

At higher laser powers (>100 kW cm^{-2}) ablation occurs. Positive ion spectra of the toluene residues indicated the presence of higher fullerenes (Figure 1). The most interesting observation from these experiments was the observation of odd numbered carbon clusters (see Figure 1). Thus some open ruptured fullerenes or fullerenes with odd chain length appendages must be formed. As far as we are aware this is the first reported observation of higher molecular weight odd numbered clusters.

As predicted from the infra-red data, the pyridine extracts were shown to contain both C_{60} and C_{70} by laser ablation. Negative ions were observed at threshold values of 2 kW cm^{-2} indicating the presence of fullerenes up to m/z ~1800 daltons (C_{150}). Increasing the laser power resulted in the appearance of fullerenes of m/z up to 2400 daltons (C_{200}), but further increase in power caused a loss of intensity in negative ions as reported previously for C_{60}/C_{70} mixtures[8].

In summary, these results clearly show that during the formation of fullerenes by arcing techniques C_{60} and C_{70} fullerenes are often formed entrapped within other molecules, possibly other fullerenes. On laser ablation these other molecules can react either alone or possibly with C_{60} and C_{70} to form species that have odd numbered molecular weights. These species must be ruptured fullerenes or species containing

odd-numbered side chain lengths. These results are consistent with the hyperfullerene or Russian egg structure recently proposed by Curl and Smalley[11] for fullerene soot or an encapsulating tube model. In these structures C_{60} is encapsulated by fullerenes of higher carbon number.

REFERENCES

1. W. Kratschmer, L.D. Lamb, K. Fostiropoulos and D.R. Huffman, Nature 347 (1990) 354.
2. R. Taylor, J.P. Hare, A.K. Abdul-Sada and H.W. Kroto, J.C.S. Chem. Commun. (1990) 1423.
3. R.E. Haufler, J. Conceicao, L.P.F. Chibante, Y. Chai, N.E. Byrne, S. Flanagan, M.M. Haley, S.C. O'Brien, C. Pan, Z. Xiao, W.E. Billups, M.A. Ciufolini, R.H. Hauge, J.L. Margrave, L.J. Wilson, R.F. Curl and R.E. Smalley, J. Phys. Chem. 94 (1990) 8634.
4. R. Diederich, R. Ettl, Y. Rubin, R.L. Whetten, R. Beck, M. Alvarez, S. Anz, D. Sensharma, F. Wudl, K.C. Khemani and A. Koch, Science 252 (1991) 548.
5. R. Ettl, I. Chao, F. Diederich and R.L. Whetten, Nature 353 (1991) 149.
6. D. Ben-Amotz, R.G. Cooks, L. Dejarme, J.C. Gunderson, S.H. Hoke II, B. Kahr, G.L. Payne and J.M. Wood, Chem. Phys. Lett. 183 (1991) 149.
7. L.S.K. Pang, A.M. Vassallo and M.A. Wilson, Nature 352 (1991) 480.
8. P.F. Greenwood, I.G. Dance, K.J. Fisher, G.D. Willett, L.S.K. Pang and M.A. Wilson, Org. Mass Spectros., 26, (1991), 920.
9. M.A. Wilson, Techniques and Application of NMR in Geochemistry and Soil Science, Pergamon Press, 1987.
10. C.S. Yannoni, R.D. Johnson, G. Meijer, D.S. Bethune and J.R. Salen, J. Phys. Chem., 1991, 95, 9.
11. R.F. Curl and R.E. Smalley, Scientific American (1991) 32.

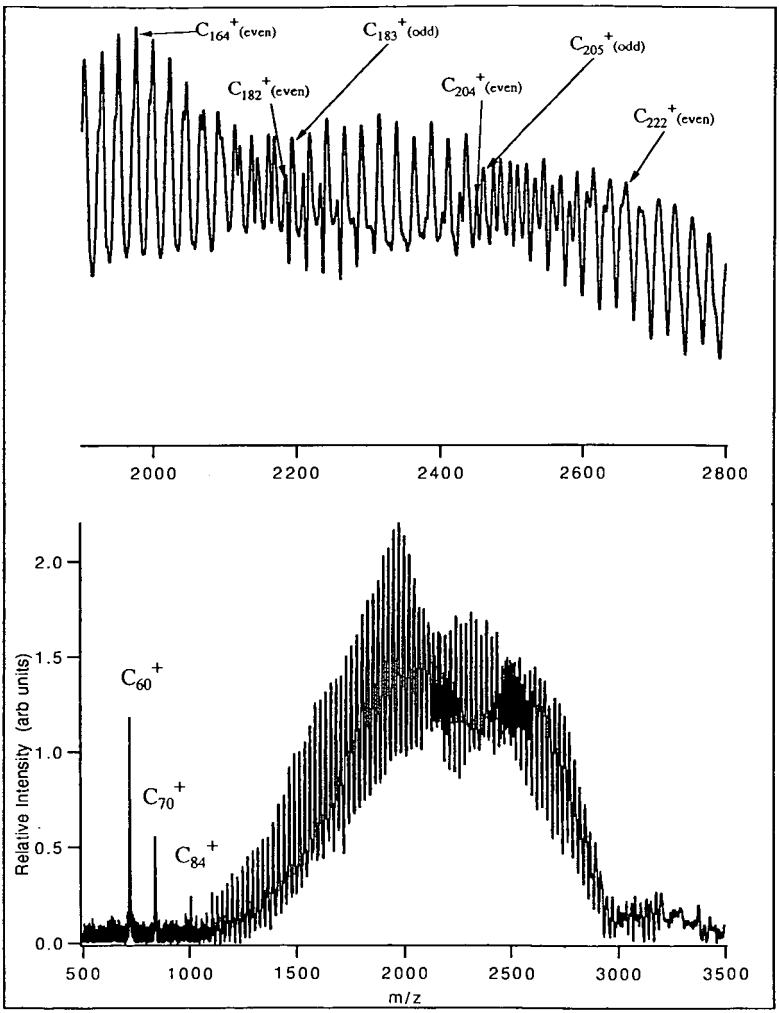

Fig. 1 Mass spectrum of the laser desorption (~4 k Wcm^{-2}) of an insoluble residue

EVALUATION OF THE ASPHALT APPLICATION POTENTIAL OF AN EASTERN US SHALE OIL

K. Mahboub[1], S. D. Carter[3], R.E. Robertson[4], P.M. Harnsberger[4], P. K. Oduroh[2], A. L. Simpson[2], and D. N. Taulbee*[3]

[1]Kentucky Transportation Center
[2]Dept. Civil Engineering
[3]Center for Applied Energy Research
University of Kentucky, Lexington
and
[4]Western Research Institute, Laramie, Wy.

Keywords: Asphalt, shale oil, KENTORT II.

Abstract. A 3" fluidized bed retort was used to generate oil samples from a Devonian oil shale from Fleming County, Kentucky. Following distillation, samples of heavy end materials were subjected to a battery of tests aimed at evaluating their potential utilization as an asphalt cement, additive, or recycling agent. Due to the unusually rapid aging characteristics of the shale oil, emphasis was placed on the latter applications. Preliminary tests of the asphalt recycling potential were generally favorable, indicating that the eastern shale oil exhibits good dispersant and rejuvenation properties.

Introduction. This manuscript describes the results of a scoping study directed at evaluating the potential road paving applications for oils derived from the eastern U.S. oil shale deposits, more specifically, for eastern shale oils (ESO) produced in a KENTORT II prototype reactor.[1,2] The KENTORT concept comprises a series of three fluidized bed reactors,i.e., pyrolyzer, gasifier, and combustor, that fully utilize the available carbon during oil shale processing. This process has been under continuing development at the CAER since about 1984 and has demonstrated that significant enhancements over Fischer Assay oil yield can be obtained using proven technology without resorting to high H_2 partial pressures. Further, this process was designed to mitigate many of the environmental concerns often associated with related technologies. However, in the present era of plentiful and reasonably priced petroleum, commercial production of motor fuels from oil shale is viewed as a high risk venture by those capable of lending financial support. Thus, the prospects for a near term commercial oil shale development is not promising.

Coincidental to the advances in oil shale technology of the past decade has been a continuing decline in both the quality and availability of road asphalts. The decline in availability has led to the recycling of road asphalts (milling and reapplication) in many areas of the country. The decline in quality, attributed primarily to advanced processing (e.g., fluid-cat crackers) used to recover more heating or motor fuel per barrel, has resulted in asphalts which do not have the desirable properties or longevity as asphalts from 3-4 decades past. Though this is bad news for motorists, this situation has created a potential niche market for shale oils,[3,4] particulary since these materials often exhibit physical/chemical properties that suggest they may be a viable alternative to petroleum derived asphalts. Accordingly, a test program was implemented to evaluate KENTORT oils in three different paving applications; i.e., as an asphalt cement, an asphalt modifier, and an asphalt recycling agent. The study included a series of binder and mixture characterization procedures for evaluation of both

short- and long-term performance potential.

Details of the test methods along with preliminary results are described elsewhere[5,6] and so only a brief description of test methods is given here. The conclusion from this earlier work was that unmodified ESO showed an unacceptable rate of 'aging' or hardening which would ultimately lead to pavement failure if used directly as an asphalt cement. However, the potential for use as an asphalt modifier and particularly, as an asphalt recycling agent showed more promise. Accordingly, these latter applications are the focus of this report.

Methods and Results. Study samples. Two oil streams, produced in a 5 lb/hr KENTORT prototype unit, were selected for study. The first was a highly viscous material (3440 P @60^{0} C) recovered in an electro-static precipitator and is referred to as the 'hard' ESO. The second, referenced as the 'soft' ESO (8 P @60^{0} C), was derived from a composite of the total oil product that was subjected to a vacuum distillation prior to testing. These two oils were deliberately selected for study since it is believed they represent the types of material that would be readily available and most likely to be utilized for asphalt production in a commercial operation. Both samples were derived from the Cleveland Member of the Ohio shale acquired from a freshly exposed outcrop in Rowan County, Ky. A detailed description of the oil shale sample and retort operation is given elsewhere.[1,2]

Binder Characterization. If eastern shale oil is to be useful as an asphalt modifier, then the blend of asphalt and ESO must exhibit aging characteristics and rheological properties that are superior to the unmodified asphalt. Likewise, if ESO is to find application as an asphalt recycling agent, it must exhibit properties that are equivalent to or better than conventional agents. In an effort to determine if ESO could meet these criteria, the research was divided into two parts. The first part focused on evaluation of the 'hard' ESO as an asphalt additive and the second on evaluation of the 'soft' ESO as a softening agent for aged asphalt and aged asphalt mix (pavement recycling).

Evaluation as an asphalt additive involved determining the rheological properties of an AC-20 asphalt, a 7 wt. % blend of "hard" ESO and AC-20 asphalt, and neat "hard" ESO. The rheological properties of the three samples were also determined after they were subjected to an accelerated aging procedure. Evaluation of ESO as an asphalt recycling agent entailed measuring the viscosity of an asphalt extracted from a laboratory-aged pavement mixture, the "soft" ESO, and an AC-5 asphalt (representative of a commercial recycling agent). Two "recycle" blends, with a target viscosity of 10,000 poise at 60°C, were prepared by blending the laboratory-aged asphalt with 1) the "soft" ESO and 2) with the AC-5 asphalt. Rheological properties of the two blends were then examined.

Dynamic viscosity measurement were made on a Rheometrics RMS-605 mechanical spectrometer using a shear frequency range of 0.1 to 100 rad/sec at 25, 45, and 60°C from which the two components of shear modulus, G' and G", were determined. The storage modulus or the elastic component (G') quantifies the elastic rebound capability of the material. The loss modulus or viscous component, G", is a measure of damping capacity. Higher G' values indicate good resistance to permanent deformation (rutting) but greater susceptibility to cracking failure. Higher G" values indicate the reverse behavior. Since there is always a trade-off between rutting performance and cracking performance, the term Tan Delta (ratio of G"/G') is used as a measure of the balance between damping and elastic properties. For a fresh asphalt, a Tan Delta value higher than 3 indicates better than average resistance to cracking but less than average resistance to rutting.[7] Values less than 3 indicate the opposite.

Aged Asphalt Binder Rejuvenation. The 60°C viscosities of the laboratory-aged asphalt, the soft eastern shale oil, and the AC-5 asphalt as described above were determined to be 5.98 x 10^{6}, 15, and 515 poise, respectively. Three trial blends each of the laboratory-aged asphalt/soft ESO and the aged asphalt/AC-5 were prepared in an effort to produce samples whose viscosity would bracket the 10,000 poise target value (see Fig. 1 and 2). Unfortunately, the trial blends did not bracket the target

viscosity for either blend series. Nonetheless, from the trial blends data, the mixing ratios required to produce 10,000 P blends were estimated to be 66% aged asphalt/34% soft ESO and 42% aged asphalt/58% AC-5 asphalt. The measured viscosity of the test blends prepared at these ratios are shown by the unfilled square symbols in Figures 1 and 2. The amount of soft ESO needed to achieve the target viscosity is considerably less than for the AC-5 due to the lower viscosity of the ESO.

Nearly identical viscosity-temperature relationships are shown for the test blends in Figure 3. Likewise, tan delta values were similar at all three temperatures with the AC-5/aged asphalt blend being slightly lower at 60°C and slightly higher at 25 and 45°C (Table 1). These results are favorable indicating good asphalt rejuvenation potential for the soft ESO both in terms of adequate dispersal of the aged asphalt and the ability to provide an equivalent viscosity as the AC-5 with less sample.

Mixture Characterization. The term mixture refers to a combination of asphalt and road aggregate. The mixture characterization program was designed so that the potential pavement performance of ESO modified asphalts could be related to that of an asphalt modified with a more conventional material with known field performance. This was accomplished by on-site sampling of ~40 Kg of hot mix (containing no modifier) during construction of an asphalt overlay research project during September 1990 (Pulaski County, Ky.). For this project, several test strips were constructed from a single asphalt blended with different commercial modifier agents. The test strips were placed on a long term monitoring schedule and samples of each asphalt/modifier blend were returned to the laboratory for testing. So, by blending the ESO with the same hot mix and subjecting this asphalt/ESO blend to the same lab tests as the field samples, a more realistic assessment of pavement performance could be obtained.

The field sampled hot mix was divided into two portions. The first portion was mixed with the "hard" ESO at the same proportions as the polymer modified mixtures. This was to compare the behavior of the hard ESO modified asphalt to the asphalts modified with commercial agents. The second portion was aged in a forced draft oven at 80°C for two weeks prior to mixing with the "soft" ESO. This was in order to test the soft ESO as a pavement recycling agent. An additional 4 Kg of the aged mixture was set aside for extraction and binder characterization. Mixture characterization included a series of mechanical response tests on compacted specimens (Marshall procedure; ASTM 1559) directed at evaluating the performance potential of the "hard" ESO modified asphalt mixture relative to the conventional polymer modified asphalts (brands "A" through "D"). All statistical comparisons were conducted at 95% level of confidence.

Tensile Strength Characterization. Fatigue and durability of asphalt pavements are believed to be related to tensile strength. It is customary to characterize tensile strength of pavement materials indirectly in accordance with ASTM-4123. Figure 4 shows the 'hard' ESO blend has tensile strength properties that are superior to the control mixture (unmodified, aged hot-mix) and are on par with two of the high tensile strength polymer modified asphalts. Taken alone, these results indicate desirable fatigue and durability performance potential for the "hard" blend ESO. However, previously reported results suggest that the aging characteristics of a 'hard' ESO blend that has not been subjected to some sort of pre-aging treatment may lead to early pavement failure.[5,6]

Moisture Damage Characterization. Asphalt binder stripping from aggregate is a moisture induced effect. The potential for this type of damage is often characterized in the laboratory in accordance with the Root-Tunnicliff test[8]. The mean tensile strength data shown in Figure 4, along with statistical analyses of the data, indicates that the 'hard' ESO moisture damage susceptibility compares favorably with the control mixture and was not significantly different than at least two of the polymer modified mixtures. Nonetheless, the data show that 'hard' ESO modified asphalt is somewhat susceptible to binder stripping.

Freeze-Thaw Damage Characterization. The potential susceptibility to freeze-thaw damage was characterized, again using tensile strength as an index parameter. Mixtures were subjected to 100

cycles of freeze and thaw (3 hours at -18°C, followed by 3 hours at +4°C). Cross comparisons (Figure 4), along with statistical data analyses, revealed no statistically significant change in tensile strength after 100 cycles of freeze-thaw. Evidently, more freeze-thaw cycles would be necessary in order to induce significant mixture differences.

Rejuvenated Mixture Characterization. Asphalt aging/oxidation severely reduces the tensile strength properties of an asphalt-aggregate mixture as demonstrated by the substantial decline in tensile strength of the aged control sample plotted in Figure 5. Addition of "soft" ESO to the aged mixture resulted in a notable increase in tensile strength, comparable to that from adding AC-5 asphalt. However, ESO addition did not restore the tensile strength to the level prior to aging. This phenomenon in not untypical and has led to a common practice of adding fresh hot mix to the recycled mixture along with the rejuvenating agent. Nonetheless, the mixture rejuvenation analysis shows the "soft" ESO to have potential asphalt recycling applications and merits further examination.

Summary. Two samples of eastern shale oil (ESO), one a hard ESO and the other a soft ESO, produced in the Kentort II process, were evaluated for potential use with paving asphalts. The hard ESO material was evaluated as an asphalt additive and the soft ESO was evaluated as an asphalt recycling agent to soften both an aged asphalt and an aged asphalt-aggregate mix.

The 'hard' ESO added at 7 wt. % to an AC-20 asphalt showed unfavorable susceptibility to moisture damage. An improvement in tensile properties of the aged asphalt mixture was achieved through addition of the hard ESO, however, this effect is likely to diminish rapidly with time due to previously reported aging characteristics.[5,6]

Both soft ESO and AC-5 asphalt were used to soften a hardened asphalt extracted from a laboratory-aged pavement mixture. The rheological properties of the aged asphalt/soft ESO blend were essentially the same as those of the aged asphalt/AC-5 blend. This finding was verified by mixture rejuvenation analysis. The amount of ESO required to soften the aged asphalt was less than the amount of AC-5 due mostly to the lower viscosity of the soft ESO. However, the large negative deviation of the ESO blending curve suggests that even at equal viscosity, the soft ESO would exhibit more softening per unit weight. Overall, the soft ESO appears to have potential application as an asphalt rejuvenating agent.

Recommendations. Previously reported results indicate that the 'hard' ESO was unstable or reactive for some time following preparation. Measurement and control of this phenomenon is an important step that must be addressed prior to further testing since a chemically and thermally stable material is necessary for paving applications. Further mixture studies are needed to fully characterize both short-term and long-term performance potential of ESO modified/rejuvenated asphalts. Field trial projects are recommended for verification of laboratory test results.

Acknowledgements. The authors would like to express their appreciation to Mr. J, Button and Mr. S. Greer of TTI who extracted and recovered the aged asphalt, and to J.M. Wolf, and F.A. Reid of the WRI who conducted the blending and aging experiments under subcontract to the UK-CAER. Mr. R. Pemberton of Ashland Oil is acknowledged for supplying the AC-5 asphalt binder. This work was supported in part by the Morgantown Energy Tech. Ctr., USDOE, under Coop. Agreement DE-FC21-90MC27286 through subcontract with the UK-CAER (such support does not constitute an endorsement by the USDOE of the views expressed in this article).

References

1. Carter, S.D., Rubel, A.M., Taulbee, D.N., and Robl, T.L., The Development of the KENTORT II Process for Eastern Oil Shale: Final Report, Report to USDoE, Laramie Project Office, Coop. Agreement No: DE-FC21-86LC11086, Univ. of Ky.-Ctr. for Appl. Energy Research, Lexington, KY, March, 1990, 208 p.

2. Carter, S.D., and Taulbee, D.N., *Proc.: 1989 Eastern Oil Shale Symp.*, Univ. of Ky. Inst. Mining and Minerals Res., *pub.*, Lexington, Ky., **IMMR89/201**, 1990, 511-518.

3. Lukens, L.A., *22nd Ann. Oil Shale Symp. Proc.*, Colorado School of Mines, April, 1989, pp 199-206.

4 Sinor, J.E., DOE report **DOE/MC/11076-2759**, July 1989.

5. Mahboub, K., Simpson, A., Oduroh, P.K., Robertson, R.E., Harnsberger, P.M., Taulbee, D.N., Rubel, A.M., *Proc.: 1991 Eastern Oil Shale Symp.*, Inst. Mining & Minerals Res., Lexington, Ky., Nov. 1991, in print.

6 Mahboub, K., Simpson, A., Oduroh, P.K., Robertson, R.E., Harnsberger, P.M., Taulbee, D.N., Rubel, A.M., submitted to *Fuel*, Jan., 1992.

7. Goodrich, J.H., *Proc.: Assoc. of Asphalt Paving Tech.*, **57**, 1988.

8. Tunnicliff, D.G., and Root, R.E, Report #174, Ntl. Coop. Highway Res. Prog., Washington, D.C., 1987.

Table 1. Rheological Properties of Aged Asphalt Blended With Soft ESO and AC-5 Asphalt.

Binder	Dynamic Viscosity, 60°C, Poise	Tan Delta
66 wt.% Recovered Asphalt/34 wt.% Soft ESO	1.244×10^4	6.112
42 wt.% Recovered Asphalt/58 wt.% AC-5	1.376×10^4	5.973
Binder	**Dynamic Viscosity, 45°C, Poise**	**Tan Delta**
66 wt.% Recovered Asphalt/34 wt.% Soft ESO	1.576×10^5	2.513
42 wt.% Recovered Asphalt/58 wt.% AC-5	1.627×10^5	2.721
Binder	**Dynamic Viscosity, 25°C, Poise**	**Tan Delta**
66 wt.% Recovered Asphalt/34 wt.% Soft ESO	5.077×10^6	1.582
42 wt.% Recovered Asphalt/58 wt.% AC-5	6.187×10^6	1.738

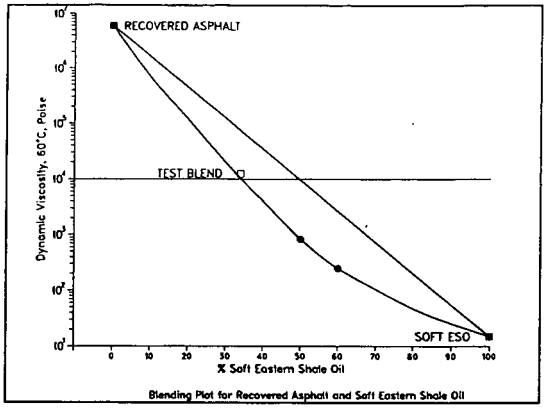

Figure 1. Viscosity of blends from aged asphalt/soft ESO blends.
●-trial blends; □-blend used for mechanical testing.

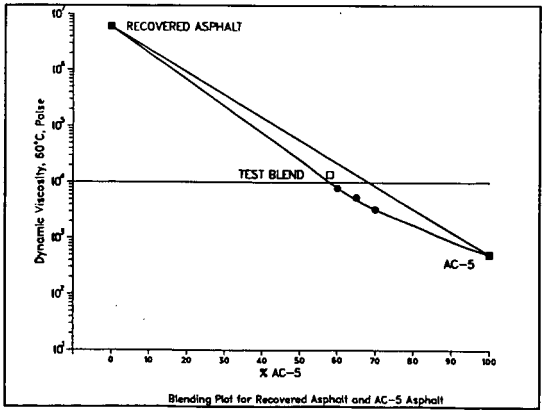

Figure 2. Viscosity of blends from aged asphalt/AC-5 blends.
●-trial blends; □-blend used for mechanical testing.

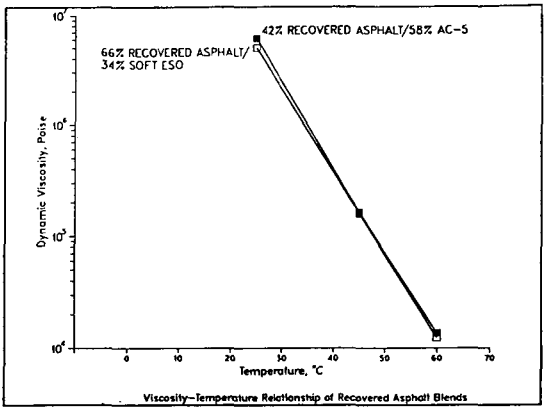

Figure 3. Viscosity-Temperature plots. □-soft ESO/aged asphalt (34%/66%); ■-AC-5/aged asphalt (58%/42%).

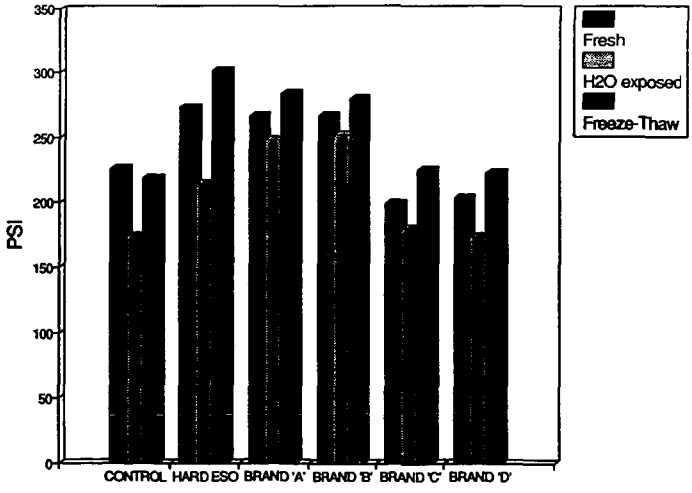

Figure 4. Tensile strength data for series of modified pavement mixtures. Samples were tested following preparation, moisture susceptibility analysis, and 100 freeze-thaw cycles. Control is pavement mixture without added modifier.

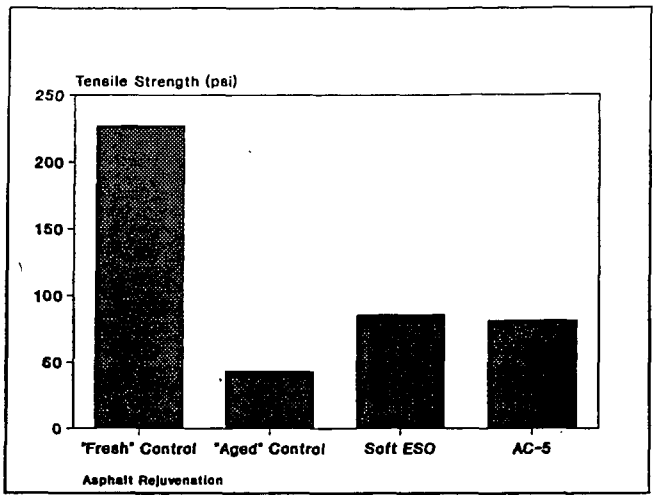

Figure 5. Tensile strength test series for fresh pavement mix, aged mix, and mix rejuvenated with either soft ESO or AC-5.

Market Enhancement of Shale Oil by Selective Separations

James W. Bunger, Prasad A. V. Devineni and Donald E. Cogswell
James W. Bunger and Associates, Inc.
Box 520037, 2207 West Alexander Street
Salt Lake City, UT 84152-0037

Joel B. DuBow, Huaying Huai and Jacek P. Dworzanski
Center for Microanalysis and Reaction Chemistry
University of Utah
Salt Lake City, UT 84112

Keywords: shale oil, separations, gc-ms

Introduction

The recent history of petroleum availability and price has shown that petroleum substitutes are not economically viable as long as there is a stable supply of conventional petroleum. The additional costs for recovery and upgrading are not sufficiently offset by product values to attract private risk capital without supports or subsidies. In order to create an economically viable synthetic fuels industry, it is becoming clear that some research must be directed at market enhancement technologies, in addition to the more traditional view of cost reduction (recovery and processing) technologies.

Recognizing this requirement, James W. Bunger and Associates, Inc. (JWBA), in concert with the Center for Microanalysis and Reaction Chemistry (MARC), at the University of Utah, has initiated a program aimed at technology for isolation and manufacture of high-value products from unconventional hydrocarbon resources. We refer to this technology as the Natural Products Extraction (NPX) technology. One such initiative is aimed specifically at high-value products from shale oil -- a U. S. natural resource of more than 1-trillion bbls-oil, in place. When compared with conventional crude oil, shale oil is characterized by its high percentage of heteroatom (N, S and O) containing molecules, its high level of mono- and di-cyclic compounds and relatively high percentage of vacuum gas oil.

For successful development of a high-value product slate from shale oil, we must focus on those structural characteristics which are present in higher concentrations in shale oil than in crude oil and which possess proven, or unique, chemical applications. Also, it is clear that isolation of distinctive structural types must, of necessity, adhere to fundamental thermodynamic principles. Therefore, separations process technology must be based on a fundamental understanding of shale oil composition and the relationship of that composition to partitioning during separation.

This paper reports results of our initial attempts to identify and isolate fractions from shale oil of potential market value, to confirm a suitable analytical methodology as a basis for process and product development, and to delineate the economic parameters of market enhancing technology.

Analytical Methodology

In prior work (1-3), it had been determined that thermodynamic properties of molecules correlate well with structural parameters 'n' and 'z' (defined by the formula $C_nH_{2n+z}N_uS_vO_w$) and 'i', a non-integer number which relates to isomeric variations. The indices 'n' and 'z' (with 'u', 'v' and 'w'), establish the molecular weight and define the essential skeletal structure. These parameters, which can be obtained from high resolution, parent peak mass spectroscopy, correlate well with enthalpic properties of the molecule. The parameter 'i', is a strong function of entropic properties. Preliminary evidence suggests that 'i' may be measured indirectly through chromatographic retention time (2).

The development of the classifying system and correlating functions has been collectively labeled the Z-Based Structural Index Correlation Method (Z-BASIC) (2). The Z-BASIC method allows, for the first time, the ability to track the separation behavior of individual species from shale oil. This provides the theoretical basis for process modeling on a molecular level. Coupled GC-MS-FTIR technologies available at the MARC, were used to demonstrate the viability of Z-BASIC for calculation of partition functions of molecular species.

Given the ability to develop separations technologies using fundamental molecular science, we organized a logical development strategy. Figure 1 shows the information flow for this strategy. The flow diagram shows that detailed analytical data is translated into mathematical terms which provide a rigorous basis for process simulation. The simulation becomes the controlling function for modifying the processes to manufacture a specification product. Where specifications cannot be met by

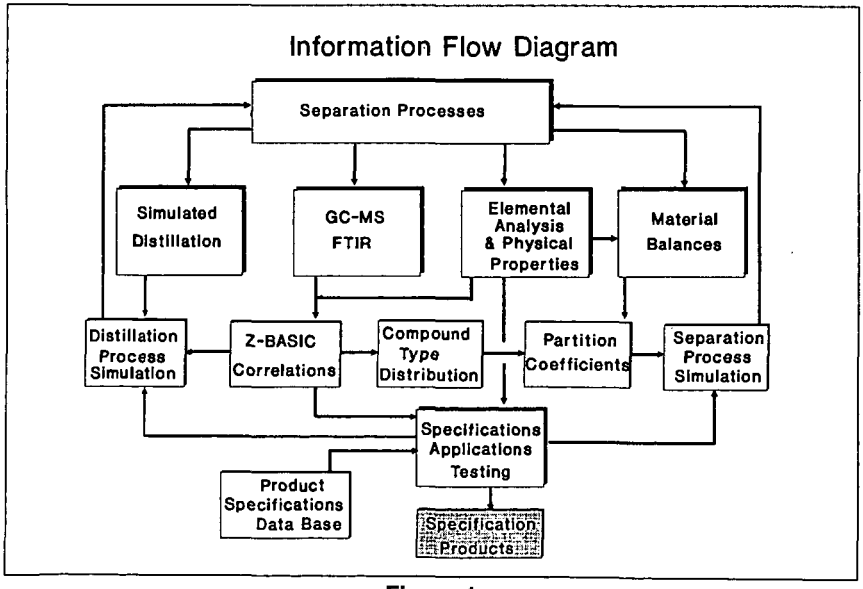

Figure 1

separations processing alone, a comparison between actual concentrate structure and desired concentrate structure will help delineate any additional processes required.

Separation of Shale Oil

Theoretical arguments suggest that attempts to separate a broad molecular weight mixture on the basis of polarity, will suffer from lack of definitiveness between molecular weight and polarity effects. Therefore, the logical initial step in a separation sequence is distillation, a process which provides fractions of narrower molecular-weight ranges.

Figure 2 shows the distillation scheme used in this study and the resulting weight percent yield of each fraction. Figure 3 shows the total ion chromatograms of the individual fractions showing the complexity of the fractions. In general, shale oil lacks homology on the basis of distillation alone, with the notable exception of the concentration of paraffins in the 350 - 440°C fraction.

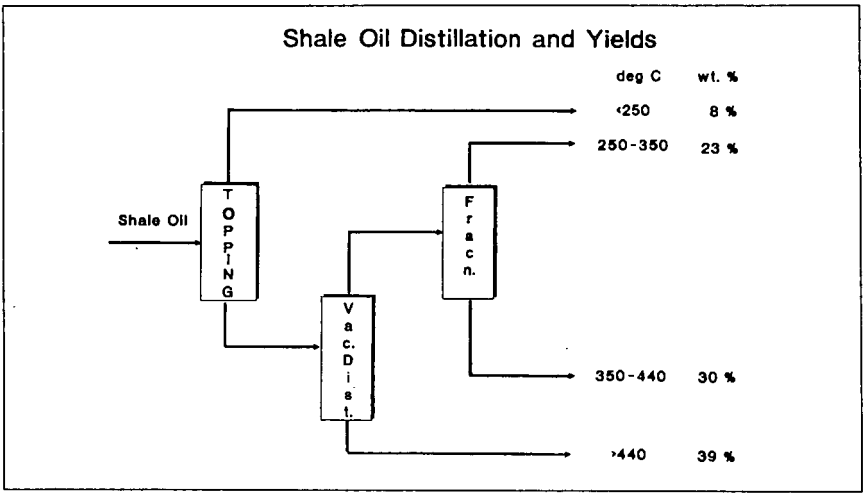

Figure 2

Figure 4 represents the heteroatom distribution as a function of boiling point and shows that while sulfur and oxygen are less dependent on boiling point, nitrogen increases significantly with boiling point. The unusual shape of the oxygen distribution is thought to be indicative of differing types dominating the lower-molecular-weight range as compared to the higher-molecular-weight range. These types have not been fully characterized.

Distillate fractions may be subjected to liquid-liquid extraction with polar solvents to separate concentrates according to polarity. Candidates for polar solvent separation include phenol, furfural, N-methyl-2-pyrrolidone and other polar solvents such as alcohols, ketones, organic and mineral acids, and organic bases. Two-phase partitioning was successfully achieved with several of the aforementioned solvent systems.

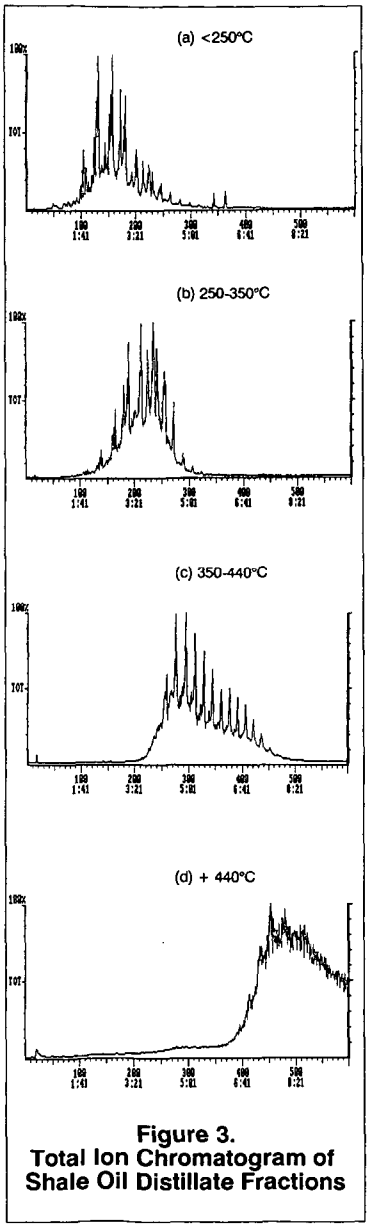

Figure 3.
Total Ion Chromatogram of Shale Oil Distillate Fractions

Laboratory separations were conducted in a small-scale, batch-type processes and quantitative results must be further confirmed before publication. Laboratory conditions were designed to simulate commercially-realistic conditions, e.g., solvent-to-oil ratios of 1:1. In commercial practice, up to five sequential separation/distillation steps are envisioned.

The laboratory separations produced 16 specific concentrates covering four boiling ranges and four polarities. The overall yield and elemental composition of the fractions separated are given in Table 1. For purposes of illustration, the fractions were lumped according to similar polarities. The four major concentrates are labeled "White Oils and Waxes", "Aromatic Oils", "Low Polarity Nitrogen Compounds" and "High Polarity Compounds".

The elemental compositions of these concentrates illustrate the differences achievable with relatively straight-forward and inexpensive separations. The white oils and waxes are extremely low in heteroatoms, including sulfur. Oxygen is calculated by difference and is, therefore, subject to a wider margin of error. The aromatic oil fraction is particularly interesting because it possesses a low nitrogen content while constituting a significant portion of the shale oil barrel.

The major fraction is the low-polarity nitrogen compounds. These materials are of a higher molecular weight and thought to possess carbazolic and aromatic nitrogen. The high-polarity compounds are of a lower molecular weight and contain acidic, phenolic, nitrilic, pyrrolic and pyridinic functionalities.

Product Slate

Based on our laboratory separations and knowledge of the structural types present, a projected product slate for shale oil was constructed. The product slate is compared to current U. S. market volumes and prices. Results are shown in Table 2.

The product slate includes oils, waxes, aromatic oils, aromatics for manufacture of sulfonates, acids, bases and resins. Functionalized intermediates are compounds containing nitrogen or oxygen and which are thought to be of particular value as starting materials for derivatization to pharmaceuticals, industrial chemicals and other pure compound systems. Pure compounds are those with particularly high market

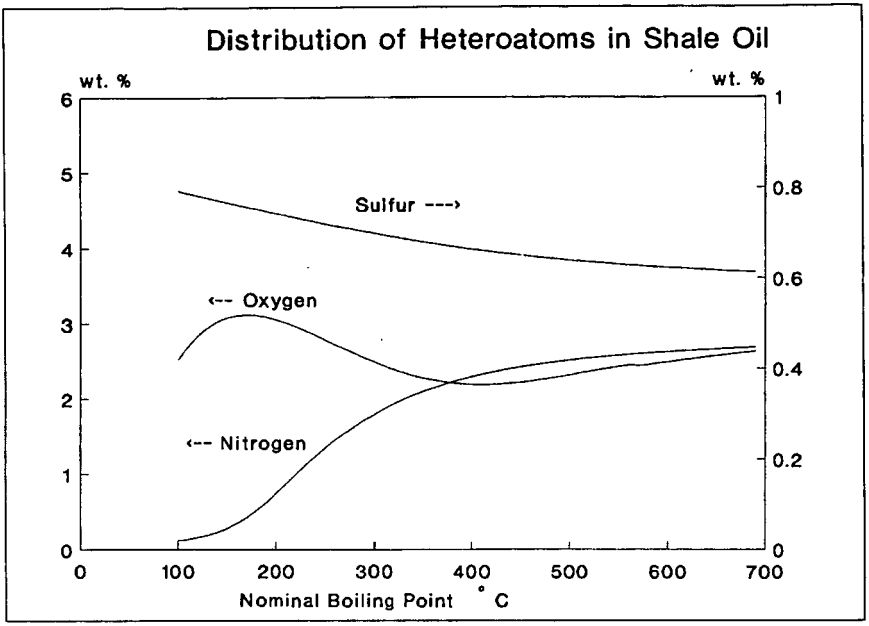

Figure 4

Table 1
Summary of Elemental Composition by Functional Concentrate

Concentrate	Wt % of Shale Oil	C	H	N	S	O (Diff)	H/C
White Oils and Waxes	13	85.7	13.8	0.05	0.02	0.26	1.92
Aromatic Oils	22	87.0	12.1	0.2	0.6	0.5	1.66
Low-Polarity Nitrogen Compounds	35	83.6	10.4	3.2	0.7	3.4	1.47
High-Polarity Compounds	30	82.7	10.6	2.8	0.8	3.2	1.52

value that may be isolable in a pure form from shale oil. Target compounds include nitriles, pyridines, quinolines, amines, amides, phenols, naphthols and carboxylic acids.

The special applications concentrates represent mixtures of particular properties which makes the concentrate marketable in its mixed form. Examples include industrial antimicrobials, coatings, wood preservatives, industrial surfactants and asphalt additives. We currently project that less than 10% of the shale oil barrel may require marketing as a fuel or refinery feed.

Table 2
Demand and Value of Products
Output of SO/NPX = 170,000 Tons/year (3,000 bbl/day)

Product	Market Volume Tons/year	Recent Price $/bbl-equivalent		SO/NPX Projected Yield Wt. % of Feed	% of Market	Revenue $/feed-bbl
White Oils	4,575,000	84	Ref (4)	13.3	0.5	11.2
Waxes	882,000	133	Ref (4)	5.0	1.0	6.6
Aromatic/ Lubricating Oils	9,526,365	60	Ref (4)	30.5	0.5	18.3
Sulfonate Feeds	333,900	142	Ref (5)	11.7	5.9	16.6
Tar Acids and Bases	830,000	210	Ref (6)	4.0	0.8	8.4
Resins	542,000	120	Ref (7)	14.7	4.6	17.6
Functionalized Intermediates	130,000	178	Ref (7)	4.3	5.6	7.6
Special Application Concentrates	500,000	28	Ref (6)	10.3	3.5	2.9
Pure Compounds	200,000	135	Ref (7)	0.7	0.6	0.9
Fuels and Refinery Feeds	large	15	Ref (8)	5.5		0.8
Totals				100		$90.90/bbl

The majority of the anticipated products are targeted for conventional commodity markets for which the market is well established. Maximum economic enhancement of a commercial shale oil facility will occur most readily when a large percentage of the shale oil product slate addresses large, well-established markets. The primary questions which remain and must be addressed in future research relate to the quality of the product and the finishing steps that are required to make the shale oil products market-acceptable.

It is recognized that certain products such as functionalized intermediates and special application concentrates may require significant market development. While this requirement may be an inhibiting factor in the short term, in the long term it raises exciting prospects for development of new materials, new chemical routes and new precursor chemicals, unique to shale oil.

Cost and Profitability Estimates

In order to establish the economic framework for our research, an attempt was made to estimate the process costs, and from projections of the product value, to estimate the profitability of a Shale Oil Native Products Extraction venture. The feed stream to the process facility is a raw, retorted shale oil which we charge to the facility, in the base case, at $30/bbl.

The capacities of the unit operations required to produce the product slate shown in Table 2, were estimated based on conceptual flow diagrams (not shown). Costs for the unit operations were determined from analogy to commercially-practiced technologies. The results are given in Table 3.

Results show that process costs of approximately $15/bbl are anticipated. Results also show that the shale oil barrel is subjected to an average of five process steps to make the product slate priceable at the values given in Table 2. Item -7 represents unspecified finishing steps through which the entire

Table 3
Estimated Process Costs for SO/NPX
(Basis: 1,065,000 bbl/year)

	Unit	Process Cost $/bbl	Throughput bbl/yr	Operating Costs $M/yr
1.	Distillation	1.5	1,065,000	1.60
2.	Liquid-Liquid Extraction	2.7	1,065,000	2.88
3.	Adsorption	4.2	958,500	4.03
4.	Dewaxing	3.2	95,850	0.31
5.	High-Efficiency Separation	4.5	60,705	0.27
6.	Hydrofinishing	2.1	777,400	1.63
7.	Miscellaneous (Filtration, Precipitation, Crystallization, etc.)	4.0	1,065,000	4.26
Annual Manufacturing Costs				$14.98M

output of the process facility is charged. This represents a contingency to account for currently unknown process requirements.

In order to account for marketing and distribution costs, a $5/bbl charge is added to the operating costs. This allows for an average shipping radius of about 500-750 miles. Higher value products, e.g., $100/bbl +, may be shipped further. Lower value products, e.g., asphalt additives, may be used locally or regionally.

Capital costs were estimated by summing the unit costs weighted for throughput capacities. A capital cost of $120-million is projected for the 5,000 bbl/day case.

The profitability estimates are shown in Figure 5. Part a) shows the capital cost and return on investment as a function of capacity; parts b) and c) provide the sensitivity to the weighted average product value and raw shale oil costs, respectively; part d) shows the profitability analysis as a function of cost of raw shale oil and plant capacity. The profitability estimates have been made for the 100% equity case, using a 10% discount rate. The profit on investment for various debt-to-equity ratios can easily be estimated by multiplying the DCF/ROI for the 100% equity case by the ratio.

The economic assessments show that an increase in average product value rapidly offsets the process and raw material costs. The incremental price/cost differential promises significant profits on investment capital and a significant return on investment could be made, even if shale oil costs were $40/bbl. Maximum profitability comes from the largest SO/NPX facility that the market will bear.

Conclusions

Commercial viability of synthetic fuels may be enhanced through technology for producing products of high market value. To pursue this objective, we have developed and demonstrated an analytical methodology which forms the basis for a process development strategy. This strategy promises an effective approach to maximizing the value of products isolable, or derivable, from shale oil.

Shale oil has been fractionated according to a simplified laboratory scheme using distillation, liquid-liquid extraction and liquid-solid adsorption, and the products have been characterized. Based on these results, a projected product slate has been constructed. The promised value of the product

Figure 5

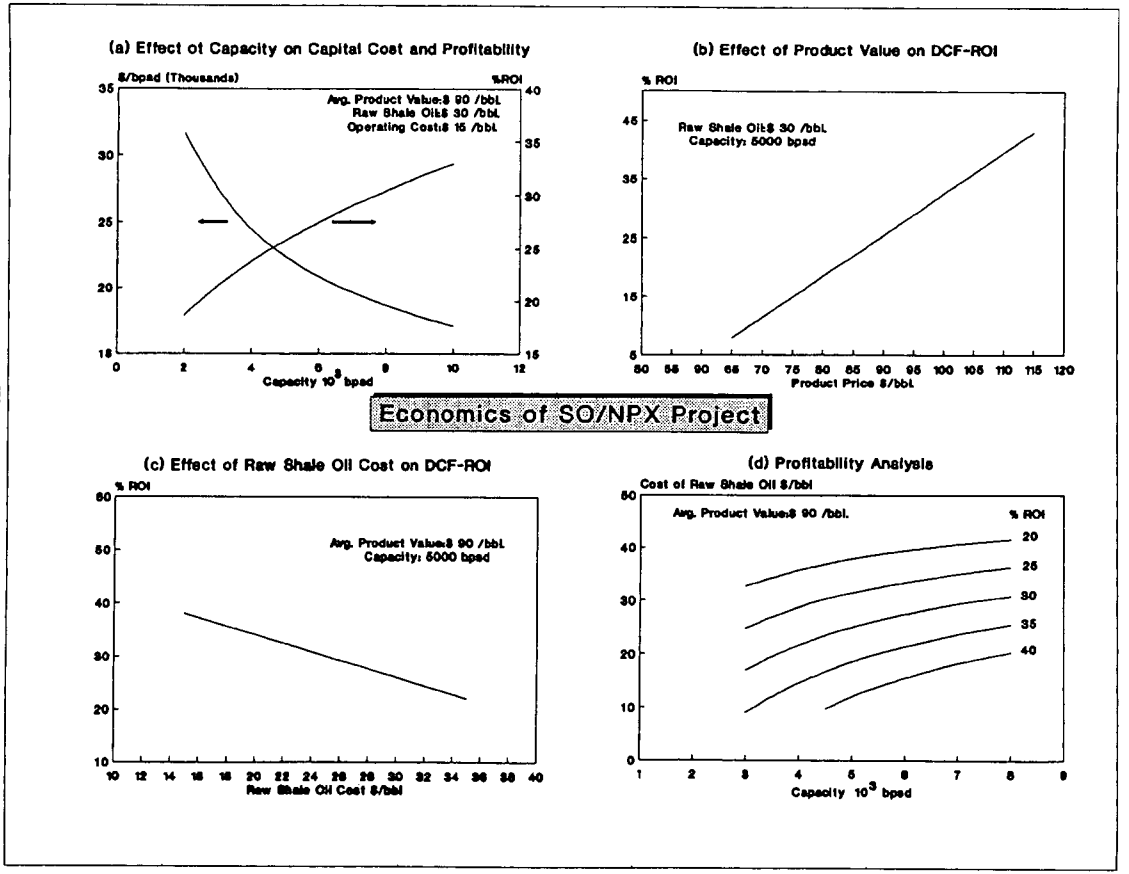
(a) Effect of Capacity on Capital Cost and Profitability
$/bpad (Thousands)
%ROI
Avg. Product Value:$ 90 /bbl
Raw Shale Oil:$ 30 /bbl
Operating Cost:$ 15 /bbl
Capacity 10^3 bpad
(b) Effect of Product Value on DCF-ROI
% ROI
Raw Shale Oil:$ 30 /bbl
Capacity: 5000 bpad
Product Price $/bbl
Economics of SO/NPX Project
(c) Effect of Raw Shale Oil Cost on DCF-ROI
% ROI
Avg. Product Value:$ 90 /bbl
Capacity: 5000 bpad
Raw Shale Oil Cost $/bbl
(d) Profitability Analysis
Cost of Raw Shale Oil $/bbl
Avg. Product Value:$ 90 /bbl.
% ROI
20
25
30
35
40
Capacity 10^3 bpad

slate readily offsets the incremental process costs and shows promise for economic profitability. This work provides a sound basis for detailed process and product research and development.

Acknowledgments

The authors acknowledge Mr. J. W. Wiser for shale oil distillation, Dr. C. P. Russell for analytical and mathematical algorithms, and Mr. S. Valerio for technical assistance in laboratory separations, all of JWBA.

The authors also acknowledge Dr. J. D. Seader for consultation on thermodynamics and separations technology, and Mr. N. Chapman for GC-FTIR analysis, both of the University of Utah.

This work was supported through cooperative agreement DE FC21-90MC27084, between the U. S. Department of Energy and Occidental Oil Shale, Inc., under the project management of Dr. Ray Zahradnik. This support is gratefully acknowledged.

References

1. Bunger, J. W., Devineni, P. A. V., Russell, C. P., and Oblad, A. G., "Structure of Future Jet Fuels - A Model for Determining Physical and Chemical Properties from Molecular Structure", Preprints, Division of Petroleum Chemistry, 30(1), 1987.

2. Devineni, P. A. V., " A Model for Correlating Properties with Molecular Structure and Its Application to Fuel/Hydrocarbon Processing", Ph.D. Thesis, Dept. of Fuels Engineering, University of Utah, 1989.

3. Devineni, P. A. V., Bunger, J. W., and Russell, C. P., "Preduction of Optimum Structure for Jet Fuel Components Using the Z-BASIC Method", Preprints, Division of Petroleum Chemistry, 1989.

4. 1988 Report on U. S. Lubricating Oil Sales - National Petroleum Refiners Association.

5. Chemical Economics Handbook - SRI International, #543.8050A, 1987.

6. Sinor, J. E., "Niche Market Assessment for a Small Scale Western Oil Shale Project", Final Report, U. S. DoE, 1989.

7. United States Production and Sales, 1988 - Synthetic Organic Chemicals - U. S. International Trade Commission Publication.

8. Chemical Marketing Reporter, August 1990.

PROCESS FOR THE PRODUCTION OF PETROLEUM TAR PITCH FOR ANODE MANUFACTURING.

León Velasco,
Francisco García, Gustavo Velutini
Intevep, S.A. PO. BOX 76343
Caracas, Venezuela

Keywords: Petroleum tar pitch, Anode, Aluminium

INTRODUCTION

The aluminium production involves the consumption of petroleum coke and pitch, which are used in the manufacturing of anodes. Normally carbon consumption, as anode, lies between 0.4 and 0.48 Kg of carbon per Kg of metal produced[1]. In the same manner, the amount of pitch used in preparing the anode lies between 14 and 18 mass %, and varies with the chemical composition of the pitch, the porosity and the structure of the petroleum coke.

The estimated amount of pitch required to meet the world aluminium production, for the early 90's, will be in the range of 1.2 million tonnes per year[2]. Additionally, almost all binders used in the manufacturing of electrodes are derived from high-temperature coal treatment during the production of metallurgical coke. However the Enviromental Protection Agency (EPA) regulations on the benzene emissions from coking oven equipment, have lead to recent announcements of numerous coking oven closures in the United States[2]. According to PACE Consultants[2], metallurgical coke output in the US is expected to plummet to 17 million short tonnes by 1996 from 25 million short tonnes in 1990.

Coke battery closures in the US, resulting from the EPA mandates, should reduce the supply of good quality coal tar pitch in the US by as much as 25 to 30 %[2]. One can assume that a similar trend should be observed in other major areas of coal tar pitch production.

Naturally, it is highly desirable to provide a continous closed-process for the producction of high quality tar pitch suitable for electrode manufacturing. In this sense, INTEVEP the R&D Center of Petroleos de Venezuela, has carried out a research project to develop a process scheme for the production of a high quality petroleum pitch for use as a binder in anode manufacturing, using Fluid Catalytic Cracking Decanted Oil as feedstock. This paper presents results of this research as well as properties of the petroleum pitches obtained.

EXPERIMENTAL RESULTS

Feedstock selection and characterization: The main characteristic of coal tar pitch is that it is a highly condensed material with an aromatic content higher than 90 volume %. With this in mind, FCC decanted oil, a highly aromatic refinery stream, was selected as the feedstock. Table 1 presents the properties of this material.

Process Description: The process for the production of petroleum tar pitch was developed using Intevep's pilot plant facilities. The process route and product yields are shown in the fig.1 and table 2, respectively. The fresh feed, decanted oil, is fed to the filter so as to remove undesirable solids, mainly FCC catalyst particles, the clean filtered stream is thereafter fed to a preheater-coil heater where the temperature is increased to 430 °C. The heated feedstock is treated in a soaker type reactor, where sufficient residence time is provided for polymerization and condensation reactions to take place. Four different residence times were considered (TR1: 39 min, TR2: 78 min, TR3: 117 min, and TR4: 156 min). The stream leaving the soaker is sent to a high pressure separator, where C_4 minus hydrocarbons and light distillates are taken off from the top, and a heavier fraction is withdrawn from the bottom. The heavier fraction is finally sent to a reduced pressure pipe still so as to produce a gasoil and a petroleum pitch. By carefull selection of pressure and temperature in this final stage a high quality petroleum tar pitch can be produced.

Pilot Plant yields and product characterization: Table 2 presents typical yields and product qualities obtained when the decanted oil is processed at a temperature of 430 °C and a pressure of 15.6 bar-a. Carbon value (CCR), density and softening point meassurements showed that residence times TR1 and TR2 were not sufficient to yield a highly condensed petroleum pitch.

Petroleum pitch selection and preparation: From table 3, pitch TR3 has properties similar to those of a typical coal tar pitch used for anode manufacturing, on the other hand, pitch TR4 has higher softening point and viscosity values than those found for coal tar pitch. Nevertheless, its higher carbon content ought to yield a denser anode. In order to improve on these properties and still benefit from the high severity conditions at which this pitch was obtained, pitch TR4 was mixed with another aromatic and lighter petroleum fraction known as light cycle oil. The resultant mixture, TR4D contained 7 volume % of light cycle oil.

Finally, bearing in mind the importance of quinoline insolubles, as a coal tar pitch quality guideline, a fourth pitch TR4DNH was prepared by adding 7 mass % of carbon black to the TR4D pitch.

Evaluation of Intevep Petroleum Pitches: Four samples of petroleum pitch (TR3, TR4, TR4D and TR4DNH) were sent to a specialized laboratory in Switzerland, for analysis as a binder material for the production of carbon anodes for the aluminium industry. The work involved the determination of physical and chemical properties of each pitch as well as production and testing of a series of bench scale test anodes according to this particular laboratory's standard procedure. Physical and chemical properties of the pitches evaluated are presented in Table 3., together with corresponding values of a typical commercially available petroleum pitch and standard coal tar pitches used in the aluminium industry. For each pitch a series of 20 cylinders (50 mm in diameter) were produced at four separate pitch levels, these are 14, 16, 18 and 20 mass %. For each series mechanical properties, reactivity in CO_2 and air, and chemical analysis were performed.

DISCUSSION:

PITCHES

General: The main differences observed between coal tar and petroleum pitches are as follows:

- At comparable viscosity levels the softening point of the petroleum pitch is about 5 to 10 °C higher. This is due to the different temperature-viscosity interdependence of the two products.
- Petroleum pitches contain hardly no quinoline insolubles (QI). The QI present in coal tar pitches are due to the carry over from the coke oven during the carbonization process of mineral coal.
- The amount of QI in coal tar pitch reflects the severity of the pyrolisis and therefore, the pitch aromaticity, so that the aluminium industry specifies QI levels very closely. However, for petroleum pitches the aromaticity is independent of the QI content thus it is not relevant to consider this property in its specifications.
- Density in water of petroleum pitches is about 5-10 % lower than that for coal tar pitches (this being due to the different nature of the organic compounds) but is not detrimental as long as the coking value lies in an acceptable and comparable range to that of coal tar pitch. Furthermore, it is important to point out that previous work found in the literature has shown that anodes produced from petroleum pitches are inferior in baked density, strength and air permeability to those produced from traditional coal tar pitches. However, petroleum pitches have been successfully used as a binder in the aluminium industry where they have been specifically developed for a particular end user[3]

Softening point: TR4 pitch was found to be extremely hard and viscous, with a softening point that would make it unpractical for mixing in the paste plant.

TR3, TR4D and TR4DNH showed softenig points that are more usual. The viscosities also fall withing the typical values found for thermally cracked petroleum pitches.

Insolubles in toluene: Toluene insolubles is the most significant property for distinguishing between a thermally cracked and oxidized petroleum pitch. Values below 10 mass % for TR3, TR4, TR4D and the commercially available pet-pitch, illustrate the fact that they were produced by a thermal process. The higher value observed for the TR4DNH pitch is a result of the addition of about 7 mass % of carbon black, as artificial QI.

Insolubles in quinoline: This fraction is almost zero, as would be expected for a thermally cracked petroleum pitch. The TR4DNH sample has been blended with 7 mass % of carbon black, therby allowing for the effect of artificial addition of QI to be quantified.

Coking value: The coking value was higher than typically expected for all four petroleum pitches under consideration. This is advantageous in anode production

since the greater the amount of residual coke, the higher the anode baked density (assuming all others parameters remain constant).

Distillation: The distillation of the TR4D and TR4DNH samples is their biggest drawback, as far as pitch properties are concerned, especially in the 0-270 °C range. The amount of these volatiles as well as their carcinogenic nature would pose significant problems in the paste plant. In the case of TR4D, this amount (6.57 mass %) in the 0-270 °C range is a direct result of the addition of a light cycle oil during the pitch preparation.

For TR3 and TR4; fractions obtained during distillation are much lower and can be considered more typical.

Density in water: TR3 pitch shows a value which is within the typical range for thermally cracked petroleum pitches, whereas the other three samples show lower but acceptable values for this property.

Elemental analysis: The elemental impurities of the four pitches are typical and would be acceptable to the aluminium industry.

BENCH SCALE ANODES AND PROPERTIES

Figures 2, 3, and 4 present the results of the evaluation of the bench scale anodes prepared with each of the INTEVEP petroleum pitches. Following is a discussion of the most relevant aspects of this evaluation:

TR3 Pitch (Fig. 2):

The optimum pitch content is around 14% this being 2% absolute less than for a typical coal tar pitch. This fact is of great financial consideration as the price of pitch is usually twice that of the coke. At this optimum the physical properties of anodes are within the range of those obtained with coal tar pitches. Although the compressive strength is at the lower end of the range this will not be too serious a problem if proper mixing, forming and baking conditions are chosen in an industrial scale plant.

As the permeability level (4.8 nPm at 14% pitch) is almost typical (3-4 nPm) for bench scale anodes and as the reactivities in CO_2 and air are quite normal, this pitch will give anodes having an acceptable burning behaviour in the pots.

TR4 (Fig. 3)

The poor wettability of this pitch, evident from the low green and baked apparent densities and the compressive strength, is a direct consequence of the high softening point and subsequent poor mixing during green paste manufacture. This effect becomes particularly evident at 20% pitch addition where the baking loss and shrinkage differ markedly form the trend observed at the lower pitching levels. The CO_2 reactivity is, despite the poor physical properties, better than typical and reflects the good quality of the baked pitch coke resulting from its higher anisotropy.

TR-4D (Fig. 4)

The physical properties of anodes made from this pitch are within the range of those measured for typical coal tar pitch based anodes, the only significant exceptions being air permeability, which is about twice the value typically expected and compressive strength which is at the lower end of the range. Although poor air permeability will result in a higher carbon consumption during electrolysis, this is offset to some degree by the lower CO_2 reactivity losses of the binder-matrix.

TR-4DNH

The addition of 7 mass % carbon black has severly affected the physical properties of the test anodes due principally to a blinding effect that has hindered the wettability of the pitch.

CONCLUSIONS

Intevep TR3

Of the four Intevep pitches tested this was found to be the most siutable as the majority of properties were within typical coal tar ranges. Although the compressive strength of the anodes were at the lower end of the range, a paste plant optimization would improve this behaviour. A significant "selling point" for this pitch is the lower optimum content needed in anode manufacture.

Intevep TR4

The TR4 pitch was unsuitable due to its high softening point resulting in inadequate fluidity and subsequently poor mixing.

Intevep TR-4DNH

The addition of 7 mass % carbon black to TR-4DNH was found to have a detrimental effect on the test anode properties.

Intevep TR-4D

The results indicate that the TR-4D pitch is promising although further investigations would be needed into production techniques that could improve its distillation behaviour, mechanical strength and air permeability.

REFERENCES

1. Grjothein, K. and B. J. Welch, "Aluminium Smelter Technology", 2th. edition, Aluminium Verlag Dusseldorf, Germany, chapter 4.
2. The pace consultants Inc. Petroleum Coke Markets Potential. November 1990.
3. R&D Carbon Ltd. Evaluation Program for Intevep Petroleum Pitches. April 90.

TABLE 1. FCC DECANTED OIL CHARACTERIZATION

SPECIFIC GRAVITY	1.078
API	-0.2
SULFUR % WT	2.6
CCR % WT	6.3
SOLIDS, PPM	15
ASH, PPM	41
FLASH POINT, °C	68
KINEMATIC VISCOSITY, cst	
KV @ 38°C	476
KV @ 60°C	118
AROMATICS, % WT	79
DISTILLATION D-1160	
% VOL	TEMP. °C
5	318
30	408
50	436
80	517

TABLE 2. TYPICAL YIELDS AND PRODUCT QUALITY

YIELDS	
GASES	9.3
LIGHT DISTILLATES	21.1
GASOIL	40.8
PITCH	28.8
LIGHT DISTILLATES CHARACTERIZATION	
SPECIFIC GRAVITY	0.8610
SULFUR, % WT	1.36
DISTILLATION:	
IBP	114
10	167
30	231
50	280
90	370
FBP	372
GASOIL CHARACTERIZATION	
SULFUR, %WT	3.8
SPECIFIC GRAVITY	1.1014
VISCOSITIES, cst	
KV @ 60°C	28.5
KV @ 100°C	5.9
FLASH POINT, °C	207.7
DISTILLATION	
IBP	261
10	334
30	366
50	390
90	442
FBP	490

TABLE 3. PITCH PROPERTIES

PROPERTIES	UNIT	COAL TAR PITCH TYP. RANGE	COMM PET. PITCH	TR-3	TR-4	TR-4D	TR-4DNH
SOFTENING POINT METTLER.	°C	100-110	121.7	129.8	148.5	114.5	121.8
VISCOSITY BY 140 °C	cP	3000-6000	n.m	n.m	n.m	10'250	12'720
VISCOSITY BY 160 °C	cP	600-1500	2140	4280	n.m	1952	2590
VISCOSITY BY 180 °C	cP	150-300	406	696	4820	458	676
DISTILLATION 0-270°C	%	0.1-0.6	0.1	1.4	0.5	6.5	6.8
DISTILLATION 0-360°C	%	4-8	8.4	9.8	8.4	17.5	15.0
DENSITY IN WATER	Kg/dm³	1.30-1.32	1.244	1.240	1.257	1.148	1.151
COKING VALUE	%	54-60	52.8	55.7	58.3	57.2	61.4
WATER CONTENT	%	0-0.2	< 0.1	< 0.1	< 0.1	< 0.1	< 0.1
INSOLUBLE IN QUINOLINE	%	8-14	0.5	1.0	0.4	0.65	7.9
INSOLUBLE IN TOLUENE	%	28-36	8.5	8.9	8.2	10.0	17.5
ASH CONTENT	%	0.1-0.3					
ELEMENTS							
S	%	0.3-0.5	3.01	2.52	2.77	2.48	2.41
Na	ppm	100-400	110	98	82	70	97
Ca	ppm	20-80	21	25	23	17	38
Cl	ppm	100-300	41	34	30	30	37
Al	ppm	50-200	96	285	232	237	227
Si	ppm	50-200	74	271	276	284	398
Fe	ppm	50-300	63	199	146	166	191
Zn	ppm	100-600	15	17	4	5	5

FIGURE 1. INTEVEP PILOT PLANT PROCESS ROUTE FOR THE PRODUCTION OF PETROLEUM TAR PITCH

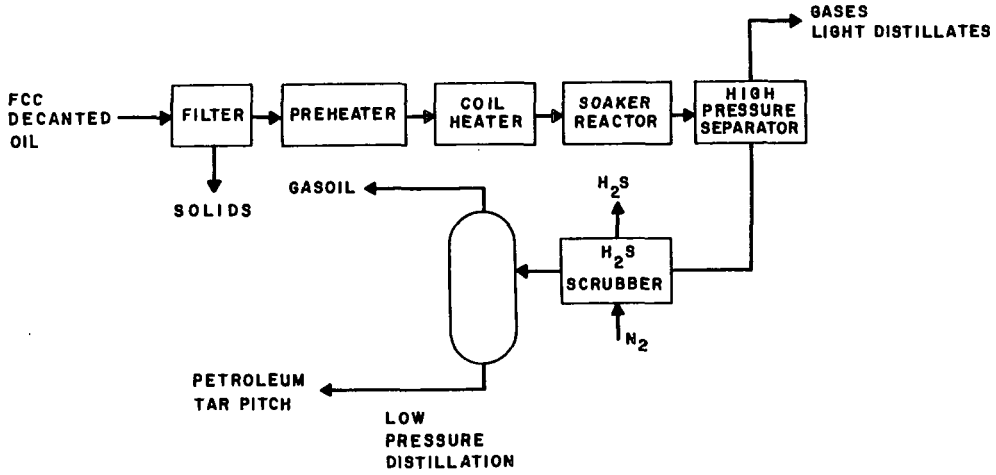

FIGURE 2. BENCH SCALE ANODE EVALUATION USING PITCH TR3

PITCH CONTENT: A = 14% B = 16% C = 18% D = 20%

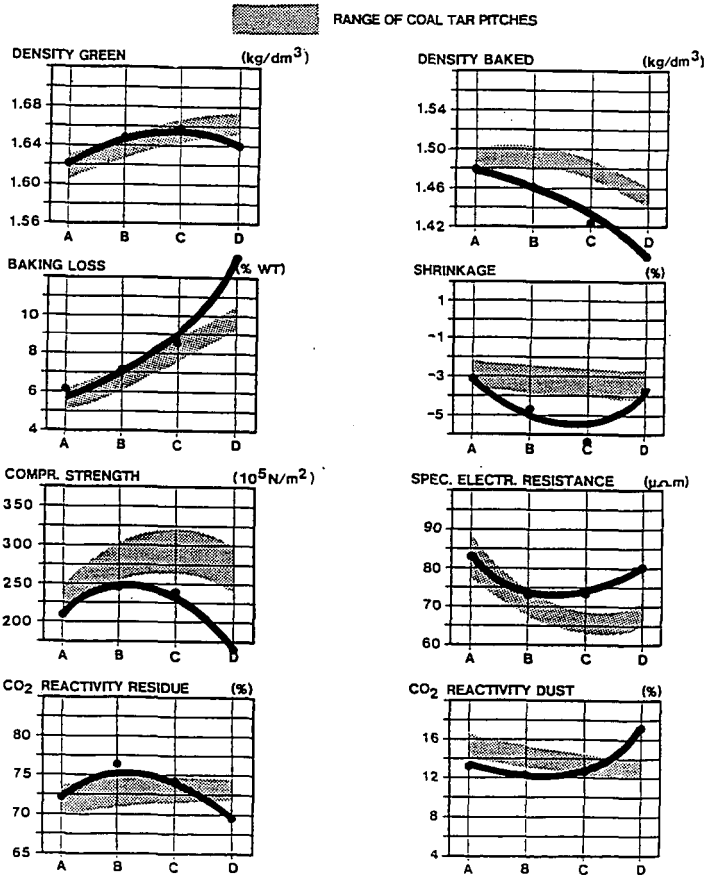

FIGURE 3. BENCH SCALE ANODE EVALUATION USING PITCH TR4

PITCH CONTENT: A = 14% B = 16% C = 18% D = 20%

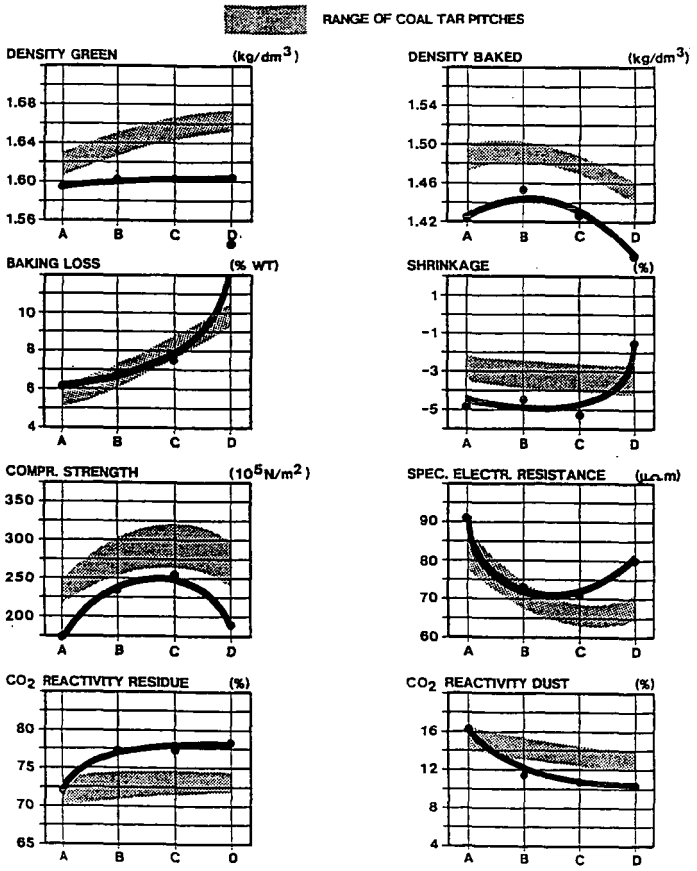

FIGURE 4. BENCH SCALE ANODE EVALUATION USING PITCH TR4D

PITCH CONTENT: A = 14% B = 16% C = 18% D = 20%

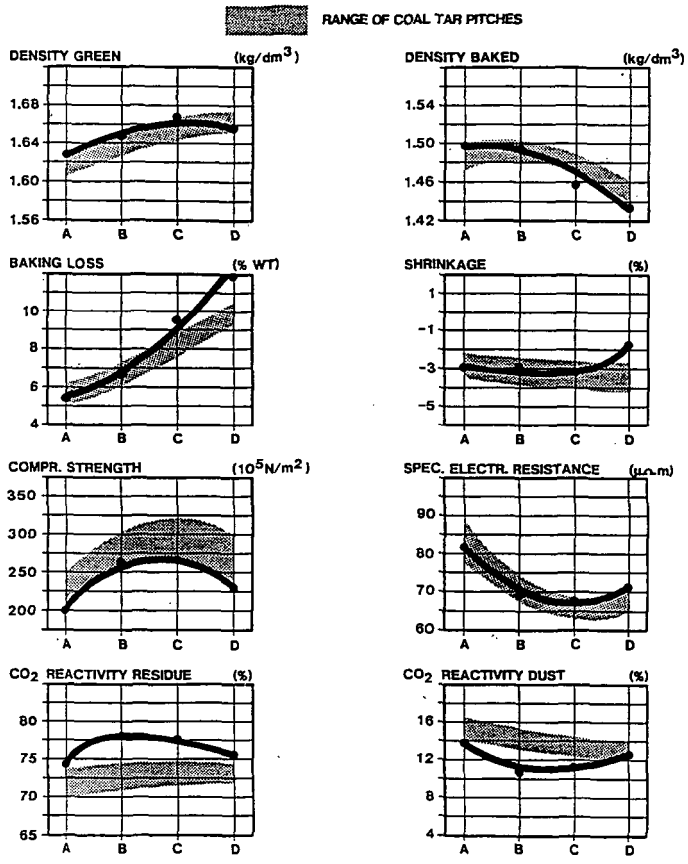

PREDICTING PETROLEUM COKE QUALITY FROM FEEDSTOCK PROPERTIES

Joaquín Rodríguez, Carola Acuña,
Jorge Guerrero and León Velasco
Intevep, S.A.PO. BOX 76343
Caracas, Venezuela

Keywords: Polarized light microscopy, NMR spectroscopy, coefficient of thermal expansion.

ABSTRACT

A method for predicting petroleum coke quality (Coefficient of Thermal Expansion, CTE) has been developed by correlating feed material properties such as aromatics carbons (wt. %) and optical size texture determined by ^{13}C NMR spectroscopy and polarized light microscopy, respectively.

Correlations used to develop this method are based on characterizations and studies of venezuelan feedstocks such as FCC Decanted Oil, Lube Oil Extract, Flexicoker Recycle Oil and several blends of these materials using the above mentioned analysis, as well as, an evaluation of needle grade coke obtained from the referred feedstocks.

INTRODUCTION

Needle grade coke is a special product obtained from the delayed coking of highly aromatic refinery streams. This special grade coke is used in the fabrication of electrodes for the electric arc furnace in the steel industry. Its a carbonaceous residue of a fibrous nature made up of needle like structures.

Feedstocks used in needle grade coke production are characterized by high aromatic content (>60 wt %), low sulfur content (<1wt %) and a relatively low Conradson Carbon (<10 wt %)[1].

One of the most important properties in assesing needle grade coke quality is the coefficient of thermal expansion (CTE).

In order to determine this property significant amounts of coke are required and pilot plant production of this material becomes necesary.

The fact that coke quality is strongly dependant upon the properties of the feedstock and the operating conditions and therefore on the growth of the mesophase[2,3] which in turn determins the degree of crystallinity of the final product suggests that it should be possible to predict coke quality from feedstock properties at predetermined operating conditions.

The present paper presents the results of the evaluation of a variety of raw materials as potential feedstocks for needle grade coke production. The evaluation includes feedstock characterization by NMR[4], observation of mesophase formation and

growth[5] and pilot plant production, calcining and characterization (CTE) of needle grade coke.

The results establish that there is a relationship between the aromatic carbons in the feedstock and the CTE; and between the optical texture size and CTE.

EXPERIMENTAL

NMR spectra of the feedstocks to be evaluated where obtained from a Bruker 300 MSL spectrometer using deuterated chloroform as solvent and TMS as internal reference (0.0 ppm). ^{13}C spectra of the liquid samples were taken at 75.468 MHz and those of ^{1}H at 300 MHz.

Mesophase growth and optical texture size where observed by polarized light microscopy. Samples placed in a micro cell (Figure 1) were subjected to a heat treatment at temperatures between 430°C and 470°C and a H_2 or N_2 pressure up to 2000 psig.

Additionaly the feedstocks were used to produce delayed coke in a 4 litre drum capacity pilot plant with a feedrate between 1500-2000 gr/h, drum internal temp of 400-500°C and two operating pressures (60 and 140 psig).

Green cokes produced were later dried and crushed to 3 mesh in size and after calcined at 850/1250°C.

Several electrode recipies where prepared using the cokes, a coal tar pitch and puffing inhibitors with which 5/8″ diameter and 5″ long bench scale electrodes were made in order to determine the CTE.

RESULTS AND DISCUSSION

Characterization of the feedstocks evaluated (FCC decanted oil, lube oil extract and flexicoker recycle) are shown in table 1. FCC decanted oil subjected to thermal treatment and observed through polarized microscopy exhibits extended fluid domains.

On the other hand flexicoker recycle tends to yield coarse flow mosaics where as Lube Oil Extract due to its low aromaticity gives rise to small mesophase spheres that do not generate mosaics.

Mixture of these feedstocks show intermediate behaviour. Optical texture size depends on the heating rate. Tables 2 and 3 show time of mesophase formation, coalescence period and the optical texture size of the feedstock considered, as well as values of CTE of the needle grade cokes produced from such feedstocks. It can be seen that the optical texture size is inversely proportional to the CTE of the cokes. This suggests that feedstocks that give rise to a greater degree of mesophase development yield higher quality cokes that is, less CTE. Figure 2 illustrates this point. This tendency can be accounted far by the fact that greater degree of mesophase development leads to a greater level of alignment in the aromatic layers which later form a microcrystalline structure that resembles graphite.

Furthermore, a relationship was found between the aromatic carbon content of the feedstock as determined by NMR and the quality of the needle coke. This dependence is shown in Figure 3. No relationship was observed between coke quality and the aromatics content determined by HPLC, which suggests that coke quality does not only depend on the amount of aromatic structures but also the type of structure.

CONCLUSION

Feedstocks evaluation by NMR spectroscopy and polarized light microscopy allows for the quality prediction of needle grade cokes produced at pilot plant scale.

REFERENCES

1. **Feintuch, H.M.et al.,** in Handbook of Petroleum Refining, pp. 3-61, McGraw-Hill (1986)
2. **Lewis, I.C. and Singer,** in Polynuclear Aromatic Compounds, pp. 269-285, ACS (1988)
3. **Marsh, H. and Smith, J.,** in Analytical methods for coal and coal products, Vol. 2, pp. 371-414, Academic Press (1978)
4. **Gillet, S. et al.,** FUEL, 60 (3): 221-225 (1981)
5. **Perrota, A.J. et al.,** High Temp. High Pres., 13(2): 159-166 (1981)

TABLE 1. CHARACTERIZATION OF FEEDSTOCKS

PROPERTY	FCCDO	LOE	FCR
API Gravity	6.9	14.6	6.3
KINEMATIC VISCOSITY			
at 60 °C, cSt	61.9	-	-
at 135 °C, cSt		11.0	45.8
Conradson Carbon, wt%	4.26	1.76	15.6
Sulfur, wt%	1.36	2.60	2.77
HPLC fractions, wt%			
Saturates	26.8	25.6	18.2
Aromatics	67.3	69.2	57.1
Polar aromatics	4.7	5.2	18.2
Asphaltenes	1.2	0.0	6.5
^{13}C NMR, wt%			
Parafinic	25.00	42.94	37.41
Naphtenic	22.27	24.76	21.16
Aromatic	52.73	29.30	41.43
-protonated	27.75	11.86	15.54
-quaternary	24.98	17.44	25.89
^{1}H NMR, wt%			
Aliphatic	73.8	64.6	70.3
Aromatic	26.2	35.4	29.7

TABLE 2. EFFECT OF MIXING FCC DECANTED OIL AND FLEXICOKER RECYCLE

FCR wt%	Mesophase formation min.	Coalescence period min.	Size µm	CTE 10^{-7}/C
		20 °C/min. (450°C)		
0	2	5	157	4.1
30	6	10	140	7.3
50	9	12	140	7.6
100	>9	>17	<50	17.3
		50 °C/min. (450°C)		
0	2	3	250	4.1
30	10	7	380	7.3
50	16	9	<3	7.6
100	9	13	<50	17.3

TABLE 3. EFFECT OF MIXING FCC DECANTED OIL AND LUBE OIL EXTRACT

Lube Oil wt%	Mesophase formation min.	Coalescence period min.	Size µm	CTE 10^{-7}/C
		20 °C/min. (450°C)		
0	2	5	157	4.1
30	3	6	150	5.3
50	na	na	na	7.3
100	no	no	no	na
		50 °C/min. (450°C)		
0	2	3	250	4.1
30	5	no	80	5.3
50	na	na	na	7.3
100	no	no	no	na

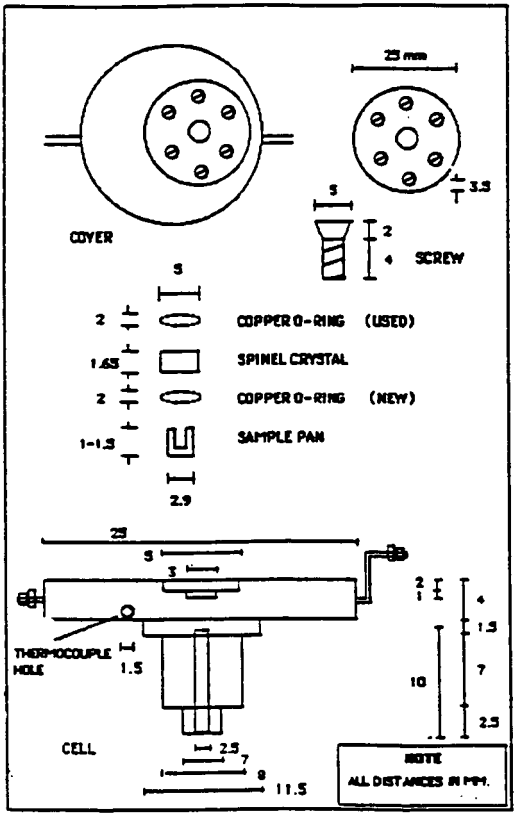

Figure 1. High temperature high pressure micro-cell

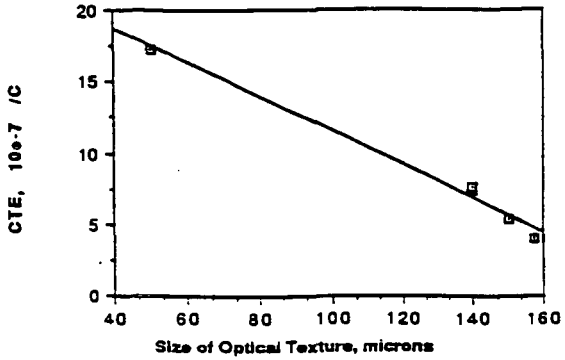

Figure 2.

Relation between Optical Size Texture of mesophase and the Coefficient of Thermal Expansion of cokes

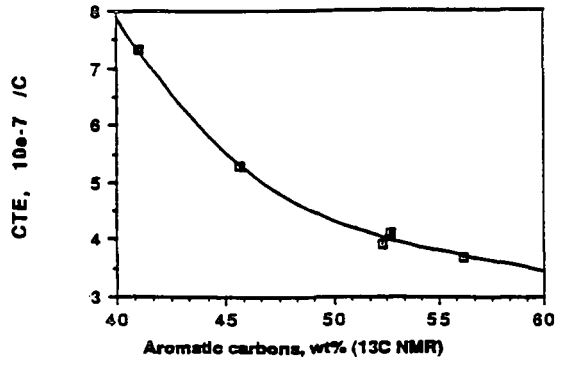

Figure 3.

Relation between NMR characterization of feedstocks and Coefficient of Thermal Expansion of cokes

SELF REDUCED IRON ORE PELLETS USING FLEXICOKE AS REDUCTANT

María Specht — INTEVEP, S.A. Apdo. 76343, Caracas, Venezuela
Carlos Seaton and Arianna Morales — Simon Bolívar University (Dept of Materials Science). Caracas, Venezuela

INTRODUCTION:

The use of flexicoque as a replacement of higher valued raw materials, has been considered, since the implamentetion of flexicoking technologies for upgrading heavy Venezuelan crude oil would increase the production of this by product.

One of the most promissing alternatives is to use this material as reductant of iron ore, because of the large amount of this mineral in Venezuela and the high demand of reduced iron for steel production.

This work is concerned with the use of flexicoke as solid reducing agent for producing direct reduced iron ore in pellet form and with the evaluation of the product obtained by the fusion of these reduced pellets.

REDUCTION OF IRON ORE USING SOLID REDUCING AGENT:

The direct reduction of iron oxides by carbon has been extensively investigated in recent years. The work done has demonstrated that such process occurs via the gaseous intermediates CO and CO_2. Initially the carbon monoxide is produced by a reaction of carbon with oxygen from the oxide in contact with the carbonaceous materials. This carbon monoxide reduces the oxides, producing carbon dioxide which reacts with carbon to form more CO; thus restoring the reducing potential of the gas phase that allows the reduction to continue. According to Baldwing [1], the chemical reactions associated with the process are as follows:

$$3Fe_2O_{3(s)} + C_{(s)} = 2Fe_3O_{4(s)} + CO_{(g)} \quad (1)$$

$$Fe_3O_{4(s)} + CO_{(g)} = 3FeO_{(s)} + CO_{2(g)} \quad (2)$$

$$FeO_{(s)} + CO_{(g)} = Fe_{(s)} + CO_{2(g)} \quad (3)$$

$$CO_{2(g)} + C_{(s)} = 2CO_{(g)} \text{ Bouduard reaction} \quad (4)$$

Previous investigation work related with the reduction of iron oxide with carbonaceous materials: charcoal, carbon, graphite, lignite coke [2, 3, 4, 5, 6, 7 and 8] have reported that the variables of major influence on this type of reduction process are: temperature, carbon content and reactivity of the carbonaceous materials. Also they demonstrated that the rate of reduction, increases with: increasing reduction temperature, increasing carbon percentage and decreasing particle size.

PRODUCTION OF COLD BOND SELF REDUCING PELLETS (SR-PELLETS):

SR-pellets are produced when carbon is incorporated in the mixture with iron ore and binders. Then an internal solid-solid reduction occurs according to the following general reactions [9].

$$Fe_2O_3 + 3C \rightarrow 2Fe^\circ + 3CO \quad (5)$$

$$Fe_2O_3 + 3CO \rightarrow 2Fe^\circ + 3CO_2 \text{ (secondary reaction)} \quad (6)$$

Fig. 1, illustrates the different mechanisms involved in the reduction of a self-reducing pellet and a conventional one reduced with external carbon [9]. Here it can

be seen that the rate and percentage completion of reduction, is higher for the self-reducing pellet than for the conventional pellets with external carbon.

Fig. 2 shows schematically the different steps for producing self-reduction pellets (SR-pellets). The self-reduced pellets can not be hardened thermally, because the reduction process would occur before the temperature for pellet induration is achieved (conventionally, $\sim$ 1300°C), since reduction reactions of iron ore by carbon may start at temperatures higher than 600°C. Therefore, SR-pellets must be produced by other pellet hardening processes i.e without firing. Such processes are designated as cold bond pelletizing.

The binders in the cold bond processes play an important role, because they must have the ability to improve green ball formation as well as the mechanical properties of green, dry, and indurated pellets [9]. Four types of binders are evaluated in this work; Portland cement, $Ca(OH)_2$, a cellulose base binder called Peridur [13] and SiO_2 (clay).

EXPERIMENTS

Methodology used

The experimental procedure is shown schematically in Fig. 3.

The reductibility of the iron oxide in the presence of flexicoke, was determined experimentally by using a thermogravimetric set up (continuous tests) and the tubular furnace (discontinuous tests) as shown in Figs. 4 (a) and (b), respectively. The removal of oxygen was measured by the loss in weight of the sample, this is known as the Loosing - weight method. By plotting the percentage loss in weight or the lost weight fraction versus time, a measure of the of the reducibility can be obtained.

For the evaluation of flexicoke as a solid reducing agent of iron ore and for determining the optimum mixture for manufacturing SR-pellets, briquettes of 10 mm in diameter and 5 mm height, were prepared by using a compressive strength of 2700 kg/cm². Two parameters were considered in the reduction of the samples, flexicoke percentage and its particle size. The experiments were performed at the same temperature (1050°C). This temperature was selected, since it was found high conversion rate at this temperature when reacting it with CO_2 [12]. Fifteen mixtures of iron ore plus flexicoke were tested, with three types of binders: hydrated lime, peridur and clay. Portland cement was evaluated as binder by making SR-pellets of iron ore and flexicoke [10]. Once was the optimum mixture determined, the effect of temperature on the reduction processes was analysed. Each experiment was run out three times for checking results reproducibility.

The SR-pellets reduction experiments were carried out using an inert atmosphere (argon), and five different temperatures: 950°C, 1000°C, 1050°C, 1100°C and 1150°C. The fraction of weight lost of the reduced samples were determined as a function of the maximum weight loss, in order to compare the behaviour of the pellets reduced at these different temperatures.

The remnant carbon content after reduction was determined by a carbon and sulphur analyser LECO. A qualitative analysis of reduction products, was carried out by X-ray diffraction, using a difractometer PHILLPS, model 1840, with the following experimental conditions: 35kv, 20mA, 0,03 2Ø seg with Ni filter. The metallic iron oxide phases present in the reduced products were determined by Mosbaüer spectroscopy. The values for metallic iron obtained by this technique were used to determine metallization percentage (%MET) according to the following relationship:

$$\%MET = [MFe^{\circ}/MFe_{tot}] \times 100 \qquad (9)$$

Where: %MET = percentage of metallization.
MFe° = iron mass.
MFe_{tot} = total iron mass as obtained by chemical analysis.

The mechanical compressive strength (crushing strength) of self-reduced pellets was determined by using a universal mechanical test equipment INSTRON of 500 kg capacity. The fracture surface of reduced products was also observed using a scanning electron microscope (SEM): PHILLIPS model 505. Attached to it a X-ray energy dispersive system (EDAX) and a wave length spectrometer of X-ray (WDAX) for qualitative and semiquantitative analysis.

The characteristics of the raw material used in the present work are shown in Table 1.

RESULTS AND DISCUSSION

FLEXICOKE AS IRON ORE REDUCTANT:

It was found that flexicoke acts as solid reducing agent of iron ore and the reduction rate increases with flexicoke content up to 17% (see Fig. 5). The curve shape indicates that there is an initial high rate of weight lost, and 15 to 30 minutes after the test started the slope of the curve tends to cero. The initial stage of the curve is related to loss of the water contained in the SR-pellets, the pirolysis of the volatile materials present in the flexicoke and the reduction of hematite to magnetite and magnetite to wustite by $CO_{(g)}$ generated by the flexicoke gasification, according to Bouduard reaction (4). The second stage of the curve is related to the reduction of wustite to iron. Fig. 6 (a) shows the effect of reduction temperature on the reduction of iron ore, from these curves it can be observed that the higher the reduction temperature, the higher the fraction of weight lost, and hence, the higher the reducibility. Fig. 6(b) shows the effect of reduction temperature on the presence of magnetite, wustite and iron. Also it was found that decreasing flexicoke particle size, increases reduction rate.

MANUFACTURE AND EVALUATION OF COLD BOND SELF REDUCING PELLETS (SR-PELLETS):

Table 2 shows the mixtures used for SR-pellets manufacturing, and also pellets quality before and after reduction tests at 1150°C for 90 minutes. Here it can be observed that the SR pellet manufactured with cement as a binder showed the highest strength 20,4 kg/pellet, although this value is lower than the required for the thermally indurated pellets (320 kg/pellets). The reduced SR pellets showed cracks, peeled surface, double structure (layer-core), and the mechanical strength decreased in 82%.

On the other hand, the SR-pellets with $Ca(OH)_2$, as a binder, showed an increment of 214% in mechanical strength after reduction. Although thes value obtained: 40 kg/pellet, is lower than the required by steel making industry for reduced pellets (60 kg/pellet).

Peridur and SiO_2 binders were used to evaluate the possibility of improving mechanical strength, however no improvements were noted when using them. Therefore the evaluation was focused on SR-pellets with cement and $Ca(OH)_2$ as binders.

The highest percentage of metalization was obtained for the SR-pellets with $Ca(OH)_2$ as binder.

STRUCTURAL CHANGES OBSERVED IN SELF REDUCED PELLETS:

The fractured area of SR-pellets with cement, as binder, reduced at 950, 1000, 1100 and 1150°C showed an internal structure of interconected pores giving a "sponge" like appearance, which indicated high degree of particle decohesion.

Whiskers or fibers of iron emerging from the oxide phases were present (see Fig. 7). The iron fibrous growth tended to be favored in the areas of oxide phases close to flexicoke particles, similar results were reported by Seaton, et al. [8]. When using charcoal as iron ore reducing agent. Internal fusion was also observed (see b in same figure), which may have occurred when the carbon was transferred from the gaseous phase to the reduced iron, producing an eutectic which fusion point is close to 1000°C [11].

Similar morphology was observed in the fractured area of SR-pellets with $Ca(OH)_2$ as binder, when they were reduced at 950 and 1000°C (see Fig. 8a). This phenomena could be accounted for by a low rate in the reaction of carbon gasification (4) and combined with a decrease in the wustite activity by the presence of calcium oxide, inhibiting iron nucleation [8].

The scanning photomicrograph of the SR-pellet with $Ca(OH)_2$, reduced at 1100°C (see Fig. 8b) showed isolated porous in a continuous matrix, indicating a more compact structure (compare with Fig. 8a).

Table 3, indicates, the volumen contraction of pellets containing $Ca(OH)_2$ as binder and the incidence of whiskers. Here it can be observed that the presence of whiskers is associated with either swelling or low volume contraction of the reduced pellets, and that these whiskers tend to dissappear as the massive iron sinterization takes place at longer periods of residence time, and at higher reduction temperatures. Also, from here can be inferred that the strengthening mechanism of SR-pellets is the massive iron sinterization during reduction. If this process does not occur the reduced pellet is highly porous and easily disintegrable, which was the case of the SR pellets with cement as a binder. The lack of massive iron sinterization is associated with the high amount of coarse remnant flexicoke particles, and to phases rich in calcium (from the high percentage of cement used as a binder) which act as barriers for iron nucleation. This lead to iron whiskers growth which are unable to sinterize each with other, promoting swelling and cracks in the reduced pellets.

FUSION TESTS RESULTS:

Table 4 shows the metallic charge patterns used for performing the fusion tests in the induction furnace, and the chemical analysis of the fusion products. If fusion 1 and 2 are compared, it can be seen that the product obtained from fusion 1, contains the double amount of carbon, vanadium and sulphur with respect to fusion 2. This is due to the fact that the remnant carbon content in SR-pellets with cement, is larger, and also that in the manufacture of these pellets a combination of two types of flexicoke (low and high vanadium content) were used.

In general, a relative high carbon and vanadium content could be acceptable, depending on the final use of the pellets, for example: as raw material for foundry (grey iron) or alloyed steels of high carbon content, providing the use of a desulphurizer during fusion process.

The fusions 3 to 7 were performed using only SR-pellets containing $Ca(OH)_2$ as binder. It can be observed that the amount of carbon and sulphur, increase with the amount of pellets in the metallic charge, except in fusion 7, where the volume of slag generated did not allow good interaction of the added pellets with the liquid phase.

Fig. 9, shows the optical photomicrographs indicating the microstructure of the fusion products, Fig. 9(a) corresponds to fusion 1, the light areas correspond to ferrite which are distributed along boundaries of very coarse prior austenite grains, and as plates within the grains; the matrix is fine perlite, a morphology characteristic of medium carbon steels. Fig. 9(b) corresponds to fusion 2 where can be observed widmanstatten patterns of proeutectoid ferrite in a matrix consisting of ferrite and fine perlite. This type of microstructure is characteristic of low carbon steels.

CONCLUSIONS:

The results of this investigation lead to the following conclusions:

- Flexicoke acts as solid reducing agent of iron ore and is effective at temperature >1100 °C.

- It is possible to agglomerate the iron ore with flexicoke by using cement, $Ca(OH)_2$, clay and peridur as binders, and manufacture cold bond self reducing pellets. The hardening mechanism is the massive iron sinterization during reduction, however these pellets do not fulfill the minimum value required for conventional pellets mechanical properties, because of the lack of a stable skeleton for binding together all the particles and the sufficient strength to support handling and transportation conditions prior to reduction; as well as sufficient compressive strength to overcome the pressure of conventional metallurgical reactors (rotary kiln or shaft type) during reduction process.

- Self reduced pellets with flexicoke as iron oxide reductant can be used as raw material for producing gray iron, or carbon steels.

RECOMENDATIONS:

An alternative for the reduction of SR-pellets with flexicoke, would be the rotary grid or a rotary open hearth furnace under isothermal conditions with high heating rates that warranties no temperature gradient in the pellets. Under these circunstances the SR-pellets residence time, in the low temperature zones would be disminished and the problems of disintigration by abrasion would be overcome. Fig. 10 shows schematically the suggested process for reducing SR-pellets. But further investigation is requiered to determine optimun operational conditions.

REFERENCES:

1. BALDWING, B. G. J. Iron Steel Inst., 179, 101 (1955).
2. OTSUKA, K. and KUNII, D. J. Chem. Eng. Japan, 2, 46, (1969).
3. ABRAHAM, M. and GOSH, A. Iron Making and Steelmaking, N 1, 14, (1979).
4. RAO, Y. K. Met. Trans. B., 8B, 279, (1979).
5. FRUEHAN, R. J. Met. Trans. B., 8B, 279 (1977).
6. GOSH, P. C. and TIWARI, S. N. J. Iron Steel Trans. B. 8B, 171 (1979).
7. SRINIVASAN, N. S. and LAHIRI, A. K. Met Trans. B., 6B, 269, (1975).
8. SEATON, C. E.; FOSTER, J. S. and VELASCO, J. Trans. ISIJ, 23, 497, (1983).
9. GOKSEL, M. A. Agglomeration, ASM, Vol. 1, Chap. 52, 877, 1981.
10. SPECHT, M. I.; MORALES, A. and SEATON, C. "Evaluation of Pellets Manufactured by Lurgi Gm6H Using Flexicoke as Solid Reducing Agent", INTEVEP, S.A., INT-EPTM,00030,87, July, 1987.
11. GOSH, P. C. and TIWARI, S. N. J. Iron Steel Trans. B, 8B, 46, 1969.
12. SEATON, C.; SPECHT, M. I.; ESTELLER, D.; CONTRERAS, G. and MORALES, A. "Potential Uses of Flexicoke in the Venezuelan Steel Industry", Iron Making Conference Proceedings, 1989.
13. From Dreeland Colloids Inc., 1670 Broadway Suite 3335, Denver, Colorado.

Table 1. Characteristics of the raw material used (weight).

Analysis	Flexicoke (Bed)	Flexicoke (Filter)	Iron ore		Binders (*) Cement Portland		Binders (*) Hydroted lime	
Fixed C	88,4	39,22	Fe_2O_3	94,33	CaO	64,0	CaO	70,00
			Al_2O_3	0,64	SiO_2	20,0	MgO	0,90
S	2,4	2,3						
			P	0,065	Al_2O_3	5,0	A_2O_3	0,60
V	1,34	16,22	S	<0,03				
					TiO_2	0,3	SiO_2	1,10
Ni	0,39	0,46	SiO_2	1,24				
					P_2O_5	0,1	Fe_{tot}	0,10
Volatile material	3,1	11,6	Fe_{tot}	64,3				
					Fe_2O_3	2,5		
As h	4,1	30,2			Mn_2O_3	0,1		
High Heating value (Cal/gr)	7305	5265			MgO	1,5		
					Na_2O	0,2		
					K_2O	0,9		

(*) Peridur is a cellulose base binder (13)
Clay was from Guárico Mines (Venezuela)

Table 2. Mixture patterns for manufacturing SR-pellets (weight %):

Binders	13,2 cement	2,0 $Ca(OH)_2$	0,08 Peridur	0,9 SiO_2
Iron ore	65,8	80,77	82,43	81,67
Flexicoke	5,3 (bed)	17,23 (bed)	17,49 (bed)	17,34 (bed)
	15,8 (filter)	-	-	-
Hardening time	7 days	-	-	-
Crushing Strength (kg/pellet)	20,4	1,78	1,64	1,60
Reduction results: (argon atmosphere at 1150°C).				
% Fe°	96,9	82,94	49,82	36,16
% Metalization	75,9	89,90	55,17	45,90
% Remnant Carbon	9,7	2,00	-	-
% FeO	13,0	6,27	26,02	11,45
Crushing strength (kg/pellet)	3,7	40	-	-

Table 3. Incidence of iron whiskers and volumen contraction percentage for reduced pellets containing $Ca(OH)_2$ as binder.

Reduction temperature (°C)	Residence time (min)	Presence of iron whiskers yes	no	Partial volume changes percentage
950	5	x		0.65
	60	x		-13.58
	90	x		3.56
1000	5	x		-7.22
	60	x		6.91
	90	x		13.34
1050	5	x		1.73
	60		x	25.69
	90		x	34.69
1100	5	x		-6.23
	60		x	27.82
	90		x	46.06
1150	5	x		-4.38
	60		x	50.68
	90		x	51.16

Table 4. Metallic charge patterns for fusion tests and chemical analysis of fusion products.

		Fusions						
		1 (*)	2 (**)	3 (**)	4 (**)	5 (**)	6 (**)	7 (**)
Metallic charge pattern	Self-reduced pellets (weight %)	13.1	13.1	15	15	30	30	45
	(g)	500	500	522	522	867	867	878
	Scrap (Steel SAE 1010) (g)	3316.2	3316.2	3048	3048	2036	2036	2968
	Elements							
Chemical composition of fusion products (Weight %)	C	0.51	0.25	0.60	0.37	0.64	0.53	0.03
	S	0.13	0.09	0.09	0.08	0.22	0.23	0.29
	Mn	0.20	0.12	0.29	0.16	0.14	0.20	0.05
	Ni	0.06	0.04	0.04	0.04	0.04	0.05	0.05
	Si	0.03	0.06	0.09	0.08	<0.01	0.05	<0.01
	V	0.15	0.03	0.04	0.05	0.08	0.08	0.04
	P	0.03	0.02	0.03	0.02	0.03	0.03	0.04

* Self-reduced pellets containing cement as binder
** Self-reduced pellets containing $Ca(OH)_2$ as binder.

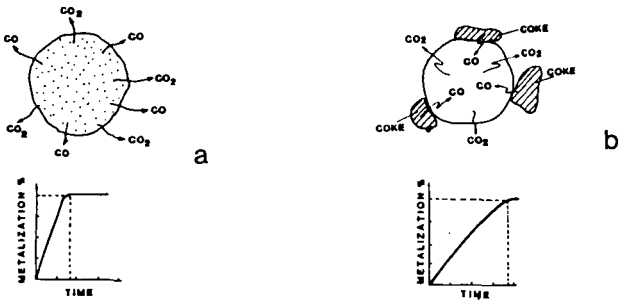

Fig. 1. (a) Self reducing pellet. Reaction (5) and (6) occurs internally.
(b) Conventional pellet with external carbon. Reaction (5) occurs at the pellet-carbon contact area and (6) inside the pellet by diffusion.

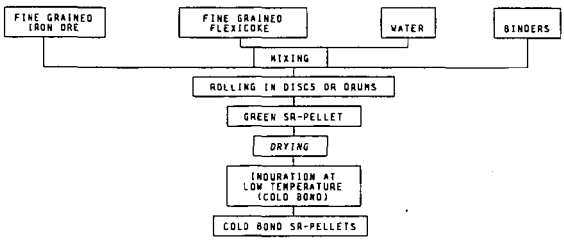

Fig. 2. Steps for producing cold bond self-reduced pellets.

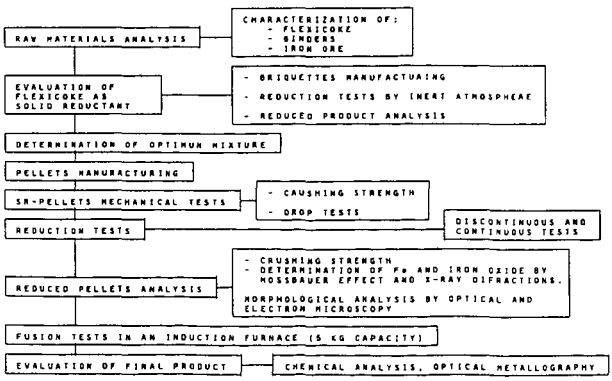

Fig. 3. Methodology used.

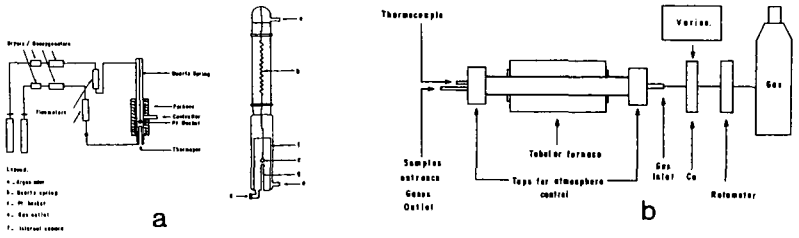

Fig. 4. (a) Thermogravimetric set up for continuous tests
(b) Tubular furnace for discontinuous tests.

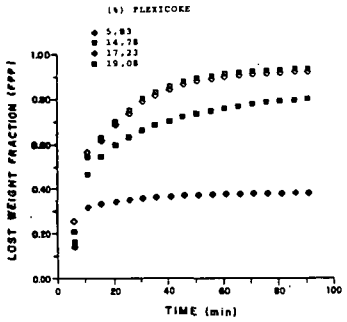

Fig. 5. Effect of flexicoke content in the reduction of iron ore.

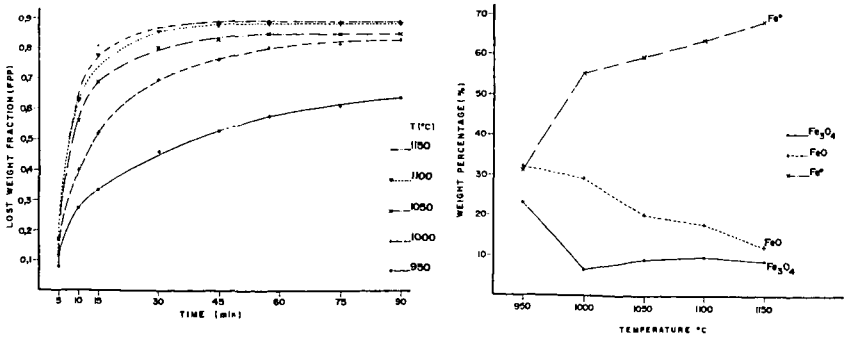

(a) (b)

Fig. 6. Effect of temperature on (a) reduction rate (b) the presence of magnetite, wustite and iron.

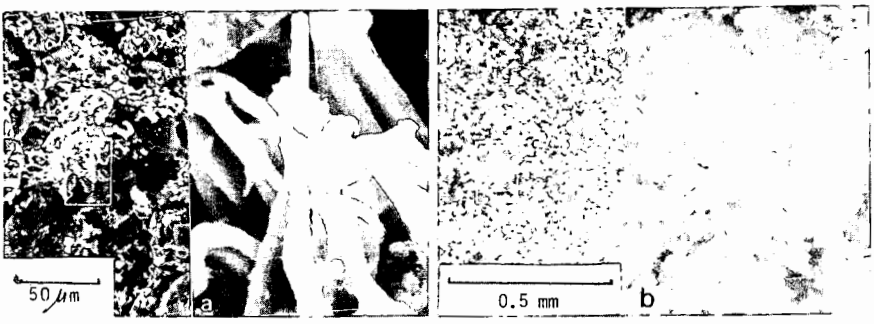

Fig. 7. (a) Scanning photomicrograph showing whiskers of iron, found in reduced pellets containing cement as a binder. (Reduction temp. 950°C).
(b) Scanning photomicrograph showing internal fusion when these pellets where reduced at 1150°C.

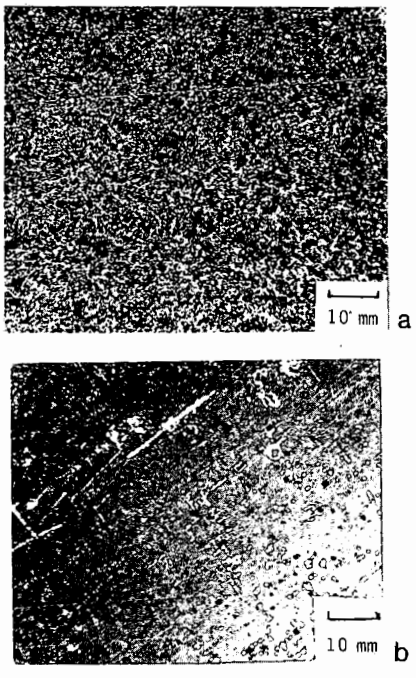

Fig. 8. SR-pellet containing $Ca(OH)_2$ as a binder. (a) reduction temp. 950°C (b) 1100°C.

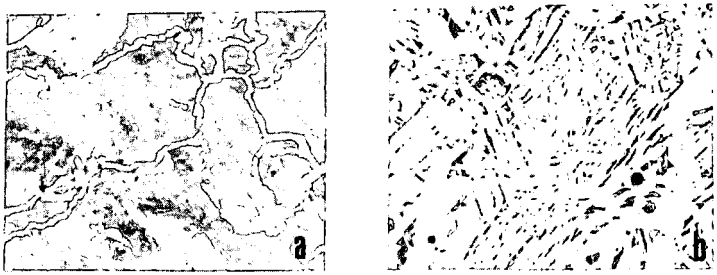

Fig. 9. (a) Optical photomicrograph of fusion 1 (100x).
(b) Optical photomicrograph of fusion 2 (100x).

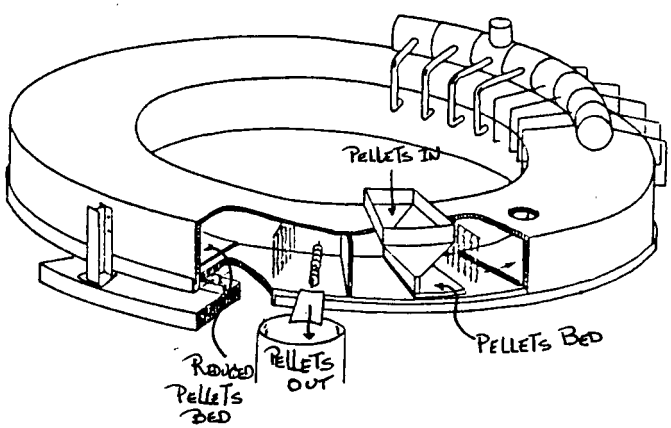

Fig. 10. Schematic view of a rotary open hearth furnace.

FLEXICOKE APPLICATIONS IN THE VENEZUELAN STEEL MAKING INDUSTRY

Druso Esteller SIDOR (Centro de Investigación). Matanzas, Edo. Bolívar, Venezuela
María Specht INTEVEP, S.A. Apdo. 76343, Caracas, Venezuela

INTRODUCTION:

In 1983 the oil refinery of LAGOVEN in Amuay installed a noncatallytic conversion process of heavy feedstock called Flexicoking. The plant has been in operation for seven years producing a by product known as flexicoke, at an aproximate rate of 300 metric tons per day. As a result, aproximate 400 thousand metric tons of solid are currently stored, posing serious problems of solids waste disposal. The flexicoke has a high carbon content, low volatile material and high heating value which makes it attractive for metallurgical applications. In 1987 a research group conformed by SIDOR (Venezuelan Steel Making Plant), INTEVEP (Venezuelan oil research institute) and LAGOVEN started activities oriented to investigate the different possibilites of flexicoke metallurgical applications. Among the possibilities studied were: flexicoke as pyroconsolidating agent, (added during pelletizing) and as foaming slag promoter for steel electric arc furnaces. The work reported here has been performed at laboratory, pilot plant and industrial scales. The laboratory work dealt with the characterization of the flexicoke. The pilot plant work dealt with the production of iron ore pellets using flexicoke as an addietive to improve the pyroconsolidating process and the mechanical behaviour of the iron oxide pellets. And the industrial work dealt with the evaluation of flexicoke as a foaming slag promoter.

EXPERIMENTAL PROCEDURE:

The experimental procedure followed in this work is shown esquematically in Fig. 1. The main characteristics of the flexicoke used in this work is shown in Table 1. If this material is compared with the metallurgical coke, used by SIDOR (see Table same) it can be observed that the main difference is the sulphur content which may impose limitations to flexicoke applications in the steel making industry. The main objective of the investigation was to determine up to which level flexicoke could substitute metallurgical coke.

Besides the chemical and physical analysis of the flexicoke given in Table 1, a morphological characterization and element distribution was performed by using scanning and transmision mycroscope analysis in order to have a better understanding of flexicoke behaviour in these particular metallurgical applications.

In order to evaluate flexicoke as pyroconsolidating agent, the procedure shown schematically in figure 2 was followed. The chemical analysis of the iron ore, dolomite, hydrated lime and sand used are indicated in Table 2.

The mixture patterns are given in Table 3. It was added 8% of water to the mixture and pelletized in a 120 cm diameter disc at 14 rpm, this configuration has a pellet production of 60 kg/h. During pelletizing more water was added up to achieve 10% in the pellet. The compresion strength and drop resistance were the two parameters evaluated in the product obtained (ie, green pellet). The drop resistance test consists of register the number of times a pellet drops from 46 cm height before it presents cracks. The reported value is often the mean value among 10 pellets. The compression strenght, also called crushing strength is the force applied on a pellet up to it breaks, it is generally reported as kg/pellet.

The pellets were burnt in a pot grate. The temperature ranged between 1260°C and 1320°C; for 30 to 45 minutes. The parameters considered for the burnt pellets evaluation were compression strength, porosity, drum abrasion index and pellet

reducibility. The criteria of acceptance or rejection of these pellets were the same considered by SIDOR for their conventional iron oxide pellets (ie, with no carbon addition). The reducibility tests were performed in a vertical reactor when 500 g of burnt pellets were heated up to 850°C in a N_2 atmosphere. When achieved this temperature a reducing atmosphere composed of CO, CO_2, H_2, H_2O was run for 90 minutes. During this period the loss weight fraction was recorded to calculate the metallization percentage according to the following equation:

% Met = (iron mass/total iron mass as obtained by chemical analysis) x 100.

The drum abrasion index was determined by reducing 500 g of burnt pellets at 550°C for 2 h in a rotary tubular furnace (Linder type). The heating up and cooling down of the sample was performed with a flow of N_2. The cold reduced sample was screened and the percentage < 6,35 mm was taken as the drum index, according to SIDOR, this must be less than 10%.

For the evaluation of flexicoke as foaming slag promoter the procedure shown in figure 3.

The slag in the steel making electric arc furnace has not only the function of trapping steel impurities but also as thermal barrier. The heat introduced inside the furnace is from tipically three carbon electrodes arc, where temperatures higher than 3500°C are generated. This is much higher than the melting point of the furnace refractory linning. Therefore, after the furnace metallic charge is melted, the furnace sidewalls are exposed to this intense radiation except for the portion of the arc that can be submerge below the slag cover that is created on top of the molten metal. The common practice is to add CaO not only for sulphur and phosphorous removal, but for covering the arc as much as possible.

In order to increase SIDOR electric arc furnace operability and decrease refractory consumptions refrigerated panels were installed on the outside walls of the furnaces, this modification implies the use of a foaming slag promoter. When carbonaceous materials such as graphite, metallurgical coke, lignite coke, etc, react with the ferrous oxide contained in the slag, CO gas in generated, the entrapped CO bubbles tend to increase the slag volume, covering in this manner the electric arc and dissipating the heat radiation that erode the refractory linning.

Previously, SIDOR tested fine metallurgical coke (mean particle size aproximately 1 mm) by injecting it through the system showed schematically in figure 4 but the usage of this material implied high consumption of valves, hoses and conexions due to its high abrasivity. Taking this into consideration, it was decided to test with flexicoke. The parameters considered during the evaluation were: operability of the injection and remnant sulphur content in the steels, since flexicoke has a sulphur content of 2,6% (62% higher than metallurgical coke).

120 metric tons of flexicoke were charged to a silo of 150 tons capacity through an air pneumatic system, at a pressure of 6 kg/cm² by a hose and pipe of 101,6 mm diameter. The flexicoke was injected on the incipient slag already formed in the electric arc furnace due to the melting of the initial metallic charge. Two electric arc furnaces were used one of 150 tons of steel capacity, where carbon steels for bars are produced, here the maximum sulphur content in the steel is 0,030%. The other, was 200 tons of steel capacity where carbon steels for slabs are produced, here is programed the production of steels with maximum sulphur content of 0,010%; 0,015% and 0,025%. Aproximately 1 or 2 tons of flexicoke per steel heat where injected. A total of 85 steel heats were evaluated.

RESULTS AND DISCUSSION

CHARACTERIZATION OF FLEXICOKE:

The flexicoke is formed during thermal cracking of the heavy residues. The break down of the large hydrocarbon molecules occurs at the surface of the heated solid particles (seed). As a result, light hydrocarbons are produced and the seeds grow in size due to the continous deposition of carbon, sulphur and metallic compounds: vanadium and nickel. A fraction of these particles stay within the reactor and the heater of the flexicoking unit, exiting the process at the elutriator when they reach an approximate mean size of 100 microns. This fraction constitute the bed coke particles and represents 80% of the total flexicoke production, their typical shape is shown in figure 4 as, can be seen, they are rounded with smaller protuberances on their surface. The inner structure of the bed coke is shown in figure 4b where also can be observed, the metals and sulphur distribution in the particle. Notice the onion like structure produced by continuous deposition of heavy, inorganic and organic substances on the solid substrate during the reactor-heater, heater-reactor cycle. Also, it can be observed that sulphur and nickel are homogeneously distributed in the particle, while vanadium tends to concentrate in the inner of the particle. The sulphur is present as organic compound as it is revealed by the transmission electron micrograph in figure 5.

FLEXICOKE AS PYROCONSOLIDATING AGENT:

Table 3 summarizes the results obtained when using flexicoke as an additive in the manufacture of iron oxide pellets. Here, it can be observed that pellets mechanical properties have increased with the addition of flexicoke up to 1%. After it, the mechanical properties decrease abruptly.

Figure 6 (a) and (b) show that the production rate and the productivity of the pelletizing process increases with additions of flexicoke up to 1%. SIDOR plans to increase the pellet plant production from 6,6 million tons/year up to 8,0 million tons/year. Flexicoke additions to pellets manufacturing would help to increase the productivity of this plant with minor equipment modifications, that would represent the instalation of a flexicoke feeder. This represents to SIDOR a consumption of 80 thounsand tons/year of flexicoke.

FLEXICOKE AS FOAMING SLAG PROMOTER:

The operability of the injection system was 100%, after being used 120 tons of flexicoke, a visual inspection of the valves, hoses and conexions revealed no erosion of the internal parts.

The flexicoke was injected during the fusion period, parallel to reduced sponge iron feeding. The optimum rate of injection was 30-40 kg/min. With this value the "swelling" of the slag was continuous improving furnace operation and decreasing noise level. At higher flexicoke injection rates, explosion between the electrodes and incontrolable flames were observed that led to decrease the furnaces between working power and the feeding rate of sponge iron.

With respect to the sulphur and carbon transference from the slag to the molten steel due to flexicoke injection; it was found that in the 150 tons capacity steel making electric arc furnace, 30% of the heats evaluated, the sulphur increments were from 0.001 up to 0.007%. The distribution of these sulphur increments in the steel heats are indicated in figure 7. In the 70% of the heats no sulphur increments were detected, on the contrary, it tend to decrease due to the simultaneous addition of CaO.

The carbon content was also evaluated, but in the 92% of the heat, no increments were detected, mainly because the flexicoke injection was on the incipient slag and flexicoke low density and high reactivity did not allow to get into the molten steel.

In the 200 tons steel capacity electric arc furnace, 66% of the heat evaluated showed increments from 0.002 up to 0.008 of sulphur. The distribution of these sulphur increments are indicated in figure 1, where it can be observed that 61% of the heats showed sulphur increments less than 0.004%. Since in this furnace, steels with more sulphur restrictions are produced, it was recomended to inject flexicoke for steels with maximum sulphur content of 0.025%. For those steels with maximum sulphur content of 0.015% the injection of flexicoke should be only during first stage of fusion period. And for those steels with maximum sulphur content of 0.010% not to use flexicoke as foaming slag promoter.

The potential consumption of flexicoke for this particular application in SIDOR is 31 thousand tons/year (11 thousand tons for 20 tons steel capacity electric arc furnace and 20 thousand tons for the 150 tons steel capacity furnace).

Only in this two applications 121 thousand tons of flexicoke per year has to be handled and transport through 18000 km distance from LAGOVEN Amuay to SIDOR through marine transportation. Although there is proven technical feasibility of using flexicoke in the steel making industry. The transportation of high tonage of this material with 100 micros mean particle size is critical, due to powder emissions to the atmosphere. The handling and transportation involves pneumatic systems increasing its costs. The evaluation of agglomerate flexicoke in briquettes is considering now in order to diminuish transportation costs and reduce environment impact. These results will be published later on.

CONCLUSIONS:

Flexicoke can be used in the venezuelan steel making industry as pyroconsolidating agent for iron oxide pellet manufacturing, improving its mechanical strength, level of porosity and reducibility when added up to 1%. The pellet plant production and productivity is also increased with flexicoke additions.

Flexicoke can be used as foaming slag promoter in the steel making electric arc furnace, but its sulphur content restricts its application to steel production of 0.025% - 0.030% S maximum.

Flexicoke can partially substitute metallurgical coke in these particular applications. But the handling and transportation of this material with such a fine particle size remains a critical point.

RECOMENDATION:

An economical study must be perfomed in order to evaluate the investment costs for handling and transportation of flexicoke in its original particle size and if it comparable to metallurgical coke price in powder form. Also the option of agglomerating flexicoke in briquettes must be considered from technical and economical point of view.

Table 1. Characteristics of flexicoke and metallurgical coke (traditionally used by SIDOR).

Analysis	Flexicoke (Bed coke)	Metallurgical coke
%C	91,7	88,0
%S	2,6	<1,0
%V	1,58	-
%N	0,36	-
Volatile material	2,6	<3,0
Ash	3,3	40
Density	1,89	-
Heating value (cal/g)	7305	7337
Mean particle size	100 microns	>3mm

Table 2. Chemical analysis of iron ore, binders and other additives.

Analysis (w%)	Iron ore	Dolomite	Hydrated lime	Sand
Fe_{tot}	66,21	2,11	2,13	0,728
SiO_2	1,34	4,30	1,53	95
CaO	0,03	31,96	63,68	0,61
MgO	0,02	15,44	2,83	0,11
Al_2O_3	0,51	0,33	0,32	1,46
P	0,035	-	-	-
S	-	-	-	-

Table 3. Mixture patterns (weight %).

Flexicoke	Iron ore	Dolomite	Hydroted lime	Saud
0	94,96	2,72	1,89	0,73
0,5	94,51	2,84	1,89	0,76
1,0	96,51	2,84	1,89	0,76
1,5	94,51	2,84	1,89	0,76
2,0	94,51	2,84	1,89	0,76

Table 4. Summary of the results obtained when using flexicoke as an additive for iron oxide pellet production.

% Flexicoke	Green pellets	Burnt pellets				
	Crushing strength (kg/pellet)	Crushing Strength (kg/pellet)	Abrasion Index	Drum Index	Porosity	Reducibility $K(10^{-2}/min)$
0	2.45	221	5.26	91.20	15.2	2.6
0.5	1.97	321.3	4.78	93.10	20.49	2.85
1.0	1.80	375.0	4.75	93.54	19.43	3.25
1.5	2.27	144.67	5.19	92.31	-	-
2.0	2.6	100.5	5.49	87.96	-	-

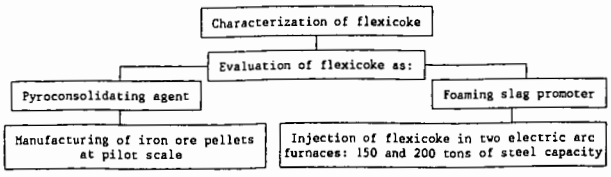

Fig. 1. Experimental procedure.

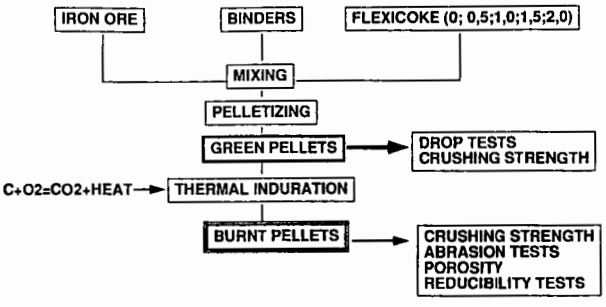

Fig. 2. Procedure followed for manufacturing iron ore pellets with flexicoke as pyroconsolidating agent.

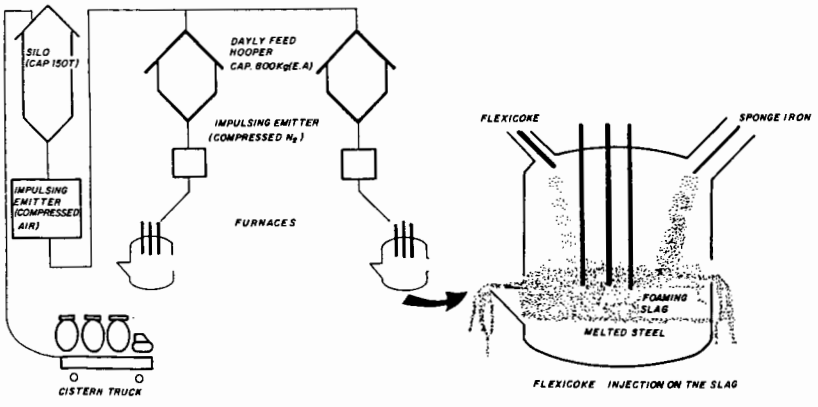

Fig. 3. Procedure for evaluation of flexicoke as foaming slag promoter.

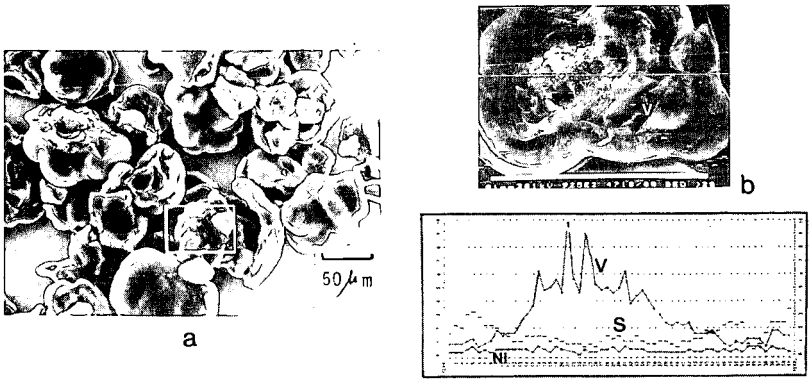

Fig. 4. (a) Scanning photomicrograph of flexicoke (bed coke). (b) V, Ni and S profile. On the photomicrograph the vanadium concentration profile is superimposed.

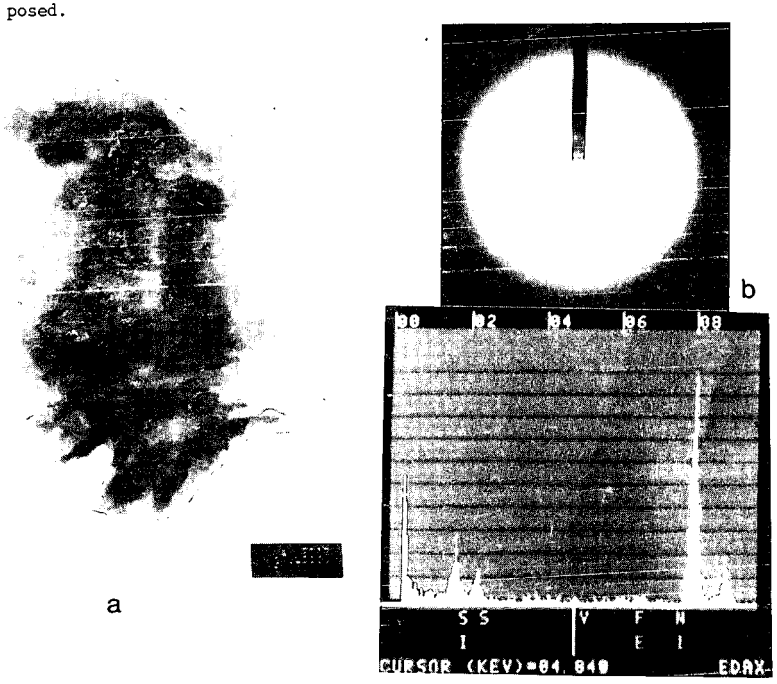

Fig. 5. Transmision photomicrograph of a bed coke particle (a). Difraction pattern of the organic sulphur compound (b).

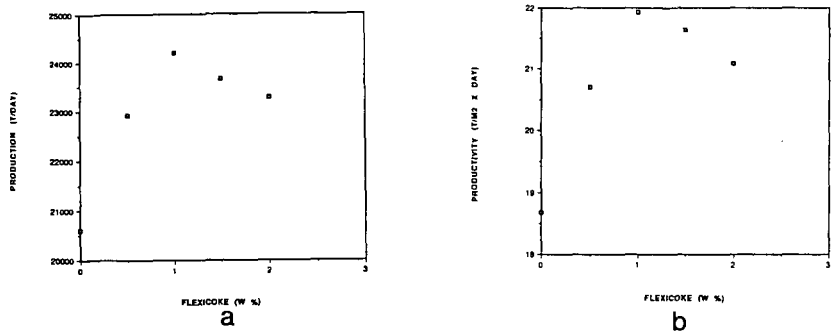

Fig. 6. (a) Production behaviour with flexicoke additions (b) Productivity.

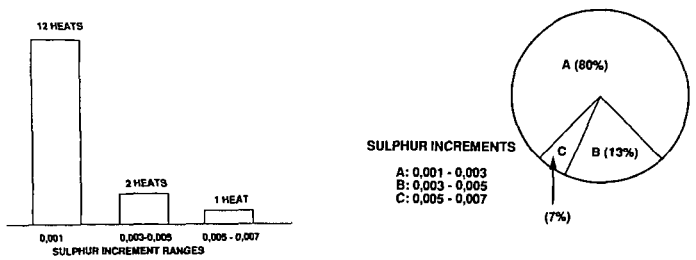

Fig. 7. Distribution of sulphur increments in the evaluated steel heats produced in the electric arc furnace 150 tons of steel capacity.

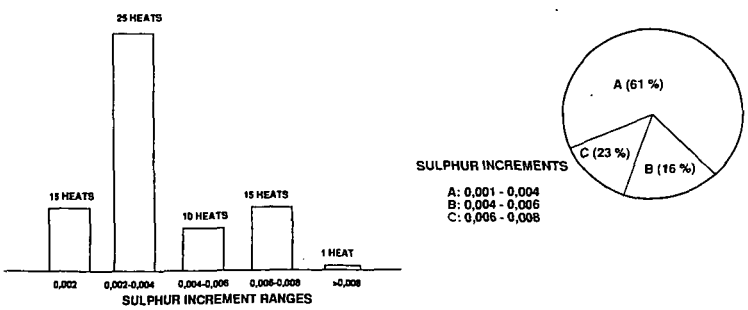

Fig. 8. Distribution of sulphur increments in the evaluated steel heats produced in the electric arc furnace 200 tons of steel capacity.